B. V. Rybakov and V. A. Sidorov

FAST-NEUTRON SPECTROSCOPY

СПЕКТРОМЕТРИЯ БЫСТРЫХ НЕЙТРОНОВ

SPEKTROMETRIYA BYSTRYKH NEITRONOV

FAST-NEUTRON SPECTROSCOPY

FAST-NEUTRON SPECTROSCOPY

B. V. Rybakov and V. A. Sidorov

Edited by N. A. VLASOV

TRANSLATED FROM RUSSIAN

Supplement No. 6

of the Soviet Journal of Atomic Energy , 1958

ATOMNAIA ENERGIIA

Press of the State Administration
for the Exploitation of Atomic Energy,
Council of Ministers, USSR, Moscow, 1958

c/b

CONSULTANTS BUREAU, INC., NEW YORK

CHAPMAN & HALL, LTD., LONDON

1960

Library of Congress Catalog Card Number: 60-8723
Copyright 1960 by Consultants Bureau, Inc.
227 W. 17th St., New York 11, N. Y.

All rights reserved. No part of this publication may be reproduced in any form without written permission from the publisher.

Printed in the United States of America

CONTENTS

Editor's Preface vi
Introduction vii

Chapter 1. Recoil-Nucleus Method 1
1. Basic relations 2
2. Choice of radiator 4
3. Scattering of neutrons on protons 5

Chapter 2. Proportional and Scintillation Counter Telescopes 9
1. Thin-radiator telescope 9
2. Thick-radiator telescope 22

Chapter 3. Nuclear Reaction Method 32
1. Ionization spectrometer with He^3 32
2. Scintillation counter with $Li^6I(Eu)$ crystal 35

Chapter 4. Time-of-Flight Method 40
1. Spectrometer with two counters. 41
2. Spectrometer with a pulsed neutron source 44

Chapter 5. Pulsed Neutron Sources 47
1. Modulation of the beam of an electrostatic accelerator 47
2. Use of the natural beam modulation in a cyclotron 52
3. Production of "time markers." 57

Chapter 6. Neutron Detectors 60
1. Efficiency of counters with organic scintillators 60
2. Resolution time 70
3. Characteristics of certain scintillators and photomultipliers 74

Chapter 7. Time Analyzer 80
1. Single-channel time analyzer 80
2. Chronotron 82
3. Fast oscilloscope 84
4. Time-amplitude converter 85
5. Principle of the "time vernier" 89

Chapter 8. Basic Features of Time-of-Flight Spectrometers 95
1. Resolving power 95
2. Efficiency 99
3. Dynamic range 101

Appendix. Energy-Time-of-Flight Table 109

EDITOR'S PREFACE

The study of interactions between fast neutrons and matter is one of the best methods of learning about the properties of the nucleus. It is also important for solving important practical problems which arise in the design of nuclear reactors. It is not surprising, therefore, that a great number of papers and investigations have been devoted to the development of various fast-neutron spectrometers. However, in general, these papers have been more concerned with technical problems and devices than with the final results of the investigations. This situation is explained by the difficulties of building a neutron spectrometer which can give good results with existing neutron sources. In recent years considerable progress has been made in the development of a time-of-flight fast-neutron spectrometer; this device offers many new possibilities in research.

The authors of the present monograph are pioneers in the development of spectroscopy methods for fast neutrons based on the time-of-flight principle. Working at the one-and-one-half meter cyclotron at the Institute for Atomic Energy they have developed one of the first and, apparently, best of the presently available spectrometers. Thus, the chapters of this monograph which are devoted to time-of-flight methods represent not only a survey of work which has been done, but, to a considerable extent, a description of their own experiments and original results.

It is natural that greatest attention in this monograph should be paid to the time-of-flight method, since it is most effective and flexible method presently available. Of the other methods, consideration is only given to those which are of importance at the present time.

There are no surveys on the time-of-flight method for fast-neutron spectroscopy. The present monograph is the first in this field. Undoubtedly it will be useful to engineers and physicists who are concerned with neutron physics. The experience of the authors has already been used in the design and construction of new cyclotrons. It is hoped that this experience will also be useful in other laboratories.

N. A. Vlasov

INTRODUCTION

The measurement of neutron energy is one of the most difficult problems in nuclear spectroscopy. Neutrons do not produce any ionization effects in passing through matter and can be detected only as a result of nuclear interactions. The study of the charged particles, γ-rays, and radioactive nuclei formed in these interactions yields information on the intensity and energy distribution of the neutron flux.

In the present monograph we consider methods of "fast"-neutron spectroscopy; by this we mean neutron energies between 0.3 and 30 Mev.

The upper limit is a natural one from the point of view of neutron spectroscopy as regards the investigation of nuclear structure and the determination of discrete spectra of nuclear energy levels. This energy region also encompasses the limiting energy of neutrons which are produced by classical sources (nuclear reactors, accelerators, van de Graaff generators and fixed-frequency cyclotrons).

The lower limit is determined only by the specific method of detection and is considerably more flexible. The method of detecting neutrons by recoil protons, which is a basic one for fast neutrons, has a lower limit of approximately 1 Mev, although in certain cases it has been possible to use this method to detect neutrons with energies smaller than 0.1 Mev [1, 2].

Until recently fast-neutron spectra have been investigated primarily through the spectrum of fast charged particles formed in the elastic interaction of neutrons with nuclei ("recoil-nucleus method") or in various nuclear reactions ("nuclear-reaction method").

With the appearance of fast scintillation counters and the development of millimicrosecond pulse techniques it has been found possible to apply the time-of-flight method to the measurement of fast-neutron energies; this method is a classical one in slow-neutron work. As applied to fast neutrons, the accuracy of the time-of-flight method is in some cases already greater than that which can be achieved by other methods. It is also found to have wider application than the other methods. This method continues to receive intensive development and represents one of the most promising methods of fast-neutron spectroscopy. However, in order to achieve good results with the time-of-flight method it is necessary to have a pulsed neutron source and a long flight path. In those cases in which these requirements cannot be met the recoil-nucleus method and the nuclear-reaction method are still valuable.

The "threshold-indicator" method, which makes use of neutron capture reactions with the subsequent formation of radioactive nucleii [3, 4], gives only a rough estimate of the neutron spectrum. The same applies to other threshold indicators such as the fission chamber.

Fast-neutron spectroscopy finds wide scientific and technological application. For example, in the development of new kinds of nuclear reactors it is necessary to study the interaction of fast neutrons with matter and to investigate elastic and inelastic neutron scattering.

Fast-neutron spectroscopy is of great value in the study of nuclear forces and nuclear structure. In spite of the advantages of work with neutrons (the fact that there is no Coulomb barrier to be penetrated by the neutron in interacting with a nucleus), up to the present time the most important work in nuclear reactions and nuclear energy states has been carried out by means of charged-particle spectroscopy. This situation is a result of the fact that the poor resolving power of neutron spectrometers made it impossible to study individual neutron energy groups corresponding to definite nuclear levels. At neutron energies up to 3 Mev useful spectroscopic investigation has been possible because of the existence of a variable-energy, monochromatic, neutron source (van de Graaff generator). As far as neutron spectrometers are concerned, however, adequate resolving powers have been achieved

only for slow neutrons. In slow-neutron experiments it is possible to obtain only a narrow range of nuclear excitation energies; these energies are close to the binding energy of the neutron in the nucleus (approximately 8 Mev). Recently, in particular because of the development of the time-of-flight method, it has also become possible to study individual levels in fast-neutron spectroscopy, at least in light and intermediate nuclei.

Before considering methods of investigating fast-neutron spectra we shall introduce certain ideas and concepts which are used in neutron spectroscopy.

The most important characteristics of a neutron spectrometer are the resolving power, efficiency, and dynamic range.

The resolving power of a spectrometer is the ratio of the line width (at half-height), corresponding to a monoenergetic neutron flux, to energy:

$$\delta = \frac{\Delta E}{E} . \tag{1}$$

The efficiency of a detector for neutrons of a given energy is usually defined as the probability that the neutron entering the sensitive volume of the detector will be detected. In other words the efficiency of the detector is normalized to the neutron flux which passes through the sensitive volume. This efficiency will be designated by ϵ.

In work with most neutron spectrometers the geometrical conditions of the experiment are very important. Hence, in comparing the properties of neutron spectrometers it is convenient to normalize the efficiency to the neutron flux per unit solid angle. The spectrometer efficiency normalized in this way will be called η. If the solid angle subtended by the sensitive volume at the neutron source is Ω

$$\eta = \Omega\varepsilon. \tag{2}$$

The dynamic range of a spectrometer is defined by the quantity

$$q = \frac{E_{max}}{E_{min}} , \tag{3}$$

where E_{max} and E_{min} are the maximum and minimum energies of neutrons which can be measured simultaneously. This quantity is useful in determining the operating possibilities of a spectrometer; in general, this quantity is not fixed for a given spectrometer.

Most neutron spectrometers require a well-collimated neutron flux; this collimation is usually achieved by virtue of the fact that the distance from the neutron source to the sensitive volume of the spectrometer is usually much greater than any transverse dimension. These conditions of spectrometer operation are called "good geometry."

It should be noted that in many cases good geometry is necessary for other reasons than the apparatus requirements: usually the source (for example, the target of an accelerator) yields an isotropic neutron flux, whereas it is necessary to study the spectrum and intensity of neutrons emitted in some definite direction.

Nuclear reactions, in which fast neutrons are emitted, may be caused by bombarding matter with charged particles or by neutrons. The conditions for studying the outgoing neutron flux in these two cases are considerably different as regards the magnitude and origin of background noise. For brevity, in what follows we will call reactions caused by charged particles "primary," and reactions caused by neutrons "secondary." This terminology is based on the fact that charged particles are usually obtained directly by means of accelerators, while neutrons result from nuclear reactions.

The particular problem of neutron spectroscopy in studying the interaction of neutrons with matter is the isolation, from a continuous (and complex) spectrum, of a narrow energy interval. The device used for this purpose is usually called a "neutron selector," as is the case in slow-neutron spectroscopy.

Almost any neutron spectrometer can be used to study the dependence of total neutron cross sections on energy since the problem reduces to the measurement of the attenuation of a neutron flux in different parts of

the spectrum. A neutron spectrometer which makes use of a time-of-flight method can serve as a selector for studying nuclear reactions in which neutrons are emitted since no requirements are imposed on the neutron detector other than speed of operation. For example, the detection of fission fragments by a gaseous scintillation counter in a time-of-flight spectrometer can be used to study the dependence of cross section and other fission parameters on neutron energy.

LITERATURE CITED

[1] G. I. Perlow, Rev. Sci. Instr. 27, 460 (1956).

[2] Granberg, Beauchamp, and Levin, Rev. Sci. Instr. 28, 89 (1957).

[3] H. A. Vlasov, Neutrons (GITTL, 1956).

[4] Hurst, et al., Rev. Sci. Instr. 27, 153 (1956).

RECOIL-NUCLEUS METHOD

The simplest interaction between a neutron and a nucleus is one in which the neutron is scattered elastically. From a knowledge of the recoil-nucleus spectrum in elastic scattering it is possible to establish the neutron spectrum. The energy transferred to the recoil nucleus by the neutron depends on the scattering angle. Thus, even monoenergetic neutrons give rise to a continuous energy distribution for the recoil nuclei.

The energy of the recoil nuclei which are emitted at a definite angle with respect to the neutron flux is uniquely related to the neutron energy. This is the basis for the "differential recoil-nucleus method," which consists of the determination of the neutron spectrum from the energy distribution of the recoil nuclei which are emitted in a narrow range of angles with respect to the direction of the neutron flux. It is apparent that this method can be used only under conditions of good geometry.

In the simplest cases (for example, if the spectrum being investigated consists of a small number of monoenergetic lines) it is sufficient to measure the recoil-nucleus spectrum, integrated over emission angle (the "integrated recoil-nucleus method"). With this method it is possible to study the spectra of neutrons from extended sources ("poor geometry").

There are numerous visual and electronic methods of studying the spectra of fast charged particles which can be used in the recoil-nucleus method.

When electronic apparatus is used, the detection and isolation of a collimated beam of recoil nuclei and the measurement of their energy is carried out by means of several proportional or scintillation counters, which form a "telescope." Spectrometers of this type are considered in Chapter II of the present monograph. Problems concerning the application of proportional counters and ionization chambers in the measurement of neutron spectra in the integrated recoil-nucleus method are considered in detail in the monograph by Rossi and Staub [1] and will not be considered further here.

Of the "visual" methods of studying the spectra of fast charged particles in neutron spectroscopy, we may make mention of the wide application of photographic emulsions. The application of photographic emulsions to nuclear physics has been discussed in a large number of original articles and survey papers. Of the survey papers which contain comprehensive bibliographies, we may mention the work of Beiser [2] and Rotblat [3]. In these survey papers rather detailed consideration has been given to the development of photographic emulsions, methods of analyzing the tracks of charged particles, and the advantages of photographic emulsions in nuclear physics. Problems concerning the application of emulsions in the measurement of neutron spectra have been considered in detail by Rosen [4]. A great deal of useful information is also contained in later papers [5-9].

A great deal of the more interesting work in neutron spectroscopy has been carried out by means of emulsions. However, this method has some important shortcomings; these are the difficulty and delay in obtaining the results after the exposures are made. With the further development of electronic methods in fast-neutron spectroscopy the use of emulsions has become less important.

The cloud chamber is cumbersome and not very efficient. At present this device finds almost no application in fast-neutron spectroscopy. In recent years increasing use has been made of the bubble chamber in the investigation of high-energy particles; this device is essentially a Wilson cloud chamber with the supercooled vapor replaced by a superheated liquid. Because of the high density of the working material, the efficiency of the bubble chamber is high, and it can be used to detect a low-intensity flux of fast neutrons. However, this device is suitable only for measurements of the spectra of very fast neutrons [10], in which case the range of the recoil nucleus is considerably greater than the bubble dimensions. The Zavoiskii scintillation chamber [11] may

also become useful in fast-neutron spectroscopy; with this device, through the use of an electron-optical image converter it is possible to observe the track of the recoil proton in an organic scintillator.

§ 1. Basic Relations

We give the basic formulas used in establishing the neutron spectrum from a knowledge of the energy distribution of the recoil nuclei. In most cases, the fast-neutron scattering can be considered in the nonrelativistic approximation. It is only close to the upper limits of the energy region being considered (approximately 30 Mev) that it is sometimes necessary to introduce small relativistic corrections.

We introduce the following notation (unless otherwise specified all quantities refer to the laboratory coordinate system):

- E – initial neutron energy;
- E' – neutron energy after scattering;
- A – mass number of the recoil nucleus;
- E_A – energy of the recoil nucleus;
- ψ – scattering angle of the neutron in the center-of-mass coordinate system;
- φ – emission angle of the recoil nucleus with respect to the original direction of motion of the neutron;
- θ – emission angle of the scattered neutron;
- σ – total scattering cross section for neutrons;
- σ_ψ – differential scattering cross section for neutrons in the center-of-mass system;
- σ_φ – differential cross section for the formation of recoil nuclei at angle φ;
- σ_θ – differential cross section for scattering of neutrons at angle θ.

We may note that σ, σ_ψ, σ_φ, and σ_θ are functions of neutron energy.

From conservation of energy and momentum we have

$$E_A = \alpha E \cos^2 \varphi, \tag{4}$$

where

$$\alpha = \frac{4A}{(1+A)^2}. \tag{5}$$

Furthermore,

$$E' = \frac{E}{(1+A)^2}\left[\cos\theta \pm \sqrt{A^2 - \sin^2\theta}\right]^2, \tag{6}$$

$$\sin\varphi = \frac{1}{2}\sqrt{\alpha \cdot \frac{E}{E_A}}\sin\psi, \tag{7}$$

$$\sin\theta = \frac{1}{2}\sqrt{\alpha A \frac{E}{E'}}\sin\psi, \tag{8}$$

$$\sigma_\varphi = 4\sigma_\psi \cos\varphi, \tag{9}$$

$$\sigma_\theta = 4\frac{E'}{E} \cdot \frac{\sigma_\psi}{\alpha\sqrt{A^2 - \sin^2\theta}} \tag{10}$$

We obtain a useful relation from Eqs. (4) and (7):

$$E_A = \frac{\alpha}{2} E (1 - \cos\psi). \tag{11}$$

The probability that as a result of scattering of a neutron with energy E the recoil nucleus will acquire an energy in the range between E_A and $E_A + dE_A$ is given by

$$W(E_A)\, dE_A = \frac{\sigma_\psi}{\sigma} \cdot 2\pi \sin\psi\, d\psi, \tag{12}$$

where the angle ψ is obtained from Eq. (11).

Making use of Eq. (11), we have

$$W(E_A)\,dE_A = \frac{\sigma_\psi}{\sigma}\cdot\frac{4\pi}{\alpha E}\,dE_A. \tag{13}$$

Eq. (13) relates the integrated recoil-nucleus spectrum resulting from the scattering of monoenergetic neutrons (the spectrum which is obtained by recording all recoil nuclei without regard to angle) to the angular distribution of scattered neutrons in the center-of-mass system.

For an arbitrary neutron spectrum the integrated recoil-nucleus spectrum is given by the expression

$$W(E_A)\,dE_A = \text{const}\,dE_A \int_{E_A/\alpha}^{\infty} \sigma_\psi \cdot \frac{F(E)\,dE}{E}\ , \tag{14}$$

where F (E) dE is the number of neutrons with energies between E and E + dE in the measured spectrum and the angle ψ is given by Eq. (11).

In the general case the differential neutron-scattering cross section in the center-of-mass system under the integral sign depends on neutron energy in a complicated way. For this reason the establishment of the neutron spectrum from the integrated recoil-nucleus spectrum is extremely difficult; in addition to the high accuracy requirements and the extremely laborious numerical calculations, it requires a knowledge of the differential neutron-scattering cross section in the center-of-mass system at all angles over the entire neutron energy range which is studied.

If the neutron scattering is isotropic in the center-of-mass system, the analysis of the integrated recoil-nucleus spectrum is simplified considerably.

In this case,

$$\frac{\sigma_\psi}{\sigma} = \frac{1}{4\pi} \tag{15}$$

and the integrated recoil-nucleus spectrum is given by the following form (for scattering of monoenergetic neutrons):

$$\begin{aligned} W(E_A)\,dE_A &= \frac{dE_A}{\alpha E} \quad \text{for} \quad E_A < \alpha E \\ W(E_A)\,dE_A &= 0 \quad\ \ \text{for} \quad E_A > \alpha E. \end{aligned} \tag{16}$$

The limits of the spectrum give the neutron energy while the area gives the total number of neutrons which undergo elastic scattering.

In the case of isotropic scattering the integrated recoil-nucleus spectrum (14) corresponding to an arbitrary neutron spectrum is of the form

$$W(E_A)\,dE_A = \text{const}\,dE_A \int_{E_A/\alpha}^{\infty} \sigma \cdot \frac{F(E)\,dE}{E}\ ,$$

whence the neutron spectrum is

$$F(E)\,dE = \text{const}\,\frac{E}{\sigma}\cdot\left[\frac{dW(E_A)}{dE_A}\right]_{E_A=\alpha E} dE.$$

Thus, by differentiation of the integrated recoil-nucleus spectrum with respect to energy it is possible to find the neutron spectrum. However, because of the distortions of the recoil-nucleus spectrum, which arises as a result of various instrument effects, this method can be used only in the simplest cases, i.e., when the neutron spectrum consists of two or three lines which are well separated.

In the general case the differential spectrum obtained by recording recoil-nuclei emitted at a given angle φ with respect to the neutron flux is related to the neutron spectrum by the simple relation

$$W(E_A)\,dE_A = \text{const} \cdot \sigma_\varphi F(E)\,dE.$$

From Eq. (4) we obtain the neutron spectrum

$$F(E)\,dE = \text{const} \cdot \frac{W(\alpha E \cos^2 \varphi)}{\sigma_\varphi} \tag{17}$$

Thus, the conversion from the differential recoil-nucleus spectrum to the neutron spectrum means essentially a calculation of the differential cross section for the formation of recoil nuclei at a given angle as a function of neutron energy and linear multiplication of the energy scale:

$$E = \frac{E_A}{\alpha \cos^2 \varphi} = \text{const} \cdot E_A.$$

In the case of isotropic neutron scattering the analysis of the differential recoil nucleus spectrum is simplified because in place of σ_φ in Eq. (17) we deal with the energy dependence of the total cross section for neutron scattering. Furthermore, there is a significant reduction in the uncertainty in the absolute measurements of the neutron flux; this quantity is determined precisely in this case, the accuracy being determined by the accuracy with which the total elastic scattering cross section is known. The total cross sections are measured by measuring the attenuation of the neutron flux and since one does not require the absolute value of the neutron flux the total cross sections can be measured with considerably greater accuracy than the differential cross sections.

In most cases the apparatus which is used to measure the differential recoil nucleus spectrum records nuclei which are emitted in a narrow forward cone ($\varphi = 0°$). The choice of the angle $\varphi = 0°$ is dictated by the fact that the recoil nuclei have maximum energy in this case (4) and the uncertainty in recoil-nucleus energy due to the spread in φ is a minimum.

§ 2. Choice of Radiator

The choice of the radiator used to determine the neutron spectrum from the spectrum of the recoil nuclei formed in the radiator material is dictated by the following considerations.

The recoil nucleus must be light. It follows from Eqs. (4) and (5) that the recoil nucleus will acquire greater energy, the smaller its mass. Furthermore, it is possible to measure the energy of light charged particles more easily than that of heavy particles. The range of particles heavier than α-particles is small and is known with considerably less accuracy than the ranges of protons or α-particles. The intensity of the flash produced by a heavy particle in a solid or liquid scintillator is very small since the light yield of scintillators falls off rapidly with increasing ionization density.

The cross section for elastic neutron scattering on nuclei of the radiator must be considerably greater than the cross sections for capture and inelastic scattering. This cross section must be well known, should exhibit a smooth dependence on neutron energy, and should be large.

It is desirable that the scattering of neutrons on nuclei of the radiator be isotropic in the center-of-mass system since this means a considerable simplification in the analysis of recoil-nucleus spectra and allows an increase in the accuracy of the absolute measurements of neutron flux.

The material which best satisfies the requirements which have been enumerated is hydrogen; this material serves as a radiator in the overwhelming majority of experiments.

In certain cases, deuterium or helium are used as radiators. The total neutron scattering cross sections for these nuclei and the total cross section for n, p scattering are rather large and are smooth functions of energy (Fig. 1). In contrast with (n, p) scattering, neutron scattering on deuterium and helium is anisotropic (in the forward direction) in the center-of-mass system.

The use of helium turns out to be convenient, for example, in studying the spectra of high-energy neutrons by means of proportional counters because the range of α-particles is smaller than the range of protons. The

anisotropy in the scattering of neutrons on helium is sometimes desirable since this effect helps in distinguishing fringing effects. Proportional counters which work at high pressures have considerably better characteristics when filled with helium than when filled with hydrogen because helium is a noble gas.

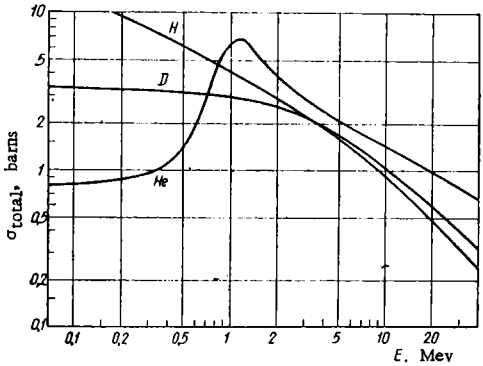

Fig. 1. Total neutron cross sections for H, D, and He^4 [12].

§ 3. Scattering of Neutrons on Protons

The formulas derived in § 1 for scattering of neutrons on protons can be simplified considerably in particular cases. The mass of the proton is essentially equal to the mass of the neutron so that $\alpha = 1$ in Eq. (5). In place of Eqs. (4) - (11), we have

$$E_p = E\cos^2\varphi = {}^1/_2E(1-\cos\psi) \tag{18}$$

$$E' = E\cos^2\theta \tag{19}$$

$$\theta = \frac{\pi}{2} - \varphi = {}^1/_2\psi \tag{20}$$

$$\sigma_\varphi = 4\sigma_\psi\cos\varphi \tag{21}$$

$$\sigma_\theta = 4\sigma_\psi\cos\theta \tag{22}$$

(the notation is that given on p. 2).

For neutron energies up to 10 Mev, (n, p) scattering is isotropic in the center-of-mass system. Taking account of Eq. (15), from Eqs. (21) and (22) for this energy region we have

$$\sigma_\varphi = \frac{\sigma\cos\varphi}{\pi} \tag{23}$$

$$\sigma_\theta = \frac{\sigma\cos\theta}{\pi}, \tag{24}$$

where σ is the total cross section for n, p scattering at a given neutron energy.

For neutron energies greater than 10 Mev the differential scattering cross section in the center-of-mass system depends on angle and may be given in the form

$$\sigma_\psi = \sigma_\psi\left(\frac{\pi}{2}\right)(1 + C\cos^2\psi). \tag{25}$$

The anisotropy factor C increases with increasing neutron energy. The dependence of this factor on energy in the laboratory coordinate system is shown in Fig. 2. The values of C are computed on the basis of the collected data on the differential cross section for n, p scattering given in the survey paper by Fowler and Brolley [13].

A paper by Bame et al. [14] presents a semiempirical formula obtained by Hammel for the differential n, p scattering cross section. This formula has been derived under the assumption that the anisotropy in n, p scattering is the result of interference between S and D waves. The coefficient of the interference term, which varies as E^2, has been obtained from experimental data obtained at neutron energies of 90 Mev. The Hammel formula is in good agreement with experiment in the neutron energy region between 10 and 90 Mev.

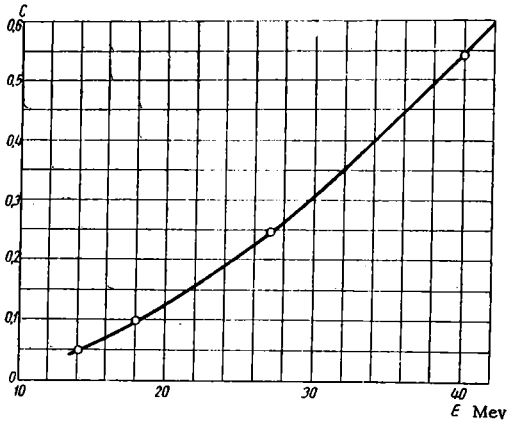

Fig. 2. Dependence of the anisotropy factor in n, p scattering on neutron energy.

In the present notation this formula is given by

$$\sigma_\psi = \frac{\sigma}{4\pi}\left[\frac{1+2\left(\frac{E}{90}\right)^2\cos^2\psi}{1+{}^2/_3\left(\frac{E}{90}\right)^2}\right],$$

where E is given in Mev.

Whence, in view of Eq. (22), the differential cross section for neutron scattering in the laboratory system is:

$$\sigma_\theta = \frac{\sigma\cos\theta}{\pi}\left[\frac{1+2\left(\frac{E}{90}\right)^2\cos^2 2\theta}{1+{}^2/_3\left(\frac{E}{90}\right)^2}\right]$$

The total cross section for n, p scattering has been thoroughly investigated over a wide energy region. This cross section is given with good accuracy by a semiempirical formula also derived by Hammel [14]:

$$\sigma = \frac{3\pi}{1{,}206E+(-1{,}8600+0{,}09415E+0{,}000130E^2)} + \\ + \frac{\pi}{1{,}206E+(0{,}4223+0{,}1300E)^2}; \qquad (26)$$

where σ is expressed in barns and E in Mev.

In many cases it is possible to use a simpler empirical formula:

$$\sigma\,(\text{barns}) = \frac{4{,}83}{\sqrt{E\,(\text{Mev})}} - 0{,}578. \qquad (27)$$

In the neutron-energy region between 0.3 and 30 Mev this formula gives 3% accuracy with the experimental data.

The values of the total cross section for n, p scattering calculated by Eq. (26) are given in Table 1.

TABLE 1

E, Mev	σ, barns	E, Mev	σ, barns	E, Mev	σ, barns
0,1	12,790	3,6	2,029	15,5	0,6281
0,2	9,700	3,8	1,959	16,0	0,6088
0,3	8,003	4,0	1,893	16,5	0,5905
0,4	6,919	4,5	1,747	17,0	0,5731
0,5	6,161	5,0	1,623	17,5	0,5566
0,6	5,596	5,5	1,515	18,0	0,5409
0,7	5,156	6,0	1,421	18,5	0,5260
0,8	4,801	6,5	1,337	19,0	0,5117
0,9	4,507	7,0	1,262	19,5	0,4981
1,0	4,259	7,5	1,195	20,0	0,4851
1,1	4,045	8,0	1,135	21,0	0,4608
1,2	3,858	8,5	1,080	22,0	0,4384
1,3	3,693	9,0	1,029	23,0	0,4178
1,4	3,546	9,5	0,9833	24,0	0,3988
1,5	3,414	10,0	0,9408	25,0	0,3812
1,6	3,293	10,5	0,9016	26,0	0,3648
1,8	3,082	11,0	0,8652	27,0	0,3496
2,0	2,903	11,5	0,8314	28,0	0,3354
2,2	2,747	12,0	0,8000	29,0	0,3221
2,4	2,609	12,5	0,7706	30,0	0,3096
2,6	2,487	13,0	0,7430	31,0	0,2979
2,8	2,378	13,5	0,7172	32,0	0,2869
3,0	2,279	14,0	0,6929	33,0	0,2765
3,2	2,188	14,5	0,6700	34,0	0,2668
3,4	2,106	15,0	0,6485	35,0	0,2575

LITERATURE CITED

[1] B. Rossi and G. Staub, Ionization Chambers and Counters III. (1951).

[2] A. Beiser, Rev. Modern Phys. 24, 237 (1952); Usp. Fiz. Nauk 52, 377 (1954).

[3] J. Rotblat, Progress in Nuclear Physics 1, 37 (1950).

[4] L. Rosen, Nucleonics 2, 7, 33 (1953); 11, 8, 38 (1953).

[5] Bujdoso, Medveczky, and Torok, Acta phys. Acad. Sci. Hung. 7, 373 (1957).

[6] J. R. Bird and R. H. Spear, Austral. J. Phys. 10, 268 (1957).

[7] W. H. Barkas, P. H. Barrett, P. Cüer, H. Heckman, F. M. Smith, and H. K. Ticho, Nuovo Cimento 8, 185 (1958).

[8] W. H. Barkas, Nuovo Cimento 8, 185 (1958).

[9] J. H. Roberts, Rev. Sci. Instr. 28, 677 (1957).

[10] H. E. Adelson, H. A. Bostick, B. J. Moyer, and C. N. Waddel, Bull. Am. Phys. Soc. ser. 2, 3, 189 (1958).

[11] E. K. Zavoiskii and G. E. Smolkin, J. Atomic Energy 4, 34 (1956).

[12] H. H. Barschall, Encyclopedia of Physics 45, 437 (1958).

[13] J. L. Fowler and J. E. Brolley, Revs. Mod. Phys. 28, 103 (1956).

[14] S. J. Bame, E. Haddad, J. E. Perry and R. K. Smith, Rev. Sci. Instr. 28, 997 (1957).

PROPORTIONAL AND SCINTILLATION COUNTER TELESCOPES

A system consisting of several counters, with which it is possible to define a collimated beam of recoil protons and measure its energy, is called a telescope. The source of recoil protons in the telescope is a layer of hydrogenous material ("radiator"). We may distinguish telescopes by means of the radiators, which can be "thin" or "thick". In the first case the radiator is a layer of solid hydrogenous matter which is located in front of the first counter of the telescope. Its thickness determines the resolving power of the spectrometer directly and comprises a small part (several percent) of the range of the recoil protons. In the second case, the radiator is the total sensitive volume of the first counter of the telescope. Its thickness may comprise a considerable fraction of the recoil proton range (for instance one half) and is limited only by the necessity of detection of the recoil proton by the remaining counters of the telescope.

A telescope with a thin radiator can have a rather high resolving power (up to 5%) and has been used for the study of complex neutron spectra [1-5]; however, intense neutron sources are required in order to obtain satisfactory results. A basic feature of a spectrometer of this type is the possibility of computing the efficiency for a monoenergetic neutron beam with an accuracy which is limited only by the uncertainty in the knowledge of the n, p scattering cross section. For this reason, telescopes with thin radiators are frequently used for absolute measurements of monoenergetic neutron fluxes [6, 7].

A telescope with a thick radiator has considerably greater efficiency and is generally used for studying low-intensity neutron fluxes.

§ 1. Thin-Radiator Telescope

A diagram of an experimental arrangement for measuring neutron spectra by means of a telescope with a thin radiator is shown in Fig. 3. At a distance b_1 from a neutron source S is located a hydrogenous radiator of diameter 2a. The recoil protons which are emitted in the direction of the detection system are collimated by an aperture which is located at a distance b_2 from the radiator. In practice conditions for good geometry are usually satisfied so that the neutron source may be considered a point source; the diameters of the radiator and aperture are small compared with the distances b_1 and b_2. The diameter of the aperture is usually made equal to the diameter of the radiator. We will consider this case only.

Between the radiator and the aperture and beyond the aperture there are located charged-particle counters and sometimes stopping filters. The counter telescope along with the auxiliary apparatus isolates, from all the charged particles produced, only those recoil protons which are emitted from the radiator and pass through the aperture; thus the system can be used to measure the energy distribution.

We now consider the resolving power (1) and efficiency (2) of a telescope with a thin radiator. The line width of the telescope is determined by the thickness of the radiator and the collimation of the recoil protons and depends on the method by which the proton energy is measured. The first two "partial" widths are general and are characteristic of all thin-radiator telescopes.

In order to determine the width due to the radiator it may be assumed that all the recoil protons are emitted at an angle of 0° since the collimation angle is usually small ($\alpha_1 + \alpha_2 \approx 20°$). Under these conditions the energy of the recoil protons is equal to the neutron energy. Part of the proton energy is lost in the radiator. The recoil-proton spectrum (for monoenergetic neutrons) is rectangular in shape. In order to determine the width we make use of an approximate relation between the range and energy of the proton,

$$R = cE_p^{3/2}, \tag{28}$$

the accuracy of which is completely satisfactory in the present case. We find

$$\frac{\Delta R}{R} = {}^3/_2 \frac{\Delta E_p}{E_p}.$$

Hence, it follows that the partial line width due to the finite thickness of the radiator is given by

$$\delta_1 = {}^2/_3 \frac{\Delta R}{R}, \tag{29}$$

where R is the range of a proton with energy $E_p = E$ in the material of which the radiator is made and ΔR is the thickness of the radiator.

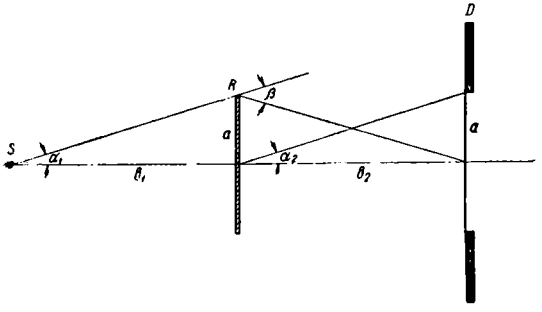

Fig. 3. Schematic diagram of a telescope with a thin radiator:
S) neutron source; R) radiator; D) aperture.

The criterion for the choice of a material for use in a radiator is the hydrogen content in a layer of the material corresponding to a given stopping power and the absence of nuclei which have a large cross section for n, p reactions in the neutron energy region being used. Earlier radiators were fabricated from glycerol tristearate ($C_{57}H_{110}O_6$) or from paraffin, the composition of which is given approximately by CH_2. There can be a large variation in the paraffin content from sample to sample and this variation is one of the greatest hinderances to making absolute measurements of neutron fluxes. At the present time polyethylene is used for radiators; this material has a well-known composition (CH_2) and has considerably better mechanical properties.

In Figs. 4 and 5 are shown curves for $\frac{dE_p}{dR}(E_p)$ and $R(E_p)$ for polyethylene calculated by us on the basis of the data reported by Hirschfelder and Magee [8].

If the recoil proton is emitted at some small angle with respect to the primary neutron its energy (neglecting energy losses in the radiator) is $E_p(\varphi) = E\cos^2\varphi \approx E(1-\varphi^2)$. Consequently, $\Delta E_p \approx E\varphi^2$ and the partial width of the neutron line due to the finite emission angles of the recoil protons is,

$$\delta_2 = \beta^2, \tag{30}$$

where β is the mean value of the angle φ for a given telescope.

From numerical integration of the area of the radiator and the aperture it can be shown [9] that when the diameters are equal and when $b_1 = b_2$, the quantity β is equal to the angle of emission of a recoil proton which goes from the edge of the radiator through the center of the aperture (Fig. 3). For a given value of δ_2 the efficiency of the telescope, which is proportional to the product of the solid angles subtended by the radiator at the source and by the aperture at the radiator; it is found to be a maximum when $b_1 = b_2$.

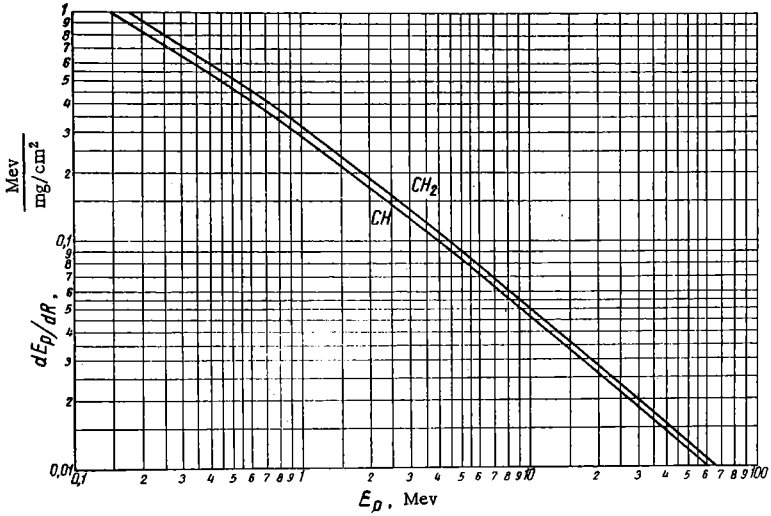

Fig. 4. Stopping power of polystyrol (CH) and polyethylene (CH_2) for protons.

As an approximation it may be assumed that the partial widths combine quadratically and that the optimum conditions obtain when they are equal. A detailed analysis shows [9] that for a given collimation angle and with $b_1 = b_2$ the thickness of the radiator should be chosen by the relation

$$\delta_1 = 0{,}9\delta_2. \tag{31}$$

In this case the resultant width is

$$\delta_{12} = 1{,}1\delta_2 = 1{,}1\beta^2. \tag{32}$$

It is apparent from Fig. 3 that for small angles the efficiency of the telescope for monoenergetic neutrons, normalized to the neutron flux per unit solid angle, is

$$\eta = \pi^2\alpha_1^2\alpha_2^2\Delta R n \sigma_\varphi(0°), \tag{33}$$

where ΔR is the thickness of the radiator in mg/cm², n is the number of atoms of hydrogen in 1 mg of the material of the radiator, $\sigma_\varphi(0°)$ is the differential cross section for the scattering of a neutron on a proton corresponding to the emission of a proton at an angle of 0°.

In many cases we can make use of Eq. (22):

$$\sigma_\varphi(0°) = \frac{\sigma}{\pi},$$

where σ is the total cross section for n, p scattering. In carrying out exact calculations attention must be paid to the anisotropy of n, p scattering in the center-of-mass system which appears at neutron energies greater than 10 Mev.

For optimum geometry $\left(\alpha_1 = \alpha_2 = \frac{\beta}{2}\right)$ and optimum radiator thickness (31), taking account of (29) and (32) we can find the upper limit of the telescope for a given neutron energy for a given resolving power:

$$\eta = 0{,}2Rn\sigma\delta_{12}^3, \tag{34}$$

where R is the range of a proton (with energy equal to the neutron energy) in the radiator.

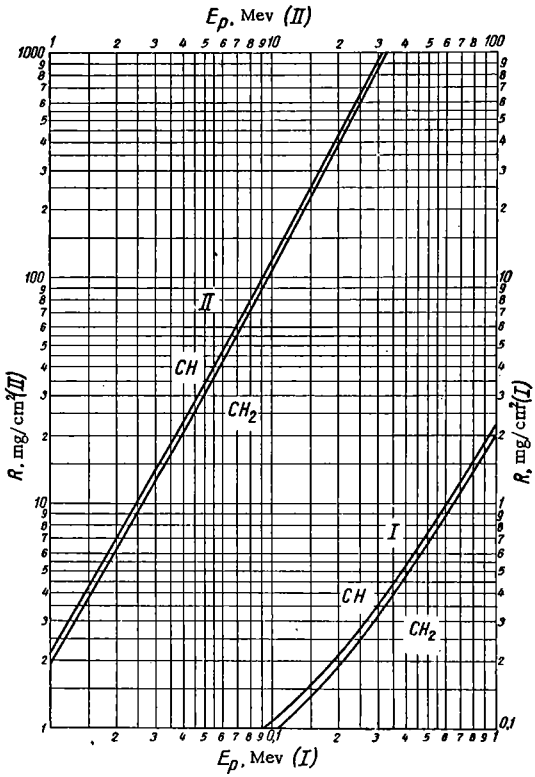

Fig. 5. Range-energy curves for protons in polystyrol (CH) and polyethylene (CH_2).

In Fig. 6 is shown the function $\eta(E)$ for $\delta_{12} = 10\%$ (corresponding to $\beta \approx 18°$) and a polyethylene radiator ($n = 8.57 \cdot 10^{19}$ mg^{-1}), computed from Eq. (34). For the actual ranges the efficiency is considerably lower since it is impossible to satisfy the optimum conditions over a wide energy region. Furthermore, for a given resolving power the efficiency of an actual telescope falls off much more rapidly in the low-energy region than is shown in Fig. 6 and the limiting resolving power deteriorates at lower energies. These effects depend on the method of determining the energy of the recoil protons and on the design features of the individual telescope.

In the intermediate region of the energy range being considered (0.3 - 30 Mev), for a given resolving power the maximum efficiency of a telescope is approximately proportional to the neutron energy. Substituting Eq. (28)

in Eq. (34) and assuming that the cross section for n, p scattering falls off approximately as $E^{-1/2}$ with increasing energy, (27), we have

$$\eta \sim E\delta_{12}^3.$$

The relation in (34) affords the possibility of finding a compromise between efficiency and resolving power. It does not take into account the width associated with the method of measuring the energy of the recoil protons and thus is applicable only for rather large values of δ_{12} (for good telescopes with $\delta_{12} > 5\%$). The expression which has been obtained makes it possible to choose the optimum value for the collimation angle β.

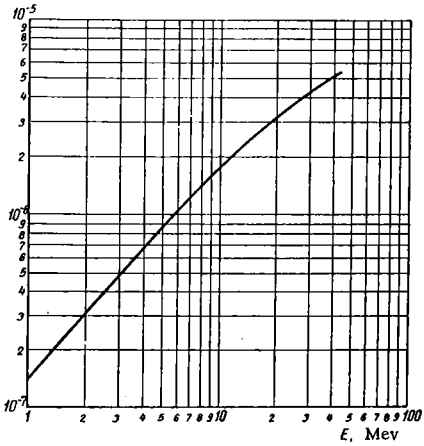

Fig. 6. The maximum efficiency of a telescope with a thin polyethylene radiator and a resolving power of 10%.

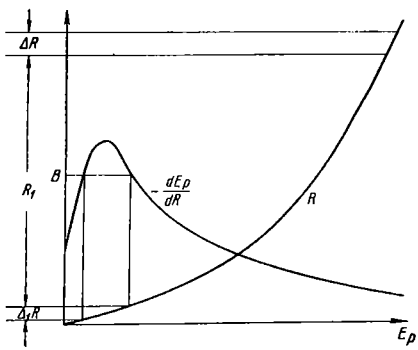

Fig. 7. Construction used in determining the resolving power of a telescope based on the measurement of recoil-proton range: ΔR) radiator thickness; R_1) effective thickness of the layer of material between the radiator and the last counter of the telescope; $\Delta_1 R$) effective thickness of the last counter; B) threshold of the last counter.

In particular, it is not immediately obvious that a small loss in resolving power leads to a significant increase in efficiency. Hence, in making absolute measurements of a flux of monoenergetic neutrons it is usually desirable to use a "wide-angle" telescope with relatively low resolving power. In this case Eq. (33) cannot be used for computing the efficiency since it applies only to small angles, the more so since it is precisely in this case that the efficiency of the telescope must be known with maximum accuracy. An exact calculation of the efficiency of a wide-angle telescope for the general case ($b_1 \neq b_2$ and different diameters for the radiator and aperture) has been carried out by Bame et al. [10]; this work contains detailed tables of the geometric efficiency factor for many values of the telescope parameters for neutron energies between 4 and 30 Mev.

Two methods of determining the energy of the recoil protons are generally used at neutron energies between 1 and 30 Mev in telescopes with thin radiators. One method consists of measuring the range of the proton in a filter located between the telescope counters or in the gas which fills the counters. The other method consists of measuring the pulse amplitudes in a scintillation counter; the protons come to rest in the scintillator, which is at the end of the telescope.

Telescopes which make use of range measurements have been widely used [1-4, 11, 12]. Most frequently, the protons are brought to rest in aluminum, the range-energy curve of which is well-known [13, 14]. The range of the recoil protons is determined by several proportional counters, which are connected in coincidence, and a system of stopping filters. The end of the range is determined to within the effective thickness of the counter located behind the filters. In order to exclude protons which have not been brought to rest in the counter, usually there is an additional counter (behind the last counter) which is connected in anticoincidence with the remaining counters. Frequently, in recording the termination of the proton path in a given counter use is made of the fact that the specific ionization caused by the proton is a maximum at the end of the range. The thresholds of the

detection circuits are set in such a way as to record only protons whose ranges are terminated in the last counter of the coincidence group [4, 15]. In Fig. 7 are curves showing the dependence of ionization loss and range on energy. The ionization loss curve exhibits a rather sharp maximum at the low proton energy. It is apparent that a change in the threshold of the detection circuit corresponds to a change in the residual path (after stopping in the filters) of the recoil protons recorded by the circuit. Thus, the effective thickness of the last coincidence counter is determined by the level of the pulse discriminator setting in a given case.

The partial width due to the finite effective thickness of the counter $\Delta_1 R$ which determines the end of the range is given by the expression

$$\delta_3 = {}^2/_3 \frac{\Delta_1 R}{R}.$$

The same expression can be used to determine the limiting resolving power of a telescope based on measurements of ranges if by $\Delta_1 R$ we understand the minimum effective thickness of the counter for which recoil protons can still be detected.

In good telescopes the limiting resolving power is 3-5%. Among other things, this means that the statistical spread in the proton ranges (straggling) has essentially no effect on the resolving power of the telescope [16].

The procedure for measuring a neutron spectrum from recoil-proton range consists of establishing a definite thickness of aluminum filter and measuring the number of protons which come to rest in the counter behind the filter. Then the thickness of the filter is changed and the measurement is repeated. At each point only those recoil protons are recorded whose energy lies within a narrow range. Thus, a range-measuring telescope is essentially a single-channel neutron spectrometer.

The effective width of a channel of the telescope ΔE is determined by the effective thickness of the detection system $\Delta_1 R$. An an approximation we may write

$$\Delta E = E\delta_3 = {}^2/_3 \; E \frac{\Delta_1 R}{R}.$$

The effective width of a channel for a given neutron energy may be determined experimentally from the shape of the line obtained in recording monoenergetic neutrons. A knowledge of this quantity is necessary for absolute measurements of complicated neutron spectra.

The time required for measuring a neutron spectrum for a given neutron-flux intensity depends not only on the telescope efficiency (32), but also on the effective channel width ΔE. The counting rate (the number of counts per second) for detecting neutrons with energy E is given by the expression:

$$P(E) = \eta(E) \cdot F(E) \Delta E,$$

where $F(E)\,dE$ is the number of neutrons with energies between E and $E + \Delta E$ emitted by the source per steradian per second. Whence, we have

$$P(E) \cong {}^2/_3 \eta(E) \, F(E) \, E \frac{\Delta_1 R}{R}.$$

Thus, in order to choose the optimum conditions for investigating a given portion of a spectrum it is necessary to be able to change the effective thickness of the detection system $\Delta_1 R$. For this purpose, a supplementary stopping filter is frequently placed in front of the anticoincidence counter which excludes long-range protons and the threshold of the last coincidence counter is varied in recording the end of the track by means of maximum specific ionization.

We now make an estimate of the maximum counting rate for a given resolving power. For simplicity we shall assume that the partial widths combine quadratically. It may be assumed that the optimum conditions for operation obtain when these widths are equal. Thus,

$$\delta_1 = \delta_2 = \delta_3 = \frac{1}{\sqrt{3}} \delta,$$

where δ is the resolving power of the telescope. Under these assumptions, taking $b_1 = b_2$, we find that the maximum counting rate for neutrons with mean energy E is

$$P(E) \cong \frac{\pi}{96} n\sigma RF(E) E\delta^4.$$

The relation which has been obtained makes it possible, in certain cases, to find compromise values between the counting rate and resolving power of the telescope for studying a given portion of the spectrum. However, it is frequently found that the allowable counting rate is lower than the maximum capacity. A measurement of the fast-neutron spectrum is usually carried out against a background of much greater intensity due to low-energy neutrons and γ-rays. These produce such large overloading of the telescope counters that the intensity of the neutron flux is generally purposely reduced in order to reduce the number of accidental coincidences. It is this factor which turns out to be one of the main practical limitations on neutron spectrometers of this type.

The high background of random coincidences is explained by the poor resolving time (10^{-6} sec) of a coincidence circuit which operates from proportional counters. The use of gas scintillation counters in telescopes (see page 75) in place of proportional counters should make it possible to reduce the resolving time of the coincidence circuit to 10^{-9} sec and thus to increase significantly the counter load which can be accomodated.

We may note that in measuring a fast-neutron spectrum by means of a single-channel device, the source of which usually is the target of an accelerator, it is necessary to operate at fairly high counting rates. It is not feasible to improve the statistical accuracy by simply increasing the exposure time at each point. This procedure increases the time required for investigating a spectrum and does not necessarily lead to results which are more reliable because of possible accelerator instabilities. A change in beam current or a redistribution of the current division between the target and a different type of aperture can lead to a considerable change in the loading of the telescope counters by background neutrons and γ-rays, thus making it difficult to take account of the accidental coincidences.

The need for continuous adjustment of the thickness of the stopping filter in measurements of neutron spectra by a telescope of this type means that the system used for changing stopping filters becomes extremely important. Because the telescope is exposed to an intense neutron flux while the measurements are being carried out, the filters must be changed by remote control. Thus, an important element in a telescope of this type is the mechanical system used for interchanging filters.

In Fig. 8 is shown a longitudinal section, and in Figs. 9 and 10 a general view, of a telescope described by Kondrashev et al. [12]. The telescope consists of four proportional counters with the first, second, and third, starting from the radiator, connected in coincidence, and the fourth connected in anticoincidence. In front of the third counter is located the main aluminum filter which serves for measurement of the recoil proton range. In addition, in front of the fourth counter there is a supplementary filter which is used to change the effective thickness of the detection system.

The interchangeable radiators and filters are located in apertures in discs; by rotating these discs, it is possible to obtain the desired radiator-filter combination. The entire system, consisting of the counters and discs, is located in a dural vacuum chamber which is sealed by rubber gaskets. Each disc is furnished with a remotely controlled mechanical rotation arrangement. The drive mechanisms and the indicator systems which indicate the disc positions are located outside the vacuum chamber. Sylphon bellows are used to transmit the rotation to the discs.

The first two counters of the telescope have a common cathode, which is in the form of a hollow cylinder. A tungsten wire, 90 μ in diameter, which is stretched along the axis is separated into two parts by a glass bead. The third and fourth counters are plane counters. The cathodes of these counters are "transparent" and are made from aluminum foil approximately 2 μ thick. The anodes are grids of tungsten wire 90 μ in diameter. The operating gas for these counters is a mixture of argon and carbon dioxide (approximately 3%) which is maintained at a pressure of 100 mm Hg. This mixture fills the entire free volume of the chamber.

In slowing-down, the protons experience multiple scattering. The mean-square scattering angle is determined basically by the fraction of the energy lost in passing through the layer of material. Thus, in slowing down in aluminum from 10 to 0.5 Mev, i.e., to 5% of the initial energy, the mean-square scattering angle of the proton

is approximately 10° [17]. After being deflected through such a large angle a proton may not strike the sensitive volume of the series of telescope counters, even if it has the required energy. This is the reason for the frequent appearance of the low-energy "tail" side which is observed in the spectrum of a monoenergetic neutron beam.

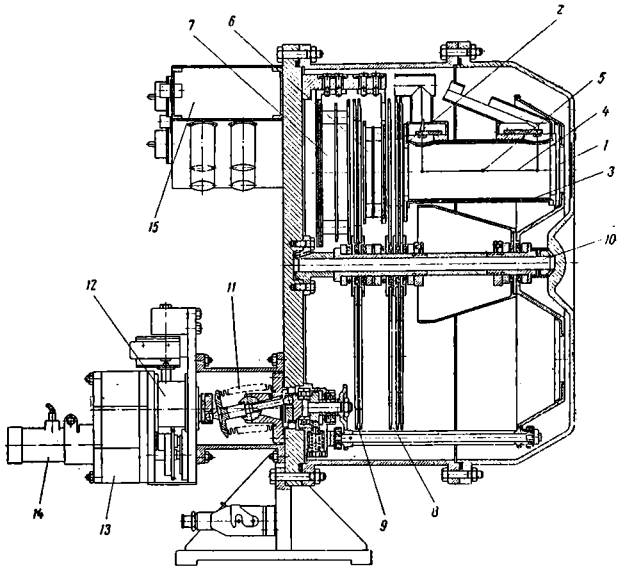

Fig. 8. Longitudinal section through a range measuring telescope [12]: 1) interchangeable radiator; 2) aperture; 3) common cathode for the first and second counters; 4) tungsten wire; 5) separation bead; 6) third proportional counter; 7) fourth proportional counter; 8) discs which carry the main assembly of aluminum filters; 9) discs which carry the supplementary assembly of filters; 10) axis of rotation of the discs; 11) sylphon bellows; 12) disc-position indicator system; 13) reducer; 14) motor; 15) preamplifiers.

To eliminate effects due to multiple scattering, usually the transverse dimensions of the counters behind the main stopping filter are increased according to their distance from this filter. In order to avoid a sharp increase in dimensions, in the telescope designed by Kondrashev et al. a minimum number of counters is used beyond the main stopping filter assembly; there are two counters: one connected in coincidence with the first counters and the second connected in anticoincidence. For the same reason plane counters has been used. An estimate made on the basis of the curve given by Dickenson and Dodder [17] shows that with this geometry (Fig. 8) less than 5% of the recoil protons are lost because of multiple scattering. The aperture which defines the solid angle inside of which the recoil protons are detected by the telescope is placed in front of the main stopping filter. Because of this arrangement multiple scattering does not introduce any errors in the determination of the solid angle.

In Fig. 11 is shown an electronic block diagram of the telescope. This system makes it possible to record simultaneously coincidences of the following types: $1+2+3$, $1+2+3+4$, and $1+2+3-4$ (the figures indicate the number of the counter and the minus sign corresponds to anticoincidence). The detection of $1+2+3-4$ coincidences gives the differential recoil-proton spectrum and, ultimately, the neutron spectrum. Simultaneous recording of the other types of coincidences is desirable for monitoring the operation of the circuit. Accidental $1+2+3$ coincidences are recorded in the anticoincidence channel $(1+2+3-4)$. It is this effect

which determines the permissible loading of the counters and, in the final analysis, the time required to carry out an experiment.

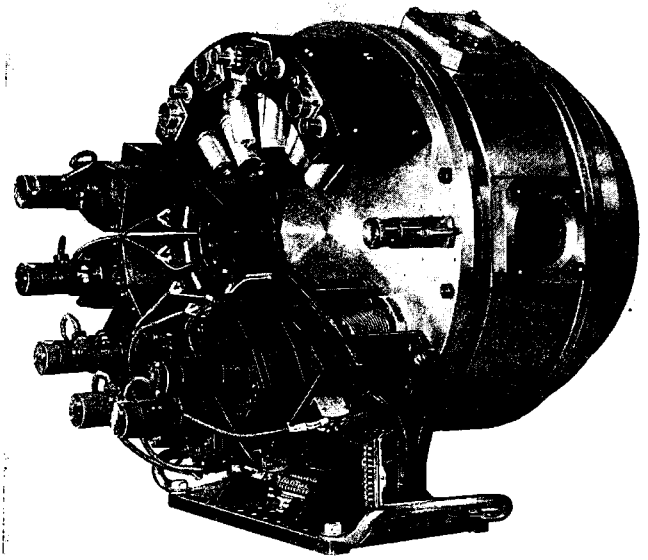

Fig. 9. External view of the telescope [12] from the motor side. The preamplifiers and two viewing windows are shown.

The main contribution to the number of 1 + 2 coincidences is due to neutrons with energy considerably less than the energy of the neutrons being studied. The flux of these neutrons is usually very large and the number of double coincidences of the 1 + 2 type is many times greater than the number of 2 + 3 and 1 + 3 coincidences so that this type of coincidence basically determines the number of accidental triple 1 + 2 + 3 coincidences. In order to measure the number of accidental coincidences use is made of a supplementary circuit which records 1 + 2 + 3 coincidences with a delay pulse (10 μsec) in a third counter (resolving time 1 μsec).

The spectrometer being described here has been used to study the excitation curve for the T (p, n) He^3 reaction in the proton energy region between 7 and 12 Mev [18]. A tritium-zirconium target on a tungsten base was bombarded by a proton beam from a cyclotron. The proton energy was varied by stopping in a platinum foil. The neutrons were produced not only by the T (p, n) He^3 reaction, but also by virtue of reactions in the platinum, zirconium and tungsten and in the lead used in several apertures which were used to define the proton beam. Two measurements were made to evaluate the neutron background; these were made with the tritium-zirconium target and with a zirconium target without tritium, which we may call the "flag". The telescope was found to give reliable isolation of neutrons corresponding to the T (p, n) He^3 reaction. The effect due to the flag was several times smaller than the effect due to the target.

In Fig. 12, is shown a neutron spectrum for the T (p, n) He^3 reaction for neutrons emitted at an angle of 0° with a proton energy of 11.6 Mev. The width of the line at half-height is 1.7 Mev or 16%. It is determined basically by the thicknesses of the polyethylene radiator (26 mg/cm^2) and the aluminum filter (22 mg/cm^2) between the third and fourth counters. The efficiency of the spectrometer is $\eta = 2.4 \cdot 10^{-5}$.

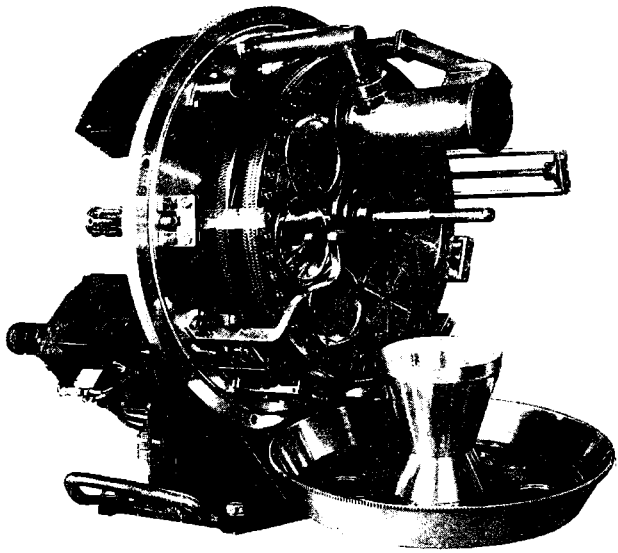

Fig. 10. View of the telescope with the vacuum cover removed. The disc which carries the interchangeable radiators is removed. The common cathode for the first and second counters is visible.

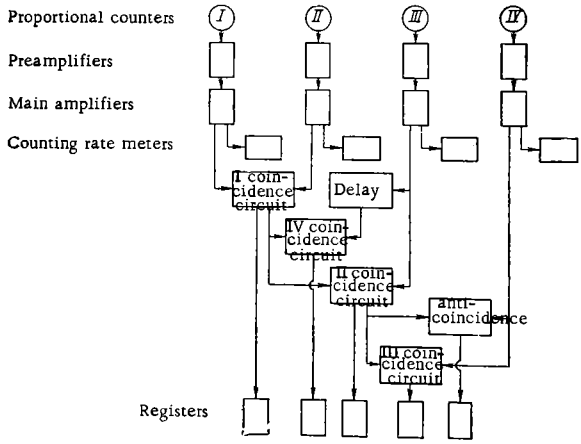

Fig. 11. Electronic block diagram of a telescope which measures range of recoil protons [12].

A considerably simpler system is a telescope in which one measures the proton range in the gas which fills the counter volume. A telescope of this kind has been described by Holt and Litherland [3] (Fig. 13). The recoil protons are detected by three ionization chambers which are located behind the polyethylene radiator.

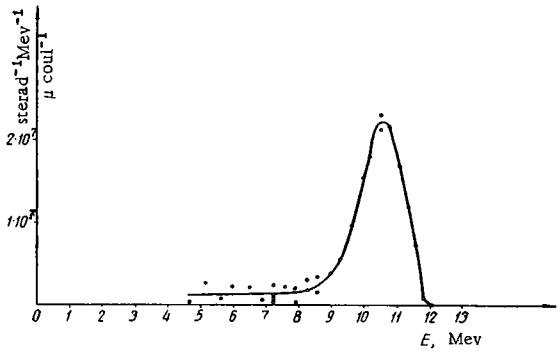

Fig. 12. Neutron spectra observed at an angle of 0° for the T (p, n) He^3 reaction induced by protons with energies of 11.6 Mev [12].

The collimated beam of recoil protons passes through two ionization chambers connected in coincidence. The pulse from the coincidence circuit triggers the sweep of an oscilloscope, which records the pulse from the third chamber in which the recoil proton finally comes to rest. The pulse from the recoil proton which comes to rest is very sharply distinguished from the spurious pulses and the background pulses; its leading edge is shifted with respect to the beginning of the sweep by the time required for electrons to drift from the point at which the proton comes to rest to the collector electrode. Thus, by determining the position of the pulse front with respect to the beginning of the sweep, it is possible to measure the residual range of the recoil proton in the last chamber. As far as resolving power is concerned, this method is no better than the emulsion method; on the other hand the difficulties are much less formidable. However, it is difficult to make an absolute determination of the energy scale because of the uncertainty in the drift velocity of the electrons. Technical difficulties in realizing a telescope of this kind are due mainly to the need of maintaining a high gas pressure in a large volume.

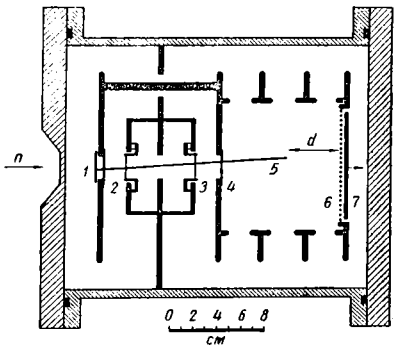

Fig. 13. Diagram of the telescope used by Holt and Litherland [3]. 1) Thin polyethylene radiator; 2 and 3) ionization chambers; 4) aperture; 5) path of the recoil proton; 6) grid; 7) collection electrode of the third ionization chamber; d) distance between the end of the path and the grid.

The telescope described by Holt and Litherland has been used by them for studying stripping reactions at deuteron energies up to 10 Mev. In Fig. 14 is shown a neutron spectrum for neutrons formed in the Al^{27} (d, n) Si^{28} reaction. The large peak at 15.5 Mev has a width of approximately 700 kev or 5% at half-height. The thickness of the target is 4 mg/cm^2 and the thickness of the radiator is 10 mg/cm^2.

Other neutron spectrometers in which the range of recoil protons is measured differ from those being considered here only in minor details.

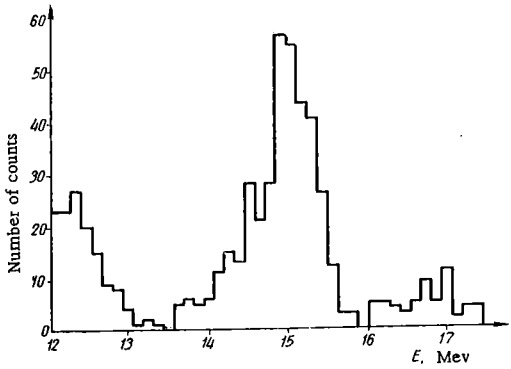

Fig. 14. Neutron spectrum from the Al^{27} (d, n) Si^{28} reaction for deuterons energies of 8.5 Mev [3]. The number of recorded recoil protons is plotted along the ordinate axis. Only the hard part of the spectrum is shown.

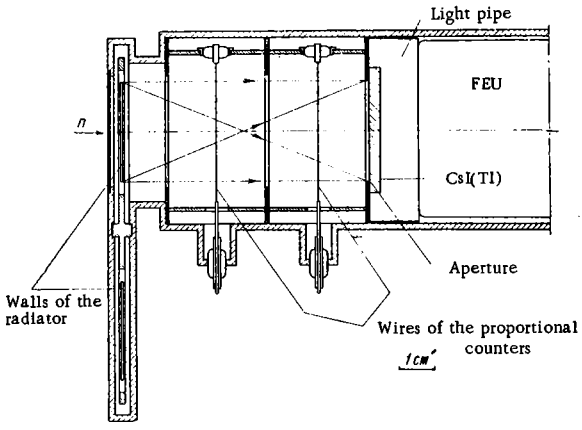

Fig. 15. Diagram of a scintillation counter telescope [10].

In recent years a telescope which has become very popular is based on the measurement of recoil proton energy by means of a scintillation counter [9, 10, 19-22]. The fundamental advantage of a telescope of this kind is the fact that since it is connected to a multichannel pulse height analyzer it is essentially a multichannel neutron spectrometer. The use of a multichannel spectrometer reduces the stability requirements of the neutron source and makes possible a reduction in the measurement time. A typical diagram for a telescope which employs scintillation counters is shown in Fig. 15. The recoil protons from the radiator pass through two proportional counters and are completely stopped in the crystal of the scintillation counter, in front of which there is a

collimating aperture. In the proportional counters the recoil proton loses only a small part of its energy (of the order of 100 kev); thus the differential distribution of pulse amplitudes in the scintillation counter gives the neutron spectrum. An electronic block diagram for a telescope of this kind is shown in Fig. 16.

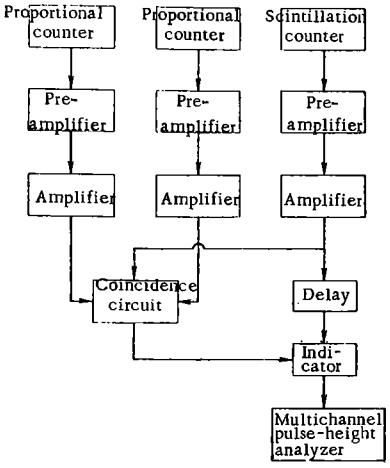

Fig. 16. Electronic block diagram of the scintillation counter telescope.

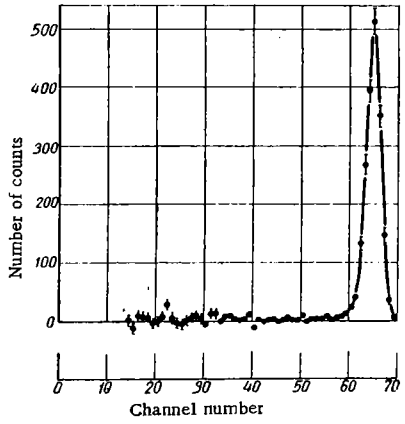

Fig. 17. Neutron spectrum from the T (d, n) He^4 reaction obtained by means of the scintillation counter telescope [9]. The line width at half-height (E = 13.7 Mev) is 5.3%.

The input to the multichannel amplitude analyzer is triggered by a pulse from the triple coincidence circuit. Pulses from the scintillation counter are applied to the analyzer through a delay line (several microseconds) because the time of operation of the proportional counter is rather long.

The limiting resolving power of a telescope of this kind is determined by the amplitude resolving power of the scintillation counter. To obtain good resolution, it is necessary to use crystals with high light output [23] and a so-called "spectrometer" photomultiplier [24] which provides good amplitude resolution. Usually NaI(Tl) crystals are used; however, it is sometimes more convenient to use CsI(Tl) crystals. These are somewhat poorer as regards light yield but are not affected by moisture and are somewhat more convenient in use. In the energy region being considered ($E_p > 0.3$ Mev), both these and other crystals exhibit a linear dependence of light yield on proton energy [25, 26]. The crystals are usually used in the form of a thin slab (Fig. 15) which is connected to the photomultiplier by means of a plexiglas light pipe. For example, in the telescope described by Johnson and Trail [9], designed for neutron energies up to 20 Mev, the NaI(Tl) crystal was 2.5 mm thick. To obtain good resolution the light pipe must provide uniform illumination over all points of the crystal. In practice, with proton energies of several million electron volts it is possible to obtain a resolving power of several percent [9].

In Fig. 17 is shown a neutron spectrum for the T (d, n) He^4 reaction [9] obtained by means of a telescope with a scintillation counter and a multichannel pulse height analyzer. The width of the line (E = 13.7 Mev) at half-height is 5.3%. The partial widths are as follows: radiator thickness $\delta_1 = 4\%$; collimation angle $\delta_2 = 1.5\%$; resolution of the scintillation counter $\delta_3 = 4\%$; channel width of the amplitude analyzer $\delta_4 = 1.5\%$; spread in primary neutron energy 1.5%. It is clear that these figures do not represent optimum conditions. An increase of a factor of 2.5 in δ_2 would have almost no deteriorating effect on the resolving power of the spectrometer but would increase the efficiency by a factor of $(2.5)^2 \approx 6$.

A shortcoming of a scintillation-counter telescope is the high sensitivity to γ-ray backgrounds.

Because a thin-radiator telescope is one of the most precise devices for absolute measurements of neutron flux, in concluding the present section we consider some of the procedures and corrections which must be made to obtain accurate results.

1. The noticeable background, especially in the part of the spectrum corresponding to low neutron energies, is due to particles which are produced by neutrons and γ-rays in the walls and in the gas of the proportional counters and in other internal elements of the telescope. It can be eliminated to a considerable degree by making measurements under the same conditions with the radiator removed.

2. The background due to the accelerator may be taken into account by making measurements with an empty target (p. 17).

3. Particles formed by virtue of the interaction of neutrons with carbon in the radiator (at neutron energies greater than 12 Mev) can be excluded by measuring the spectrum with a carbon radiator.

4. The effects due to neutrons scattered on elements which surround the telescope and on the walls of the room can be estimated by enclosing the direct neutron beam with absorbing cover. This effect is usually negligibly small since neutrons scattered at points lying beyond the plane of the radiator are not recorded by the telescope.

5. In working with intense neutron fluxes large errors can arise as a result of detection of accidental coincidences and as a result of errors due to the dead time of the detection system. Both of these effects can be corrected for from a study of the dependence of the results on source intensity and on the distance between the source and the radiator.

6. A considerable fraction of the neutrons (up to 10%) may be absorbed in the material between the source and the radiator. Along the neutron path there is usually the substrate of the accelerated target, the wall of the vacuum chamber which contains the target, and the front wall of the telescope. Corrections for this effect can be computed with rather good accuracy on the basis of the well-known total neutron cross sections for various materials (27) since under conditions of good geometry it is sufficient to take account only of the ejection of neutrons from the beam and scattering in the beam can be neglected.

In order to make precise, absolute measurements of complicated spectra, it is frequently necessary to investigate the energy dependence of the line shape experimentally. This can be done by means of monoenergetic neutrons using reactions such as

$$T(p,n)He^3, \quad D(d,n)He^3 \quad \text{and} \quad T(d,n)He^4$$

§ 2. Thick-Radiator Telescope

The sensitive volume of the first counter of the telescope can be used as a recoil-proton source if the operating material of the counter contains hydrogen. In order to determine the proton energy by the intensity of ionization or the scintillator flash, the thickness of this "radiator" must constitute a significant fraction of the proton range, since it is the energy lost in the radiator which is measured. Because of this fact, it is possible to increase the telescope efficiency and also, in certain cases, to reduce the lower energy limit at which the telescope can be used (to several tens of kilo electron volts).

We now consider several typical versions of ionization and scintillation telescopes with thick radiators.

In Fig. 18, is shown an ionization telescope [28], designed for operation in the neutron energy region between 0.05 and 1 Mev. This instrument consists of three proportional counters filled with methane to a pressure of 8-140 mm Hg, depending on the energy of the neutrons being investigated. The recoil protons formed in the gas of the first counter are collimated by nozzles. The first two counters are connected in coincidence and the third is connected in anticoincidence with the first two. Thus, only those recoil protons are recorded which are formed in a narrow solid angle and which terminate their paths in the second counter. In order to measure the proton energy the pulses from the two first counters are combined and applied to a multichannel pulse height analyzer.

The width of the line observed when detecting monoenergetic neutrons is determined by the collimation angle of the recoil protons and the resolving power of the proportional counters which are connected in the pulse combination circuit. In order to obtain good resolving power it is necessary to make the gas amplification factors of both counters precisely equal; however, this can be achieved only with great difficulty. In Fig. 19 are shown the calculated and experimental shapes of the telescope lines corresponding to a neutron energy of 0.8 Mev. The experimental width of the line is 9%.

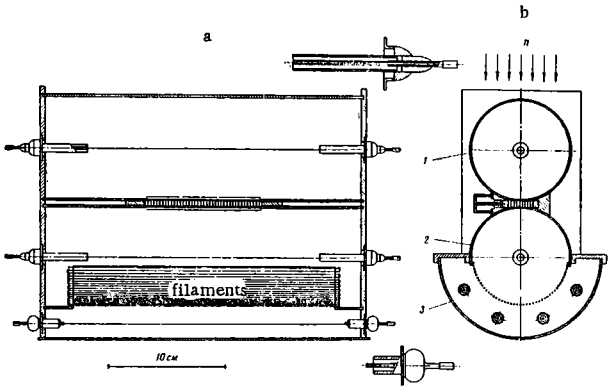

Fig. 18. Ionization telescope [28] which combines the amplitudes of the pulses from two counters. a) Longitudinal section; b) transverse section; 1) and 2) proportional counters connected in coincidence; 3) multiwire anticoincidence counter.

The dynamic range of the telescope is limited by the condition for maximum recoil proton range $d < R_0 < 2D$, where D is the diameter of the first counter and the second counter and $\underline{d}$ is the length of the nozzle. In the present case [28], for example, at a pressure of 140 mm Hg for the operating gas in the counters, it is possible to study the neutron energy region between 0.3 and 1.2 Mev. The effective thickness of the "radiator" of such a telescope is R_0, if $d \ll R_0 < D$. Under these conditions the efficiency of the telescope is given approximately by the relation

$$\varepsilon = 3{,}4 \cdot 10^{-6} \cdot \varkappa \cdot \frac{s}{d^2} \sigma R_0$$

where κ is the transmission coefficient of the nozzle; $\underline{s}$ is the area of the aperture in the nozzle; $\underline{d}$ is the length of the nozzle; R_0 is given in cm and σ in barns.

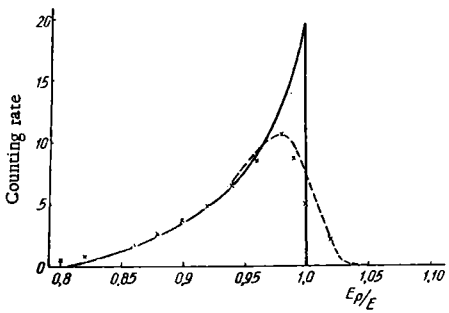

Fig. 19. Line shape for the ionization telescope with a thick radiator [28] for neutrons with energies of 0.8 Mev. Solid curve is the computed curve and the dashed curve is the experimental curve.

If, in operation with a point neutron source the angle subtended by the working volume of the telescope at the source is equal to the collimation angle (s/d^2), the telescope efficiency, normalized to the neutron flux per unit solid angle, is

$$\eta = 3{,}4 \cdot 10^{-5} \varkappa \left(\frac{s}{d^2}\right)^2 \sigma R_0.$$

The telescope being considered is characterized by the following parameters:

$$s = 4 \text{ mm}^2; \quad d = 4.6 \text{ mm}; \quad \varkappa = 0.72.$$

A similar neutron spectrometer for the energy range between 2 and 18 Mev was built earlier by Mozley and Shoemaker [29] who used scintillation counters (Fig. 20). The telescope consists of two scintillation counters with organic scintillators (anthracene crystals). The first is a thick radiator while the second separates recoil protons emitted from the first at a small angle with respect to the neutron flux. Between the scintillators there is a proportional counter which measures the specific ionization, distinguishing between recoil protons and electrons produced by γ-rays. All three counters are connected in coincidence.

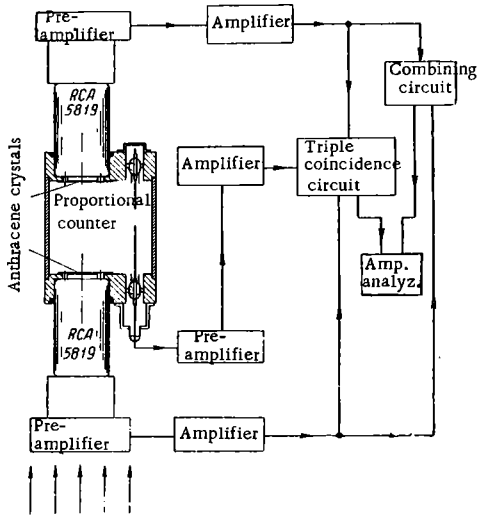

Fig. 20. Scintillation telescope in which pulse amplitudes from two counters are combined [29]. a) Preamplifier; b) amplifier; c) proportional counter; d) anthracene crystals; e) combining circuit; f) amplitude analyzer; g) triple coincidence circuit.

Pulses from the scintillation counters are combined and applied to a multichannel pulse height analyzer, the input of which is opened by the coincidence circuit. If the scintillation counters are identical the amplitude of the total pulse is determined by the energy of the recoil proton and is not affected by the way in which this energy is distributed between the two scintillators. Slowing-down of the protons in the gas in the proportional counter can be neglected. In order to determine the energy of the recoil protons from the amplitude of the pulses it is necessary to take account of the nonlinear dependence of the light yield in anthracene on proton energy.

The resolving power of a scintillation telescope of this type is considerably poorer than that of an ionization telescope because of the poor amplitude resolution of a scintillation counter with an organic scintillator. For example, in recording monoenergetic neutrons with an energy of approximately 15 Mev the telescope considered here yields a line width of 20% [29], in which the partial width due to the energy spread in the primary neutrons and the collimation angle of the recoil protons is 7%.

As in the preceding case, the effective thickness of the "radiator" of the telescope for neutrons of a given energy is equal to the range of the recoil protons. Hence, the efficiency of the telescope is approximately proportional to neutron energy. In the present case

$$\epsilon = 2 \cdot 10^{-5} \text{ for } E = 2 \text{ Mev} \qquad \text{and} \qquad \epsilon = 2 \cdot 10^{-4} \text{ for } E = 20 \text{ Mev.}$$

An improved scintillation telescope of this type has been described by Calvert et al. [30]. In this instrument the amplitude analysis of the pulses from the scintillation counters is carried out without preliminary combination. The pulse from the first counter, in the scintillator of which the recoil protons are formed, is applied to the vertical sweep of an oscilloscope while the pulse from the second scintillation counter is applied to the horizontal sweep. The beam in the oscilloscope is gated by the pulse from the proportional counter which is located between the scintillation counters. Each recoil proton formed in the scintillator of the first counter which strikes the scintillator of the second counter corresponds to a spot on the screen of the oscilloscope. The position of the spot uniquely determines the energy of the recoil proton. It is apparent that the spots from a monochromatic neutron flux will lie on one smooth curve (Fig. 21). If we plot on the screen of the oscilloscope a series of lines corresponding to definite energy values, the analysis of the neutron spectrum means essentially counting the number of spots on portions of the screen enclosed between neighboring lines. This method of analysis does not require the identification of the scintillation counters. Furthermore, with this method, an inorganic crystal (with a high light yield) can be used as the scintillator in the second counter, thus making possible a considerable increase in the resolving power of the telescope.

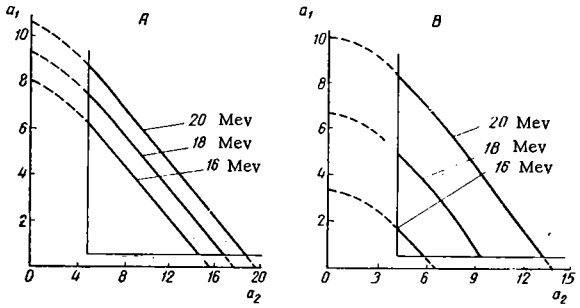

Fig. 21. Lines of equal energy on the screen of the oscilloscope used for analysis of pulses from the scintillation telescope [30]: A) without filters; B) with filters between the scintillators (300 mg/cm^2 of aluminum). The heavy lines show the operating region isolated by the discriminators; a_1 and a_2 are the amplitudes of the pulses from the first and second counters.

If necessary, the resolving power of this telescope can be improved over the resolving power of its scintillation counters by introducing stopping filters between the scintillators. Under these conditions, the resolving power is improved, since only part of the proton energy is lost in the crystals and the statistical spread in the amplitudes of the pulses in the scintillation counters is reduced in absolute magnitude. Obviously, this improvement in the resolving power of the telescope is achieved at the expense of a reduction in effective thickness of the radiator.

The scintillator in the second counter in the telescope described by Calvert et al. is an NaI(Tl) crystal. In the neutron energy region between 4 and 20 Mev, the resolving power of the spectrometer is 5-7%. The efficiency ϵ for detecting neutrons with energies of 20 Mev is $6 \cdot 10^{-5}$. The telescope has been used for studying stripping reactions (d, n) in light nuclei. In Fig. 22 is shown a neutron spectrum for the F^{19}(d, n) Ne^{20} reaction obtained with a deuteron energy of 9.06 Mev.

Another type of system has been proposed for fast-neutron spectroscopy [31-36]: this system is analogous to the two-crystal γ-spectrometer which uses the Compton effect. The practical application of this system has not been realized but a prototype of the spectrometer, which measures the neutron energy by the time-of-flight between two counters has appeared.

A schematic diagram of this spectrometer is shown in Fig. 23. Two counters with organic scintillators are located at a considerable distance from the neutron source and from each other and are connected in coincidence. A neutron scattered on hydrogen in the scintillator of the first counter may be detected by the second if the scattering angle is close to the chosen angle θ_0. A pulse-height analyzer which is controlled by the coincidence

circuit is used to measure the pulse spectrum of the first counter. It corresponds to the spectrum for the recoil protons which are emitted at an angle $\varphi_0 = \frac{\pi}{2} - \theta_0$ (20) with respect to the primary neutrons.

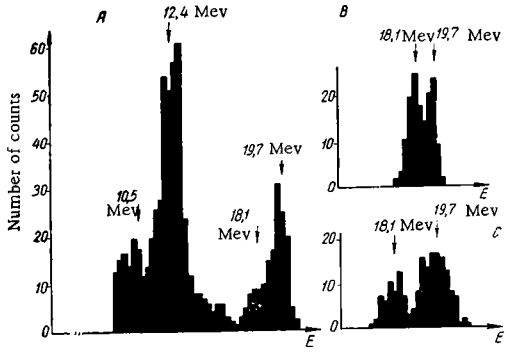

Fig. 22. Spectrum of neutrons from the F^{19} (d, n) Ne^{20} reaction at a deuteron energy of 9.06 Mev obtained with the scintillation telescope [30]. A) Neutron spectrum at an angle of 0°; B) neutron spectrum at an angle of 15°; C) the same spectrum obtained with a filter between the scintillators (260 mg/cm^2 of aluminum).

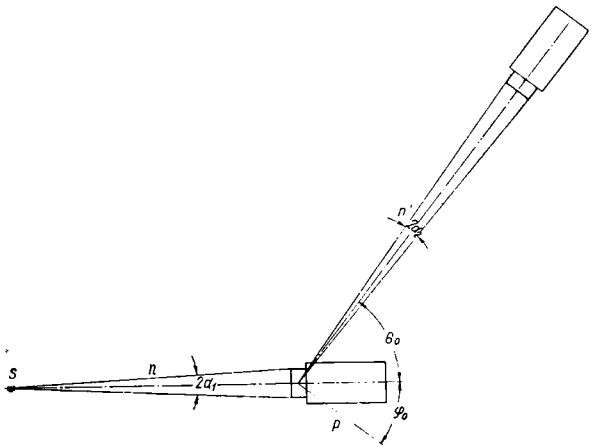

Fig. 23. Schematic diagram of the scintillation spectrometer which uses neutron scattering from one counter to another.

In order to reduce the background the resolving power of the coincidence circuit is made small enough so that it is possible to distinguish neutrons from γ-rays by time-of-flight, but large enough to encompass a reasonable neutron energy range (usually approximately 10^{-8} sec). The pulse from the first counter is delayed before being applied to the coincidence circuit by a time equal to the time-of-flight of neutrons of the energy being investigated.

The resolving power of the spectrometer is determined chiefly by the spread in the scattering angle of the detected neutrons and the amplitude resolving power of the first counter. The partial line width of the spectrometer due to the finite collimation angle of the recoil protons is given approximately by [see Eq. (19) and Fig. 23]

$$\delta_1 = 2 \operatorname{ctg} \theta_0 \Delta\theta = 2 (\alpha_1 + \alpha_2) \operatorname{ctg} \theta_0. \tag{35}$$

Because of the nonlinear light yield of the organic crystals the resolving power of the spectrometer is found to be smaller than the line width observed in the amplitude distribution of pulses from the first counter. For example, in the work of Chagnon et al. [35], with neutron energies of 4 Mev the line width was 17%, corresponding to a resolving power $\sigma = 10\%$.

If the thickness of the first scintillator is small, when it is possible to neglect the effect of multiple scattering the efficiency of the spectrometer for neutrons of a given energy is proportional to the product of the solid angles and the counter efficiencies,

$$\eta = \omega_1 \omega_2 \varepsilon_1 \varepsilon_2, \tag{36}$$

where the counter efficiencies are determined by the formulas

$$\varepsilon_1 = n\sigma(E) h_1 \frac{\cos \theta_0}{\pi},$$

where n is the number of hydrogen atoms in 1 cm^3 of scintillator; $\sigma(E)$ is the scattering cross section for a neutron with energy E on a proton; h_1 is the thickness of the first scintillator; $\frac{\cos \theta_0}{\pi}$ is the probability for scattering of a neutron at an angle θ_0 refer to unit solid angle (24).

$$\varepsilon_2 = n\sigma(E \cos^2 \theta_0) h_2 \left(1 - \frac{B}{E \cos^2 \theta_0}\right),$$

where $E \cos^2 \theta_0$ is the energy of a scattered neutron (19); h_2 is the thickness of the second scintillator; B is the energy threshold of the second counter (see p. 60) which is determined in the present case by the sensitivity of the coincidence circuit.

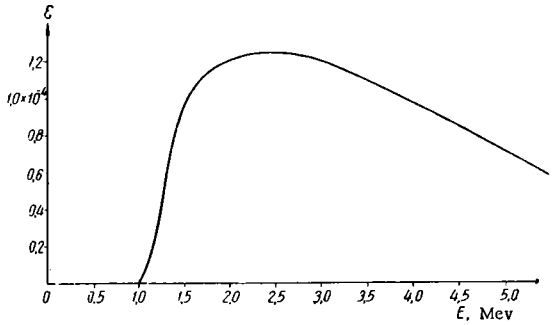

Fig. 24. Efficiency of the scintillation spectrometer which uses neutron scattering from counter to counter.

For the spectrometer whose circuit is shown in Fig. 23, we have

$$\eta = \pi a_1^2 \alpha_2^2 n^2 \sigma(E) \sigma(E \cos^2 \theta_0) h_1 h_2 \cos \theta_0 \left(1 - \frac{B}{E \cos^2 \theta_0}\right). \tag{37}$$

It is apparent that in place of the single counter shown in Fig. 23, in detecting scattered neutrons it is advantageous to use a system of several counters located in a ring at the same angle θ_0 with respect to the direction of the primary neutrons (or a solid ring of scintillators). Thus, this means the efficiency of the spectrometer can be increased by a factor of 10 or more.

Starting from the relations which have been derived, (35) and (37), it should be possible to determine the optimum value of the angle θ_0. It is easy to see that the determining factor is $\sigma(E \cos^2\theta_0)$ in the expression for the efficiency (37), which requires large scattering angles since σ increases sharply with decreasing neutron energy. However, at large angles the amplitude of the pulses in the second counter is very small. A practical operating region lies between 30 and 60°.

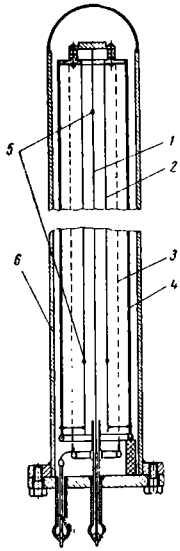

Fig. 25. Ionization telescope used by Benenson and Shurman [38]. 1) Central wire; 2) wire of the "transparent" cathode of the central counter; 3) wires of the anticoincidence counters; 4) external cathode of the anticoincidence counters; 5) beads which isolate the volume of the end anticoincidence counters; 6) vacuum jacket.

In Fig. 24, is shown the function $\epsilon(E)$ for a telescope of the type considered here [35]. The scattered neutrons are detected by a system of 10 counters (stilbene crystals) located at an angle of $\theta_0 = 45°$. The scintillator of the first counter is also a stilbene crystal which is 2 cm in diameter; this crystal is located at a distance of 30 cm from the neutron source. Consequently, the efficiency of the spectrometer is $\eta(E) = 10^{-3}\ \epsilon(E)$ (2) and for neutrons with energies of 1.5-4 Mev (Fig. 24), equal to the efficiency of a telescope with a thin radiator.

The possibility of using a telescope of this kind in practice is not very good because in studying any part of the neutron spectrum, there is a large number of accidental coincidences due to the background of neutrons of other energies and γ-rays.

An interesting version of a spectrometer has been described by Beghian et al. [31]. The angle θ_0 in this case is 90°. The energy of the recoil protons in the first counter is essentially equal to the energy of the primary neutrons. The scattered neutrons are detected by a counter with a NaI(Tl) crystal from the γ-rays emitted in the capture of neutrons by silver nuclei which surround the scintillator and by the iodine nuclei contained in the crystal itself. The counters are connected in a coincidence circuit with a resolving power of $3 \cdot 10^{-8}$ sec. The delay between pulses from the counters is chosen in such a way that of all the secondary neutrons the time-of-flight is such as to accept only those with energies between 5 and 30 kev.

The spectrometer has a rather poor resolving power (determined by the amplitude resolution of the scintillation counter) and a low efficiency; however, it does have the significant advantage of a directional sensitivity: it records only neutrons which are incident on the first counter at an angle of approximately 90°, with respect to the line which passes through the counters. This spectrometer may find application in studies of extended and anisotropic neutron sources.

The original ionization telescope, in which the thickness of the radiator is several times greater than the range of the recoil proton, was suggested by Giles [37]. In Fig. 25 is shown a section of the telescope designed by Benenson and Shurman [38]. The telescope is a cylindrical proportional counter filled with hydrogen or hydrogenous gas and surrounded by a layer of anticoincidence counters. The anticoincidence counters also have cylindrical ends. All counters have a common gaseous volume and are separated by thin wires which form a "transparent" cathode for the central counter. The axis of the instrument is parallel to the direction of neutron motion. The recoil proton produced in the central counter is detected only in the case in which its range completely lies inside the central counter. If such is not the case the anticoincidence counter operates.

The pulses from the central proportional counter are applied to a multichannel amplitude analyzer which is controlled by the anticoincidence circuit. The shape of the observed amplitude distribution of the pulses is

shown in Fig. 26. In the upper part of the figure, in polar coordinates, is shown the dependence of the recoil-proton range on emission angle which is obtained from Eq. (18) under the assumption given in (28):

$$R = R_0 (\cos^2 \varphi)^{3/2} = R_0 \cos^3 \varphi.$$

The angles φ' and φ'' in Fig. 26 represent two solutions of the equation

$$R_0 \cos^3 \varphi \sin \varphi = 2a,$$

where 2a is the diameter of the transparent cathode of the central counter, and R_0 is the range of the recoil proton emitted at an angle of 0° with respect to the telescope axis.

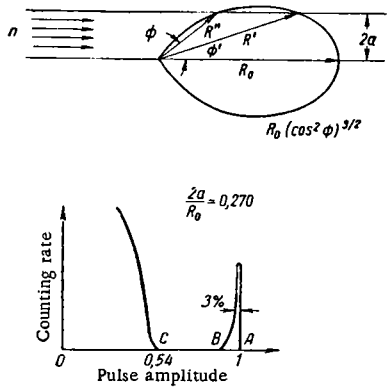

Fig. 26. Line shape obtained with the ionization telescope of Benenson and Shurman [38]. Points A, B, and C correspond to the ranges R_0, R', and R'' (see upper part of figure).

It is apparent from Fig. 26 that the telescope records recoil protons which are emitted in a narrow forward cone as well as the short-range protons corresponding to a very large emission angle. In the bottom part of Fig. 26 is shown the computed amplitude spectrum corresponding to $2a/R_0 = 0.270$. The main peak has a width of 3% but it is composed of a "group" of small pulses with amplitudes ranging from zero to half the amplitude of the maximum pulse. Consequently, the spectrometer has a relatively good resolving power but a rather narrow dynamic range (3): $q < 2$. This deficiency of the telescope is compensated by the fact that the pressure of the gas in the counters can be changed during operation and a wide neutron spectrum can be measured in sections. The investigation of the soft part of the spectrum on the background of neutrons of high energy is completely feasible since the long-range protons are rejected because of the end anticoincidence counters.

In order to obtain good resolving power, in addition to providing a narrow collimation angle it is necessary to provide a narrow threshold for the operation of the anti-coincidence counters which limit the sensitivity of the volume of the main counter. This is one of the basic difficulties in the design of the telescope. Another experimental difficulty is that of obtaining a high resolving power for the central proportional counter.

In Fig. 27 are shown the experimental spectra obtained by irradiating the telescope with monoenergetic neutrons with energies of 5.5 Mev and 6.4 Mev produced in the D (d, n) He^3 reaction. The telescope was filled with propane to a pressure of 1.15 atmos in the first case and 2.10 atmos in the second case. The line widths were 8 and 11%, respectively. In contrast with the calculated amplitude distribution, in the experimental spectra there are many pulses in the intermediate region between the peak and the "tail." The explanation of this is connected chiefly with the incomplete transparency of the cathode of the central counter and corresponds to protons which strike the wires.

A great disadvantage of the telescope is the need for calibrating its energy scale by means of neutrons with known energies since the amplitude of the pulses from the central counter depends on the gas amplification factor.

The efficiency of the telescope for neutrons of a given energy is easily computed. If the leading edge of the sensitive volume of the telescope is at a distance L from a point neutron source and the length of the sensitive volume is $l \ll L$, it may be assumed that the telescope subtends a solid angle $\pi \alpha^2$, where $\alpha = a/L$. We shall assume that the effective solid angle for all recoil protons which arise in the volume of the central counter and remain in it is $\pi \beta^2$, where β is the angle between the telescope axis and the direction of the recoil proton which arises at the axis and terminates its path within the boundary of the volume of the central counter. As can be shown by graphical integration [38], when $2a/R_0 < 0.3$, as is usually the case, this assumption introduces an

error of less than 2%. From Eq. (22), we have $\sigma_\varphi = \frac{\sigma}{\pi}$ and

$$\eta = \pi x_1^2 n_0 (l - R_0),$$

where $(l - R_0)$ is the effective thickness of the "radiator" for neutrons of a given energy. In practice the effective thickness of the radiator is limited by construction considerations but can be made several times greater than the range.

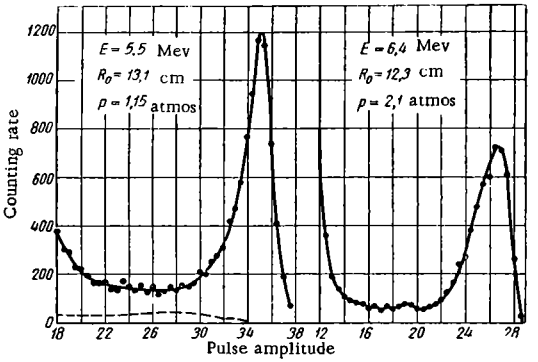

Fig. 27. Experimental line shape of the ionization telescope of Benenson and Shurman for two values of the neutron energy. a) Pulse amplitude; b) counting rate.

The maximum efficiency of the telescope is realized when it is filled with pure hydrogen. However, in order to improve the resolving power of the proportional counter and in order to reduce the range of the protons the telescope is usually filled by methane or propane. On the average the efficiency of the counter is 15-30 times greater than the efficiency of a telescope with a thin radiator and the same resolving power.

LITERATURE CITED

[1] D. L. Hill, Phys. Rev. 87, 1034 (1952).

[2] B. E. Watt, Phys. Rev. 87, 1037 (1952).

[3] J. R. Holt and A. E. Litherland, Rev. Sci. Instr. 25, 298 (1954).

[4] R. G. Cochran and K. M. Henry, Rev. Sci. Instr. 26, 757 (1955).

[5] S. J. Bame and W. T. Leland, Phys. Rev. 106, 1257 (1955).

[6] H. H. Barschall, L. Rosen, and R. F. Taschek, Revs. Mod. Phys. 24, 1 (1952).

[7] J. L. Fowler and J. E. Brolley, Revs. Mod. Phys. 28, 103 (1956).

[8] J. O. Hirschfelder and J. L. Magee, Phys. Rev. 73, 207 (1948).

[9] C. H. Johnson and C. C. Trail, Rev. Sci. Instr. 27, 468 (1956).

[10] S. J. Bame, E. Haddad, J. E. Perry, and R. K. Smith, Rev. Sci. Instr. 28, 997 (1957).

[11] A. R. Quinton and W. T. Doyle, Phys. Rev. 101, 669 (1956).

[12] L. F. Kondrashev, A. A. Kurashov, A. F. Linev, V. A. Sidorov, N. I. Sokolov, and N. N. Khaldin, Inst. and Exp. Tech. (USSR) 1, 17 (1958).

[13] J. H. Smith, Phys. Rev. 71, 32 (1947).

[14] D. H. Simmons, Proc. Phys. Soc. A65, 454 (1952).

[15] B. R. Gossick, Rev. Sci. Instr. 26, 754 (1955).

[16] D. O. Caldwell, Phys. Rev. 88, 131 (1952).

[17] W. C. Dickinson and D. C. Dodder, Rev. Sci. Instr. 24, 428 (1953).

[18] G. F. Bogdanov, N. A. Vlasov, S. P. Kalinin, B. V. Rybakov, L. N. Samoilov, and V. A. Sidorov, J. Exptl.-Theoret. Phys. (USSR) 36, 643 (1959).

[19] A. Garonsky and J. P. Judish, Phys. Rev. 100, 121 (1955).

[20] J. R. Risser, J. E. Price, and C. M. Glass, Phys. Rev. 105, 1288 (1957).

[21] S. J. Bame, and J. E. Perry, Phys. Rev. 107, 1616 (1957).

[22] M. D. Goldberg and J. M. LeBlanc, Bull. Am. Phys. Soc., ser. 2, 3, 323 (1958).

[23] Birks, Scintillation Counters, Izd. IL (1953).

[24] N. S. Khlebnikov and A. E. Melamid, Inst. and Exp. Tech. (USSR) 6 (1957).

[25] C. J. Taylor, W. K. Jentschke, M. E. Remley, F. S. Eby , and P. G. Kruger, Phys. Rev. 84, 1034 (1951).

[26] S. Bashkin, R. R. Carlson, R. A. Douglas, and J. A. Jacobs, Phys. Rev. 109, 434 (1958).

[27] Atlas of Neutron Gross Sections Izd. AN SSSR (1955).

[28] G. J. Perlow, Rev. Sci. Instr. 27, 460 (1956).

[29] R. F. Mozley and F. C. Shoemaker, Rev. Sci. Instr. 23, 569 (1952).

[30] J. M. Calvert, A. A. Jaffe, and E. E. Maslin, Proc. Phys. Soc. A68, 1017 (1955).

[31] L. Beghian, R. Allen, J. Calvert, and H. Habban, Phys. Rev. 86, 1044 (1952).

[32] P. R. Chagnon, L. Madansky, and G. E. Owen, Rev. Sci. Instr. 24, 656 (1953).

[33] J. E. Draper, Rev. Sci. Instr. 25, 558 (1954).

[34] J. Elliot, W. McGarry, and W. Faust, Phys. Rev. 93, 1348 (1954).

[35] P. R. Chagnon, G. E. Owen, and L. Madansky, Rev. Sci. Instr. 26, 1165 (1955).

[36] Yu. A. Egorov, Inst. and Exp. Tech. (USSR) 3, 21 (1958).

[37] R. Giles, Rev. Sci. Instr. 24, 986 (1953).

[38] R. E. Benenson and M. B. Shurman, Rev. Sci. Instr. 29, 1 (1958).

NUCLEAR-REACTION METHOD

If, as a result of a nuclear reaction induced by a neutron, only charged particles are produced, the energy of the neutron can be determined by measuring the total energy of the charged particles by their range in a photographic emulsion or by their ionizing properties. Since, the total energy of the reaction products is independent of the incident direction of the neutron which induces the reaction, this method does not require preliminary collimation of the neutron flux. Because of this feature, this method turns out to be extremely desirable for measurements of neutron spectra of extended sources and has been applied in investigation of nuclear reactors and in experiments designed to test neutron shielding. In these cases the use of spectrometers which use the differential recoil-nucleus method leads to two problems that arise from the necessity of collimating the neutron flux. In the first place the spectrometer must be removed by a considerable distance from the neutron source and this leads to a great reduction in efficiency (for example, in a proportional-counter telescope with a thin radiator $\eta \approx 10^{-8}$ or less). Secondly, scattering of neutrons on the walls of the collimator tends to distort the primary neutron spectrum.

The choice of nuclear reactions which can be used for studying fast-neutron spectra is very limited. The reaction cross-section must be rather large and must exhibit a smooth dependence on energy in the region being studied. Furthermore, the reaction must satisfy the following contradictory requirements.

A nucleus formed as a result of the reaction must not exhibit low-lying excited levels, because, under those conditions, the total kinetic energy of the reaction products will not be uniquely related to the neutron energy. This requirement is satisfied only by the very light nuclei.

On the other hand, the nucleus must be sufficiently heavy so that in elastic scattering of a neutron with maximum energy the energy of the recoil nucleus will be smaller than the total energy of the products of the reaction caused by a neutron of the minimum energy being investigated. This requirement is satisfied if the reaction energy Q is large. However, in cases in which Q is large and positive, the neutron energy is only a small fraction of the energy of the reaction products so that the accuracy of the measurement is low.

Finally, it is necessary that any other possible reaction between the neutron and the same nucleus be considerably less favorable energetically or much less probable.

These requirements can be satisfied in only a few of the reactions between neutrons and light nuclei. In Fig. 28 is shown the independence of the cross section for the most favorable reactions, $He^3(n, p)T$ and $Li^6(n, \alpha)T$, as a function of neutron energy.

The nuclear reaction method is useful in measuring neutron spectra when photographic emulsions are used. An additional criterion for the choice of a nuclear reaction in this case is the existence of characteristic, easily noticeable, tracks in the emulsion; these facilitate the identification of the given reaction and help to distinguish it from competing processes. Usually the emulsion used for neutron spectroscopy is filled with boron or lithium. The reaction $B^{10}(n, 2\alpha)T$ (Q = 0.33 Mev) gives a fairly well-defined three-pronged star, the total energy of the particles of which is approximately equal to the neutron energy [1]. The reaction $B^{11}(n, \alpha)Li^8$ (Q = − 6.7 Mev) is easily distinguished by the "lithium hammer" produced in the decay of Li^8 [2]. The reaction $Li^6(n, \alpha)He^3$ (Q = 4.78 Mev) is also easily identified [3, 4].

§ 1. Ionization Chamber

If the nuclei in which the neutron-induced reaction takes place is introduced into the composition of the gas in an ionization chamber or proportional counter, the energy of the reaction products can be determined by their ionizing properties.

Batchelor and others [5-9] have used a proportional counter containing He^3 for this purpose. A measurement is made of the total energy of the proton and triton formed in the reaction $He^3(n, p)T$ (Q = 0.77 Mev). In Figs 29 and 30 are shown the counter-pulse spectra for irradiation by monoenergetic neutron beams with energies of 0.12 and 1.00 Mev. In addition to the main peak, in each spectrum there is a peak due to slow neutrons which are formed as a result of the slowing down of the primary neutrons in the walls of the apparatus; there is also a continuous spectrum due to γ-rays. The peak is due to the rapid rise in the cross section for the $He^3(n, p)T$ reaction or slow neutrons. At a neutron energy of 1 Mev there are also pulses due to the recoil nuclei formed in the elastic scattering of neutrons on He^3.

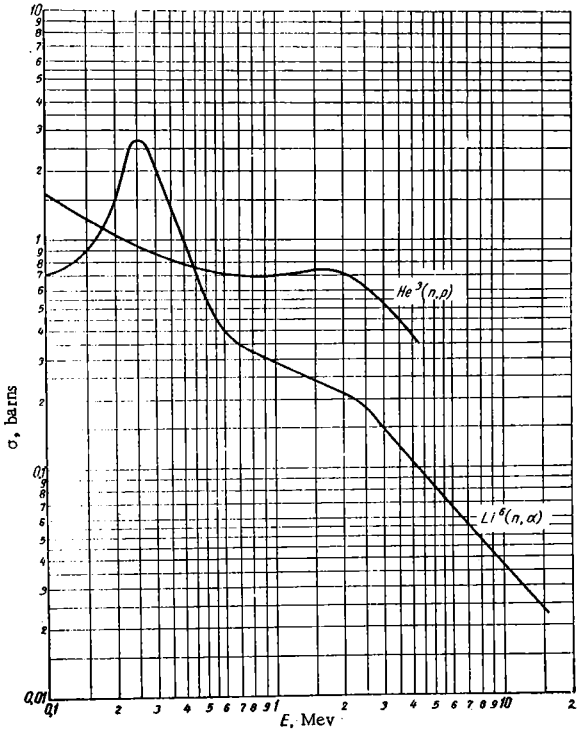

Fig. 28. Dependence of the cross section for the $He^3(n, p)T$ and $Li^6(n, \alpha)T$ reactions on neutron energy.

It is apparent from Fig. 29 that the lower limit of the energy range of the spectrometer is about 0.1 Mev, at which point the main peak runs together with the slow-neutron peak. At a neutron energy of 1 Mev the limit of the pulse spectrum due to recoil nuclei coincides with the slow-neutron peak; thus, the spectrometer is capable of measuring spectra between 0.1 and 1 Mev. As the neutron energy is increased the dynamic range of the spectrometer (3) is reduced since the lower limit is determined by the boundary of the pulse spectrum due to recoil nuclei. In this case the allowable simultaneous radiation energy region approaches one-quarter of the maximum neutron energy since the maximum energy of the recoil nuclei is three-quarters E for elastic scattering of neutrons on He^3. Consequently, the main region of application of a spectrometer which uses the $He^3(n, p)T$ reaction lies close to neutron energies of 1 Mev.

The design of a proportional counter must provide high resolving power and must eliminate edge effects. In counters of usual dimensions the range of the charged particles formed in the counter is reduced by adding a heavy gas (A , Kr, Xe) to the He^3 and increasing the pressure of the mixture to several atmospheres. The counter of Batchelor et al., which was 5 cm in diameter and 24 cm long, was filled with the following mixtures: He^3 - 270 mm Hg, Kr - 1640 mm Hg, CO_2 - 18 mm Hg. Under these conditions about 10% of the protons formed in $He^3(n, p)T$ reactions induced by slow neutrons terminated their paths at the walls of the counter. For neutron energies of 1 Mev the edge effects were about 40%. In this work edge effects were not important; they lead to the appearance of a "tail" in the region of low pulse amplitudes (Fig. 31).

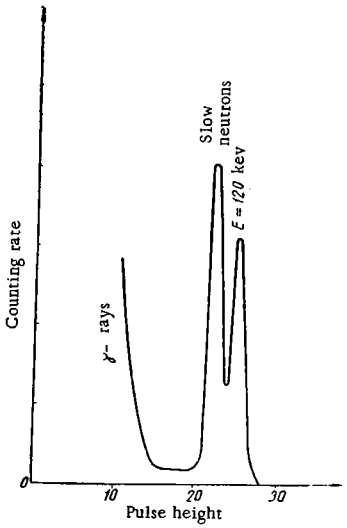

Fig. 29. Pulse spectrum for a He^3 proportional counter irradiated by monoenergetic neutrons with an energy of 120 kev [6].

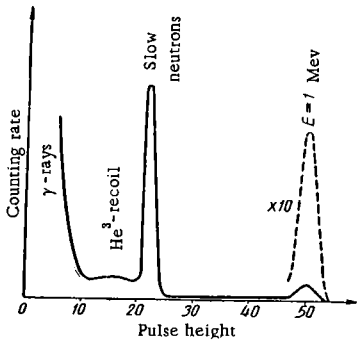

Fig. 30. Pulse spectrum for a He^3 proportional counter at a neutron energy of 1 Mev [6].

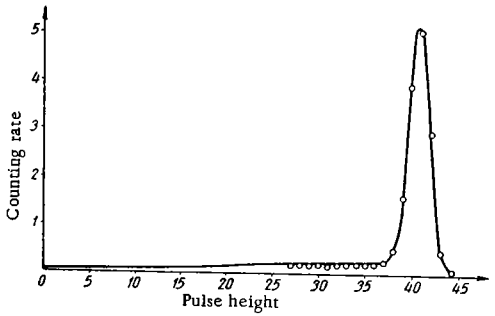

Fig. 31. Line shape for a He^3 proportional counter [6] at a neutron energy of 0.67 Mev. The theoretical curve and the experimental points are shown.

Obtaining a high resolving power in a proportional counter in which the working gas is maintained at a high pressure presents a technical problem of great difficulty. The resolving power of the counter used by Batchelor et al. was approximately 7%. Under these conditions the resolving power as a neutron spectrometer (1) was about 50% for E = 0.12 Mev and about 12% for E = 1 Mev.

Glazkov [10] has obtained almost the same resolving power in a simpler spectrometer; this instrument is essentially a spherical ionization chamber filled with He^3 [11]. A glass chamber, rather simple in design, and 20 cm in diameter, is silvered on the inside and covered with an outer layer of electrolytic copper (in order to provide stability at high pressures); the central electrode is 1.5 cm in diameter. The chamber is filled with the following mixture: He^3 - 350 mm Hg, A - 1900 mm Hg, N_2 - 90 mm Hg; the resolving power is approximately 9%.

The resolving power of proportional counters or ionization chambers depends critically on the purity of the working mixture, especially at high pressures. In the cases being considered here, careful measures are taken to free the gases from oxygen and water vapors which could form negative ions and deteriorate the collection of electrons. It is necessary to free the He^3 from traces of tritium, the radioactivity of which can cause a noticable dark current and deterioration of resolving power.

The efficiency of a He^3 spectrometer can be computed from the dependence of the cross section for the $He^3(n, p)T$ reaction on energy shown in Fig. 28. The efficiency is considerably greater than that of a recoil-nucleus spectrometer of comparable resolving power. At neutron energies of approximately 1 Mev the efficiency of the spectrometer used by Batchelor et al. [6] was approximately 10^{-5}; the efficiency of the spectrometer used by Glaskov [10] was 10 times greater.

An important advantage of the spherical ionization chamber as compared with the cylindrical proportional counter is the fact that the efficiency is independent of the direction of the incident neutrons. This feature is especially important in the present case since the main advantage of a He^3 spectrometer is the possibility of measuring neutron spectra without regard to direction.

§ 2. Scintillation Counter with a $Li^6I(Eu)$ Crystal

Efficiencies higher than those cited above can be obtained if the nucleus on which the required reaction takes place is introduced into a solid scintillator and the neutron energy determined from the magnitude of the pulse in the scintillation counter. The basic difficulty of this method lies in the fact that the light yield of a

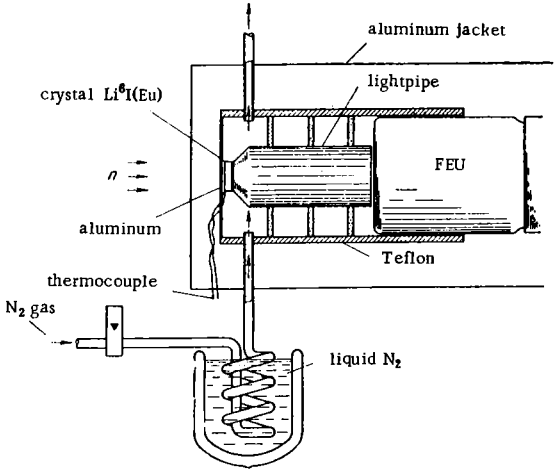

Fig. 32. Diagram of the apparatus used by Murray [12].

scintillator is reduced markedly with increasing specific ionization. If several charged particles are produced in a reaction induced by a neutron, even if their total energy is constant for a given neutron energy, it can divide differently between the particles. If different particles are formed in the reaction (for example, α-particles and tritons) this situation leads to a large uncertainty in the pulse amplitudes for neutrons of a given energy

This difficulty has been avoided to a considerable extent by Murray [12], who used a lithium iodide crystal (pure Li^6, activated with europium) as a scintillation detector for neutrons. He found that when the temperature of the crystal was reduced to $-140°$ C, the spread in the pulse amplitude produced in the crystal by the products of the $Li^6(n, \alpha)T$ reaction was reduced considerably; thus it was possible to make use of the full available resolving power.

A diagram of Murray's apparatus, with which it is possible to maintain the crystal at any temperature between room temperature and liquid-nitrogen temperature, is shown in Fig. 32.

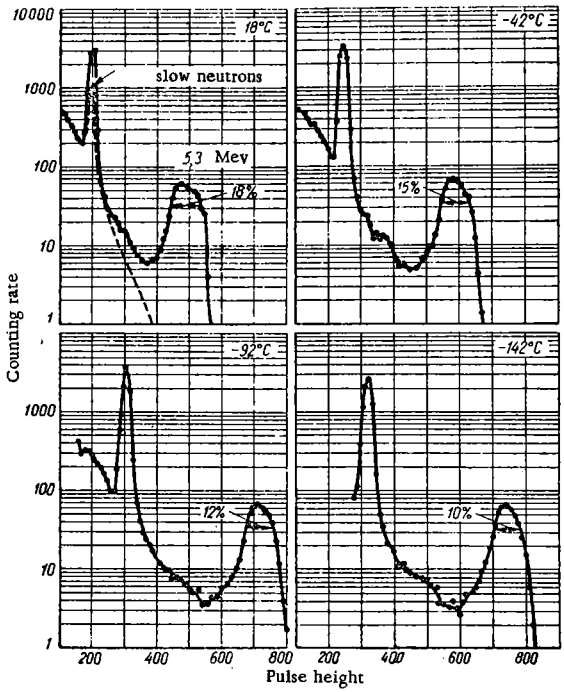

Fig. 33. Pulse spectrum for a scintillation counter with a $Li^6I(Eu)$ crystal at various crystal temperatures. The counter was irradiated by neutrons with an energy of 5.3 Mev. The dashed lines show the pulse spectrum corresponding to the background of neutrons and γ-rays.

In Fig. 33 are shown pulse spectra from the counter obtained at various crystal temperatures for irradiation by monoenergetic neutrons at 5.3 Mev. When the temperature of the crystal is reduced to $-142°$ C the width of the main peak is reduced by almost a factor of 2 while the pulse amplitude is increased by a factor of $1\frac{1}{2}$. At low temperatures the peak becomes Gaussian because of the equalization of the light yield of the crystal when excited by α-particles and tritons produced in the $Li^6(n, \alpha)T$ reaction.

Because of the fact that the reaction used here has a large positive Q (4.7 Mev), the resolving power of the spectrometer is poorer than the amplitude resolving power of a counter with the values shown in the figure. For example, at $-142°$ C the resolving power of the spectrometer is 18% for neutrons with an energy of 5.3 Mev (not 10% as shown in Fig. 33).

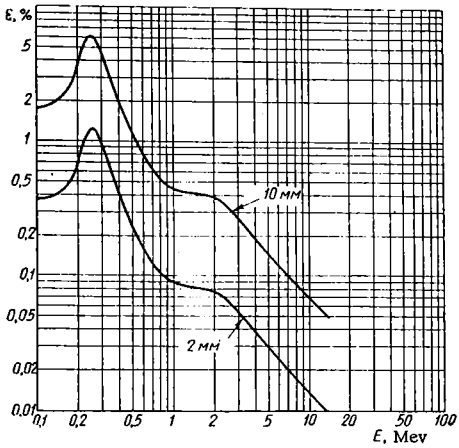

Fig. 34. Efficiency of a $Li^6I(Eu)$ crystal as a function of neutron energy for two values of crystal thickness.

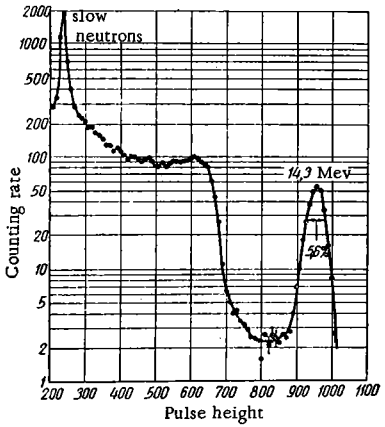

Fig. 35. Pulse spectrum from a scintillation counter with a $Li^6I(Eu)$ crystal irradiated by neutrons with an energy of 14.3 Mev. The crystal was cooled to liquid nitrogen temperature.

On the other hand, the high value of Q makes it possible to obtain good discriminations against γ-rays and to avoid one of the most common shortcomings of scintillation neutron detectors, i.e., the high sensitivity to γ-rays. Pulses from thermal neutrons are characterized by the same amplitude as pulses from γ-rays with an energy of 4 Mev. If there are interference effects due to γ-rays of higher energy the thickness of the crystal may be chosen (2-3 mm) so that the range of electrons with energies greater than 4 Mev does not make any contribution.

The dependence of the efficiency of a $Li^6I(Eu)$ crystal on neutron energy is shown in Fig. 34. The efficiency falls off rapidly with increasing energy but is still rather high at E = 10 Mev ($\epsilon \sim 10^{-3}$ for a crystal 10 mm thick).

The potentialities of the spectrometer are limited strongly by the high efficiency for slow neutrons so that even when the spectrometer is irradiated by monoenergetic neutrons a rather high slow-neutron background is observed (Fig. 33); these neutrons are produced in the parts of the holder close to the crystal. A particularly high contribution to this background is made by the plexiglas lightpipe (Fig. 32) which provides thermal isolation of the cathode of the photomultiplier from the crystal; this isolation is required because the operation of the photocathode is effected at low temperatures (photomultipliers such as the RCA 6342 or DuMont 6292 are used).

It should be noted that the use of the domestic photomultiplier such as the FEU-11 (and similar types such as the FEU-12 - FEU-16), which normally operate at liquid nitrogen temperatures [13], makes it possible to locate the crystal directly at the cathode and thus to improve considerably the spectrometer characteristics.

For neutron energies greater than 7 Mev, on the pulse spectrum due to the Li(n, α)T reaction, pulses from competing reactions begin to be observed, such as $Li^6(n, dn)He^4$, $Li^6(n, p)He^6$ and elastic scattering of neutrons on Li^6. This effect also tends to reduce the dynamic range of the spectrometer (Fig. 35). Nonetheless, the investigation of wide continuous spectra which do not contain too many fast neutrons is considered possible by Murray. It is first necessary to obtain pulse spectra for monoenergetic neutrons at several energy values. The true shape of a continuous spectrum can be obtained by the following interpretation technique. The spectrum is divided into several

intervals and, starting at the upper limit, the background corresponding to each interval is subtracted step by step. In Fig. 36 are compared neutron spectra from the fission of U^{235} obtained in this way with the results of measurements by means of photographic emulsions containing Li^6. The background, which is subtracted, represents 60% at E = 1.5 Mev, 17% at E = 3 Mev, and is negligibly small at E > 5.5 Mev.

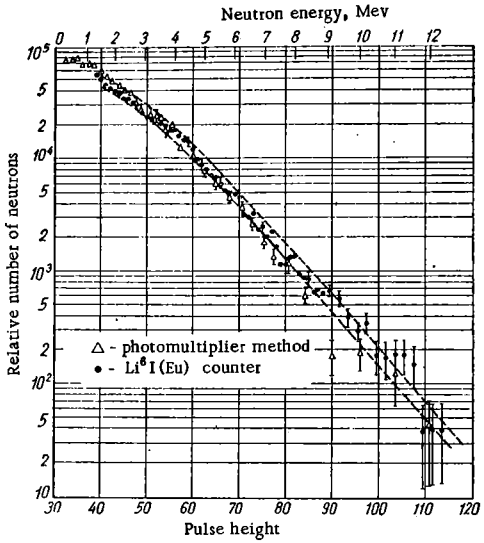
Neutron energy, Mev
0 1 2 3 4 5 6 7 8 9 10 11 12
Relative number of neutrons
10^5 5 2 10^4 5 2 10^3 5 2 10^2 5 2 10
△ - photomultiplier method
• - Li^6 I(Eu) counter
30 40 50 60 70 80 90 100 110 120
Pulse height

Fig. 36. Neutron spectrum for U^{235} fission. The dotted lines show the uncertainty in the measurements of the spectrum corresponding to the uncertainty in the cross section for the $Li^6(n, \alpha)$ reaction. This is common for both methods.

The lower limit of applicability of the spectrometer corresponds to neutron energies of 1 Mev, at which point the main peak cannot be distinguished from noise.

LITERATURE CITED

[1] C. M. J. Lattes and I. R. I. Occhialini, Nature 159, 331 (1941).

[2] E. Pickup, Phys. Rev. 74, 495 (1948).

[3] N. Kaplan and H. Yagoda, Rev. Sci. Instr. 23, 155 (1952).

[4] J. H. Roberts and F. E. Kinney, Rev. Sci. Instr. 28, 610 (1957).

[5] R. Batchelor, Proc. Phys. Soc. A 65, 674 (1952).

[6] R. Batchelor, R. Aves, and T. Skyrme, Rev. Sci. Instr. 26, 1037 (1955).

[7] R. Batchelor and G. C. Morrison, Proc. Phys. Soc. A 68, 1081 (1955).

[8] R. Batchelor, Proc. Phys. Soc. A 69, 214 (1956).

[9] R. Batchelor and H. R. Hyder, J. Nucl. Energy 3, 7 (1956).

[10] N. P. Glazkov, Inst. and Exp. Tech. (USSR) 4, 96 (1957).

[11] Kh. R. Poze and N. P. Glazkov, J. Exptl. Theoret. Phys. (USSR) 30, 1017 (1956).

[12] R. B. Murray, Nuclear Instr. 2, 237 (1958).

[13] G. S. Vil'dgrube, Dissertation (1958).

TIME-OF-FLIGHT METHOD

The determination of neutron energy by time-of-flight is one of the most direct methods for neutron spectroscopy. The time-of-flight is related to the neutron energy and the flight distance by the following simple relation:

$$t\,(\text{m}\mu\text{sec}) = \tau L = \frac{72{,}3L\,(\text{m})}{\sqrt{E\,(\text{Mev})}}, \tag{38}$$

where τ is the neutron time-of-flight for a distance of 1 meter.

Eq. (38) is written in the nonrelativistic approximation. In making an exact measurement of the energy of fast neutrons, it is necessary to take account of relativistic effects. For example, at a neutron energy of 30 Mev the relativistic correction amounts to approximately 3%. The precise relation between E and τ is tabulated in detail in the Appendix.

The relation between the neutron energy spectrum and the time-of-flight distribution is given by the expression

$$F(E)\,dE = V(t)\,dt = U(\tau)\,d\tau$$

Whence, taking account of Eq. (38), we obtain a formula for converting the neutron spectrum from the time scale to the energy scale:

$$F(E)\,dE = 0{,}957 \cdot 10^{-4}\tau^3 U(\tau)\,dE,$$

where τ is expressed in mμsec/m.

In order to measure the time-of-flight it is necessary to record the instant of time at which the neutron leaves the initial point and the time at which it arrives at the terminal point of the flight path. The latter is determined by the appearance of a pulse in the counter which records neutrons at the end of the path. The moment of emission can be fixed by one of the following methods.

1. Detection of the scattering of a neutron in an organic scintillation counter located at the origin of the flight path.

2. Detection of the radiation accompanying the formation of the neutron in a nuclear reaction by a counter placed close to the neutron source.

3. The use of a pulsed neutron source. The instant at which the neutrons are emitted from the source is noted by an electric pulse which is synchronized with the neutron pulse.

In slow-neutron spectrometers only the third method is used for denoting the time of emission. Neutron pulses approximately 1 mμsec long are produced by means of mechanical choppers at nuclear reactors or are obtained from cyclotrons or synchrotrons, the beams of which are modulated in an appropriate manner. In order to use the first method listed above the neutron energy must be very small; the second method, although feasible in principle, imposes limitations on the neutron source. In practice, in fast neutron work all three methods are important.

Slow-neutron time-of-flight spectrometers usually have a resolution time of the order of 1 mμsec. This time is limited chiefly by the techniques used to obtain the neutron pulses. By increasing the flight distance to

several tens of meters, with this resolution time it is possible to obtain a high resolving power (1%) only for neutrons with energies of approximately 10 kev.

The application of the time-of-flight method for investigation of fast neutrons became possible only recently with the advent of scintillation counters with organic scintillators, fast coincidence circuits, wide-band amplifiers and oscilloscopes, fast trigger circuits with secondary-emission pentodes, etc. These new experimental techniques are now called "millimicrosecond pulse techniques" [1].

Actually, as is easily seen from Eq. (38) (see also Fig. 37) the flight time of fast neutrons is very small. For example, neutrons with an energy of 10 Mev traverse a distance of ten meters in 230 mμsec. This means that using such a flight distance, in order to measure a neutron spectrum for neutrons with energies of 10 Mev with a resolving power of $\Delta E/E = 2\Delta t/t = 1\%$, it is necessary to have a spectrometer with a resolution time of the order of 1 mμsec (10^{-9} sec).

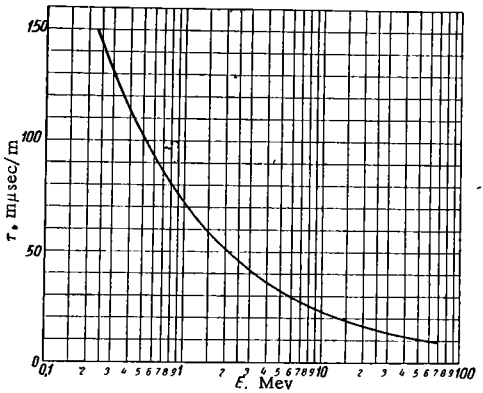

Fig. 37. Neutron time of flight over a distance of one meter (τ) as a function of neutron energy.

It is interesting to note that after spectrometers with resolution times of approximately 1 mμsec were built for the megavolt region, millimicrosecond techniques were carried over to the kilovolt region [2]. In this region, high resolving time makes it possible to use a considerably shorter flight distance and, consequently, weaker neutron sources. In addition, the upper energy limit due to the apparatus is no longer a limitation, i.e., it becomes possible to make a smooth transition from the kilovolt energy region to the negavolt region.

The development of techniques for obtaining neutron pulses was somewhat dependent on the development of fast scintillation counters and time analyzers. Hence, at the beginning the two-counter spectrometers were used; these were based on the first two methods indicated above for recording the time of emission of the neutron.

§ 1. Spectrometer with Two Counters

A spectrometer in which the time of emission is indicated by the scattering of the neutron from one counter into another is no different from the two-crystal spectrometer described in § 2, Chapter II. The sole difference is that instead of an amplitude analysis of the recoil protons in the first counter it is necessary to make a time-of-flight analysis of the scattered neutrons.

One of the first spectrometers of this type was built by Veretennikov and Averchenkov [3]. As an example we consider the apparatus of Neilson and James [4], which has been described in greater detail. It is similar to the system shown in Fig. 23. A neutron is scattered through an angle θ_0 in the organic scintillator of the first counter and recorded by the second counter. The time-of-flight distribution of the scattered neutrons is determined. The energy of the primary neutron is determined from Eq. (19).

The counters consist of stilbene crystals (first 1 × 2 × 2 cm and the second 2 × 4 × 4 cm) and RCA 6342 photomultipliers. The pulses from the photomultipliers are applied to a thirty-channel time analyzer which uses "time to amplitude" conversion (see § 4, Chapter VII). The resolution of the spectrometer is 1.5 mμsec, close to a record for devices of this type. Nevertheless, in order to obtain sufficiently good resolving power, it is necessary to keep the counters well separated, with the attendant reduction in efficiency.

In Fig. 38 are shown time-of-flight distributions for neutrons from the D(d, n)He^3 reaction (E = 4.17 Mev) obtained at $\theta_0 = 30°$ with three distances between the counters: 27 cm, 42 cm, and 67 cm.

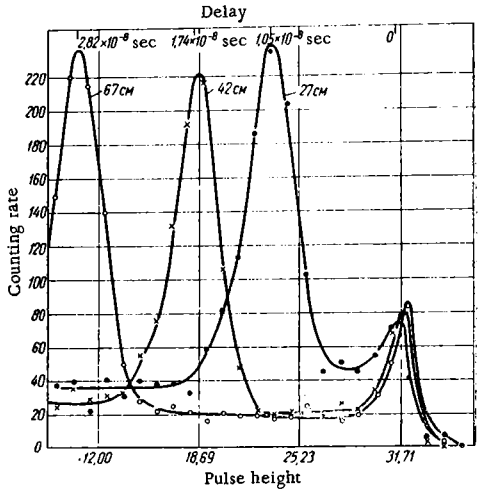

Fig. 38. Time-of-flight distribution of neutrons from the D(d, n)He^3 reaction (E = 4.17 Mev) obtained with a spectrometer which uses neutron scattering from one counter to another [4]. The curves shown correspond to three values of flight distance. Along the abscissa axis below are plotted directly the measured pulse amplitudes of the time analyzer (related linearly to the delay); above are plotted the corresponding delays.

The width of the neutron peaks is due to a considerable extent to the smearing of the scattering angle because of the finite crystal dimensions. The small peak close to t = 0 corresponds to scattering of the background γ-rays from crystal to crystal and to (n, γ) reactions in the first crystal with subsequent detection of the γ-rays in the second crystal.

A fundamental shortcoming of a spectrometer of this type is the poor efficiency which, as in the two-crystal spectrometer with the amplitude analyzer (36), is proportional to the product of the efficiencies of the two counters; the actual efficiency is still lower because of the necessity for separating the counters. With L = 0.5 m and $\alpha_1 = \alpha_2$, the efficiency of the spectrometer described above, η, for neutrons with energies of 3 Mev, is approximately 10^{-7} for a resolving power of approximately 20%. This defect cannot be remedied by using intense neutron sources since the counting rate is not limited by the source intensity but by the large background of random coincidences due to the overloading of the first counter.

This spectrometer can be used without any essential changes in a scheme based on the second method of recording the time at which the neutron is emitted (Fig. 39) for an investigation of (x, nγ) reactions. In this case, the counter which is placed close to the target of the accelerator records γ-rays which are emitted simultaneously with the neutrons.

It might appear that a scheme of this kind could be used to increase the efficiency of the spectrometer by increasing the size of the first crystal and movingit closer to the neutron source. In practice, however, this procedure gives only a very small improvement because of the high background of random coincidences which occur as a consequence of overloading of the first counter.

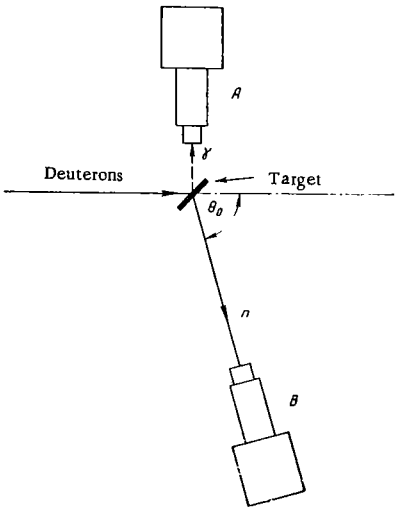

Fig. 39. Diagram of a time-of-flight spectrometer in which the neutron-emission time is indicated by means of the accompanying γ-radiation.

We may note that the high additional background is produced here by the "false" coincidences due to scattering of neutrons from crystal to crystal since, in order to obtain good resolution time in counters which record γ-rays, it is also necessary to use an organic scintillator.

The advantage of this method as compared with the first is essentially the fact that the neutrons which strike the second counter with the total energy. With all other conditions being equal this means that it is possible to raise the threshold and reduce the background.

In Fig. 40 is shown a spectrum for neutrons from the $Be^9(d, n\gamma)B^{10}$ reaction (Ed = 0.8 Mev) obtained with the spectrometer of Neilson and James, with γ-rays recorded by the first counter. On the high background due to accidental and "false" coincidences are observed three groups of neutrons, corresponding to the lowest excited states of B^{10}. The energy values found from this curve 4.20 + 0.40; 2.65 ± 0.30 and 1.28 ± 0.20 Mev, are in agreement with the values obtained with emulsions [5] but are characterized by lower accuracy. In Fig. 40 the peak at t = 0 is not shown; it is ten times more intense than the neutron peaks. It is due to γ-γ-coincidences and to cases in which a neutron is recorded in counter A and a γ-photon in counter B.

In spite of its shortcomings, a time-of-flight spectrometer with two counters has great advantages as compared with the spectrometers considered in § 2, Chapter II. In particular, with an instrument of this kind it is possible to observe several energy groups over a wide neutron energy range and to measure n-γ-correlation for each energy group against a background of neutrons with other energies [6].

A spectrometer of this kind is especially useful when the time of emulsion of the neutron is indicated by the emission of a charged particle. In this case, it is possible to achieve 100% efficiency of the counter for the accompanying particle with a rather low neutron sensitivity of the first counter.

For example, in a measurement of a fission neutron spectrum (Cranberg et al. [7]) the time of emission of the neutron was denoted by a pulse from a spiral ionization chamber which detected the fission fragments. The chamber was characterized by an electron collection time of approximately 20 mμsec, making it possible to determine the time of emission of the neutron with an accuracy of ± 4 mμsec.

If, in the reaction which is being used, only a neutron and one charged particle are produced (for example, the $T(d, n)He^4$ reaction), the two-counter method has another advantage as compared with the method based on the use of a pulsed neutron source. The direction of emission of the charged particle is uniquely related to the direction of emission of the neutron. Thus, by detecting the charged particles which are emitted in a given direction, it is possible, without the help of any absorber or collimators, to define a narrow cone of "effective" neutrons; these are uncontaminated by low energy neutrons which are so often produced due to scattering in a collimator.

This method has been used by O'Neil [8] at Cornell University (USA) for studying inelastic scattering of neutrons from the $T(d, n)He^4$ reaction on a number of elements. As a result of analysis of the neutron spectra this author was able to obtain new data on nuclear temperatures.

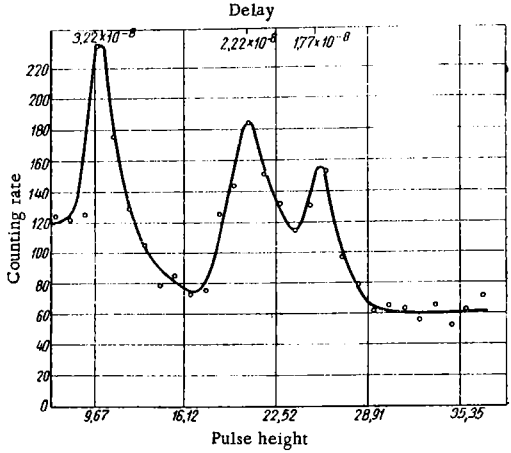

Fig. 40. Time-of-flight distribution of neutrons from the $Be^9(d, n\gamma)B^{10}$ reaction ($E_d = 0.8$ Mev) obtained with a time-of-flight spectrometer. In order to determine time at which the neutrons are emitted, the first counter records the γ-rays.

§ 2. Spectrometer with a Pulsed Neutron Source

It is possible to determine the time at which a neutron is emitted through the use of a modulated source which gives periodic short bursts of neutrons which are rather well separated in time, thus making it possible to use a time-of-flight spectrometer with only one counter. By this means it is possible to achieve a considerable increase in the efficiency of the spectrometer and to reduce the limitations on the intensity of the neutron flux which can cause overloading of the first counter and accidental coincidences. The chief difficulty in realizing this method in the negavolt region is the fact that the length of the neutron pulses (if one to obtain good resolving power) must be of the order of millimicroseconds, i.e., a thousand times shorter than the pulses obtained by means of mechanical selectors and pulsed cyclotrons.

The technique of obtaining extremely short neutron pulses has been developed only recently. Since it involves various methods of modulating beams of charged particles which are obtained from accelerators, for the time being only accelerator targets can be used as pulsed sources of fast neutrons. It is interesting to note that because of the inherent properties of its acceleration mechanism the "natural" pulsed source for fast-neutron spectroscopy is the cyclotron.

A schematic diagram of a modern fast-neutron spectrometer, in which time-of-flight is measured, is shown in Fig. 41. The basic elements of this system are the pulsed neutron source, the neutron detector, and the time analyzer.

In the investigation of primary processes the neutron source is the accelerator target itself; in the investigation of secondary processes samples are used which emit neutrons when bombarded by the pulsed flux of monoenergetic neutrons from the accelerator target.

The distance L between the source and the neutron detector which is called the "flight distance" (or the base of the spectrometer) is approximately 10 m in work on primary reactions and approximately 1 m in work on secondary reactions (for example, inelastic neutron scattering) [9].

The pulses from theneutron detector are applied to the input of a time analyzer. To the other input of the analyzer are applied signals which are synchronized with the neutron pulses. These signals, which mark the time at which the neutrons are emitted from the source, will be called "time markers" or "control pulses".

The time analyzer is used to make an analysis of the time distribution of the pulses from the counter with respect to the control pulses. The distribution which is obtained, which is characterized by a fixed time shift because of the unknown delays in the neutron counters, the shaping circuits of the control pulses, etc., is then the neutron time-of-flight distribution. The zero of the time scale is usually determined by the position of the γ-ray peak from the target which is easily detected by a scintillation counter.* Because of this situation no special phasing circuit is required. In investigating secondary processes the time reference is the γ-ray peak emitted by the sample as a result of inelastic neutron scattering or the neutron peak due to elastic scattering of primary neutrons on the sample.

Before being applied to the recording system the pulse from the time analyzer must pass through a gate (Fig. 41) which is opened by a signal from the amplitude selector (in the simplest case a threshold discriminator) only when the amplitude of the pulse from the neutron counter falls in a preassigned interval (above the discriminator threshold).

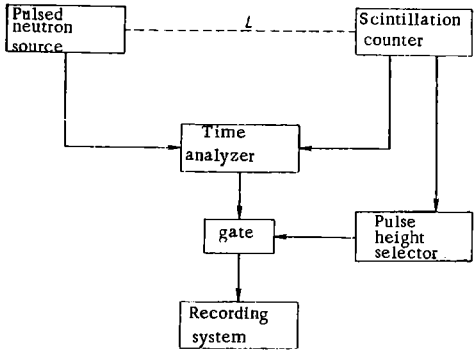

Fig. 41. Block diagram of a fast neutron time-of-flight spectrometer with a pulsed neutron source.

A pulse-height selector is not a necessary part of a spectrometer which is intended only for determination of neutron energies. However, it does provide the possibility of absolute measurement of neutron fluxes and, furthermore, is often desirable for improving the resolution time of the spectrometer.

The method of using the pulse-height selector shown in Fig. 41 is not the only possible method. For example, the selector can be used at the input of the time analyzer. It is apparent that in this case it must be "fast." However, contemporary millimicrosecond techniques do not provide sufficiently good pulse-height analysis. For this reason, one usually uses the so-called "fast-slow" switching circuit shown in Fig. 41. In this case the selector is a conventional microsecond circuit while the "gate" is a simple coincidance circuit with a resolution time of the order of a microsecond. A shortcoming of the "fast-slow" system is the fact that sometimes (in practice only in the case of single-channel spectrometers and the chronotron system) the allowable counter loading is limited by the amplitude selector and not by the basic elements of the circuit.

Problems which arise in pulsed-source spectrometers are considered in detail in later chapters because of their importance. Nonetheless, our description can not pretend to be complete since almost every month brings new developments in this field.

* The time-of-flight of γ-rays over a distance of one meter is 3.34 mμsec.

LITERATURE CITED

[1] Lewis and Wills, Millimicrosecond Pulse Techniques, Izd. IL (1956).

[2] W. M. Good, J. H. Neiler, and Gibbons, Phys. Rev. 109, 926 (1958).

[3] A. I. Veretennikov and V. Ya. Averchenkov, Inst. and Exp. Tech. (USSR) 3, 21 (1958).

[4] G. C. Neilson and D. James, Rev. Sci. Instr. 26, 1018 (1955).

[5] J. S. Pruitt, C. D. Swarts, and S. S. Hanna, Phys. Rev. 92, 1456 (1953).

[6] G. C. Neilson and J. B. Warren, Phys. Rev. 103, 1758 (1956).

[7] L. Cranberg, G. Frye, N. Nereson, and L. Rosen, Phys. Rev. 103, 662 (1956).

[8] G. K. O'Neil, Phys. Rev. 95, 1235 (1954).

[9] L. Cranberg, R. Day, L. Rosen, R. Taschek, and M. Walt, Progress in Nuclear Energy Ser. 1, 1, 107 (1956).

PULSED NEUTRON SOURCES

In all existing time-of-flight spectrometers used in the megavolt region the pulsed neutron sources are accelerator targets. The techniques of obtaining short neutron pulses are essentially the methods of modulating the intensity of a beam of charged particles. Since the time in which these particles slow down in the target and the time required for the nuclear reactions is small the time at which the neutrons are emitted coincides with the time at which the charged particles strike the target and the duration of the neutron pulse is equal to the duration of the charged-particle pulse.

The optimum pulse duration is approximately 1 mμsec. If this figure is reduced the result is a loss of average intensity and essentially no improvement in the resolving time of the spectrometer since the latter generally limited by the resolving time of the scintillation counter.

The optimum repetition rate for the pulses is considered in § 3 of Chapter VIII. In most cases, the required pulse repetition frequency is approximately 1 Mc.

§ 1. Modulation of the Beam of an Electrostatic Accelerator

An accelerator or a van de Graaff generator provides a continuous well-focused ion beam at low energies. A simple method is frequently used for modulation of such a beam. By means of a pair of deflection plates to which is applied a high-frequency sinusoidal voltage (RF), the beam of ions is deflected past an aperture. Twice in each RF period (forward and reverse motion of the beam) the ions which pass through the aperture strike the target. The duration of the particle pulse at the target is smaller the greater the deflection amplitude of the beam and for deflection frequencies of the order of a megacycle can be as small as 1 mμsec.

If necessary, it is easy to arrange things so that only one neutron pulse is produced per RF period. For example, it is possible to use a second pair of deflection plates, at right angles with respect to the first, and to apply a second deflection voltage in such a way that the beam is swept out in a circle which intersects the aperture once per period.

Because of its simplicity this method has been used widely in time-of-flight neutron spectroscopy [1-5]. However, it does have certain shortcomings.

It is apparent that the mean ion current at the target is only a small fraction of the initial beam current, being equal to the ratio of the ion pulse length at the target to the pulse repetition rate. For example, with $\Delta t_{pulse} = 1$ mμsec and 1 μsec, only $1/1000$ of the current is used.

The following situation is also important when the energy of the accelerated particle is several million electron volts. Whereas the useful current is reduced by a large factor, the total beam current and background produced by the accelerator remain the same. In chopped-beam operation the background radiation is produced mainly in the diaphragm which contains the aperture, where the greatest fraction of the beam is intercepted; thus it is possible to reduce the effect of the background by moving the target away from the aperture. However, under these conditions, it is necessary to use a supplementary focusing system after the chopper.

In Fig. 42 is shown a beam-chopping system used in the van de Graaff generator at Los Alamos (USA) [2]. The chopper is located directly at the point at which the beam leaves the magnet used to analyze the particles by mass and energy. A sinusoidal voltage (3.7 Mc) is applied to the deflection plates. By means of an electrostatic system behind the chopper, the beam is focused on a target located at a distance of 8.55 m from the aperture. The particle pulses are produced at the target twice per RF period and are 3 mμsec long. The mean beam current is 0.5 μamp.

Many of the shortcomings of this system can be avoided if the beam chopper is placed at the input of the accelerator, directly after the source. Under these conditions, the accelerator is not subject to spurious contamination and the signal-to-noise ratio is improved. In Figs. 43 and 44 are shown a chopper of the type described by King et al. [6, 7]. It consists of two pair of deflection plates which are connected in parallel with an

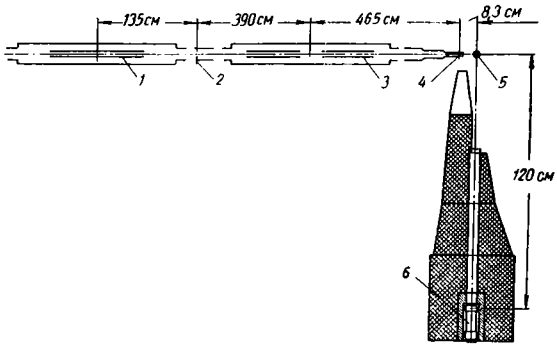

Fig. 42. Diagram of the Los Alamos apparatus used for studying inelastic scattering of neutrons by a time-of-flight method: 1) Deflection plates of the chopper; 2) aperture; 3) electrostatic focusing system; 4) target; 5) scatterer; 6) scintillation counter in the collimator.

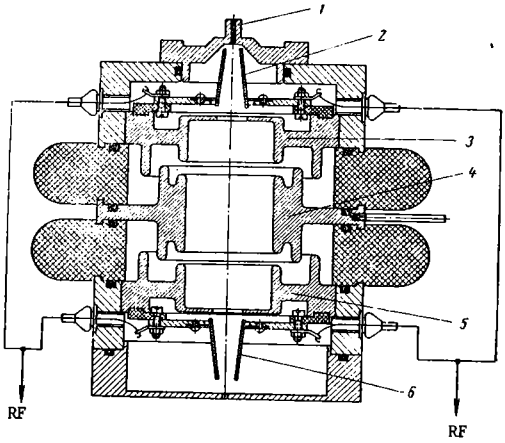

Fig. 43. Chopper used at the input of the van de Graaff generator [6, 7]: 1) Channel for ion source; 2 and 6) deflection plates; 3, 4, and 5) electrodes of the electrostatic lens.

electrostatic lens between them; this lens focuses the ion beam on the input of the accelerator aperture. Neiler et al. [8] have used this chopper with the van de Graaff generator to study the neutron spectrum obtained in (d, n) reactions on light nuclei. At a deflection frequency of 2 Mc the total resolving time of the spectrometer ranges from 6 to 4 mμsec, with mean target current of 0.6 and 0.25 μamp, respectively. The background from the accelerator is an order of magnitude smaller than that with the chopper at the output.

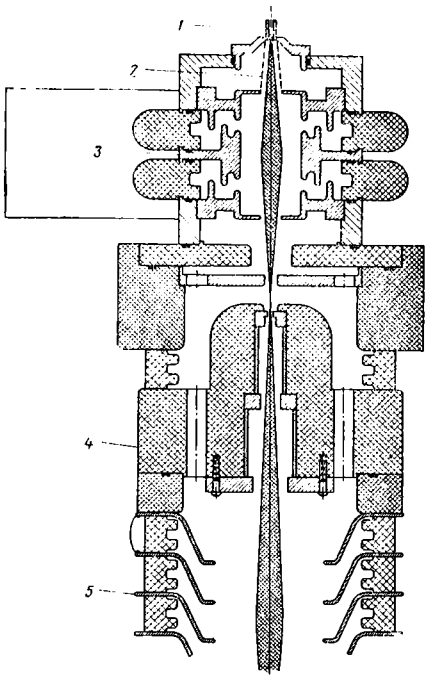

Fig. 44. Diagram of the arrangement of the chopper at the input of the van de Graaff generator [6, 7]: 1) Channel for the ion source; 2) the deflection plates of the chopper are not shown; 3 and 4) electrostatic lenses; 5) first accelerating electrode.

A similar chopper has been described in detail in a later paper by Turner and Bloom [9]. In a paper by Bertozzi et al. [10], who studied a photoneutron spectra, a chopper was used to chop the beam at the input to the van de Graaff generator which served as an injector for a linear electron accelerator.

Various methods of bumching the ions can be used in order to increase the instantaneous current of accelerated particles when pulse operation is used. In 1952 Mobley [11] proposed a method for obtaining short intense ion pulses by means of a focusing magnet. The principle is illustrated in Fig. 45. A chopper, which consists of a pair of deflection plates (1) placed at a focus of the magnet, and a diaphragm (2), is used to chop a monoenergetic ion beam. In the motion of the beam from left to right, ions which have passed through earlier must traverse a longer path in order to arrive at the second focus of the magnet. It is possible to make the geometry such that the ions arrive at the target (6) at the focus of the magnet in the form of a short bunch. When the beam moves in the reverse direction the ion bunches are spread. This situation can be avoided by using an aperture in the form of a slit in the horizontal plane (plane of the figure) and using a second pair of deflection plates which remove the beam from the horizontal plane when it reverses its motion.

When the total deflection angle is 90° the outer trajectory is longer than the inner trajectory by an amount 2s where s is the width of the beam at the input to the magnet. In order to ensure that the ions at the output from the magnet are collected in one plane, it is necessary that the sweep velocity of the beam, taken along the line AB, be half the ion velocity. In this case, the length of the ion arc at the input to the magnet will be 2s while the duration of the pulse at the target is $2x/v$, where x is the thickness of the beam at the input to the system and v is the ion velocity.

In the general case the pulse length is $\frac{x}{v'}$, where v' is the beam sweep velocity along the line AB and the pulse current is $I = I_0 \cdot \frac{s}{x}$, where I_0 is the initial beam current. When $s = 20$ cm and $x = 0.2$ cm, which is the case for the van de Graaff generator, $I = 100\ I_0$. Consequently, with all other conditions being equal, a system of this kind provides an increase in target current by a factor of 100 as compared with the simple chopper; there is a corresponding improvement in the signal-to-noise ratio. With a good monochromatic beam the duration of the pulse can easily be made 10^{-10} sec.

Although, it is inherently simple, the ion bunching method proposed by Mobley has not yet been applied because it requires a high deflection voltage (100 kv), a large magnet, and a very accurate field geometry.

Moreover, in order to change the energy of the particles, it is necessary to go through a rather complicated adjustment procedure and this nullifies one of the chief advantages of the van de Graaff generator – the possibility of smooth variation of particle energy. In order to avoid this disadvantage Mobley and Albritton [12] developed a special stabilized generator for providing a sinusoidal voltage whose frequency could be changed rapidly.

The principle shortcoming of this method is the deterioration in beam geometry: in place of a parallel beam the target sees a beam with a rather wide divergence angle (10-20°).

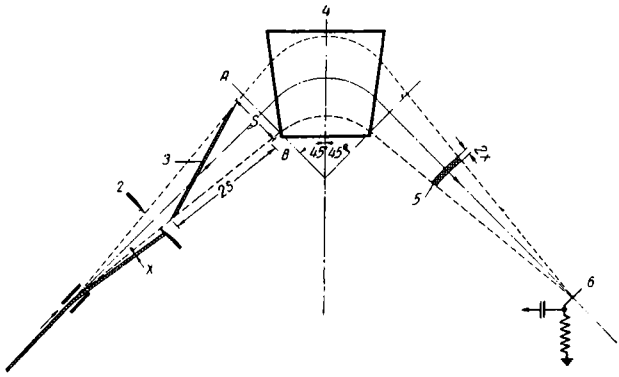

Fig. 45. Ion bunching by means of a focusing magnet: 1 and 2) Deflection plates and aperture of the chopper; 3) ion bunch; 4) magnet; 5) compressed ion bunch; 6) target.

A very effective method for bunching ions, accelerated to 200 kev, has been realized by Flerov and Tamanov [13]. This method is similar to that used in klystrons for obtaining short electron pulses. By means of a sinusoidal field, the direction of which coincides with the beam axis, the velocity of ions which enter the system at different instants of time is modified so that after passing along a definite drift length the ions are bunched and strike the target in short bunches. If a beam of monoenergetic ions is introduced into an accelerator gap, to which is applied a cosinusoidal voltage (Fig. 46) with amplitude small compared with the ion energy, ions which enter the accelerator gap at the beginning of the first half of the cycle will be slowed down while those which enter at the end of the cycle are accelerated. Because of the difference in ion velocities, ions which pass through the accelerating gap in the first half-cycle are compressed into a small bunch after a distance L, which depends on the ratio of the initial ion energy to the amplitude of the oscillating voltage. On the other hand, ions which pass through the gap during the second half-cycle are spread out. If an additional system is used to modulate the beam in such a way that ions pass through the accelerating gap only at the middle of the first half-cycle (shown cross-hatched Fig. 46) these ions will arrive at a target located at a distance L in short bunches, once per period of bunching voltage.

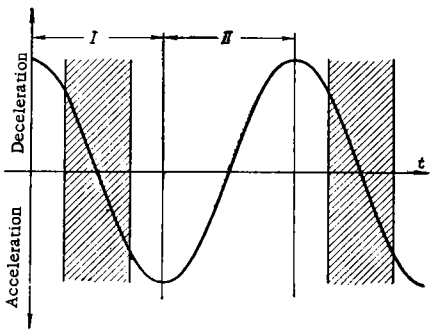

Fig. 46. Ion bunching by means of a sinusoidal accelerating voltage.

A calculation shows that with this method it is possible to obtain ion pulses of the order of 10^{-10} sec; the pulse current is increased by a factor of 100 or more as compared with a simple method of beam chopping.

A diagram of an experimental system used by Flerov and Tamanov is shown in Fig. 47. Preliminary chopping of the beam is accomplished by means of two pair of deflection plates (1) and (3) which are perpendicular to each other (separated by a distance of 22 cm) and an aperture (7) which is located at the output of the system. A sinusoidal deflection voltage (5 Mc) is applied to the deflection plates. The distance between the two pair of plates is chosen in such a way that ions with an energy of 200 kev pass through it in one quarter of a period of the deflection voltage; so the beam is swept in a circle and strikes the aperture (7) once per period (see Fig. 47).

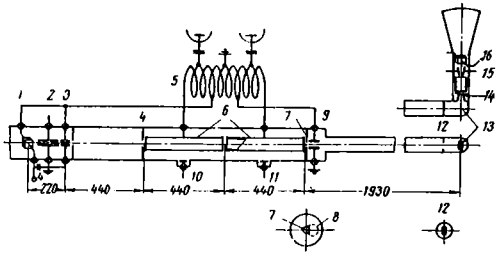

Fig. 47. Diagram of the apparatus used by Flerov and Tamanov [13]: 1, 2, 3, and 9) Deflection plates; 4, 7, and 12) apertures; 5) oscillator circuit; 6) tubular electrodes; 8) trace of the ion beam on the diaphragm; 10, 11) outputs for measuring the high-frequency voltage at the electrodes; 13) target; 14, 15, and 16) electrodes of the oscilloscope.

The ion bunching system consists of two tubular electrodes (6) and grounded diaphragms (4 and 7) which are located at the input to the first electrode and the output of the second. Thus, there are three accelerating gaps. The tubular electrodes are connected to the output tank circuit (5) of a push-pull oscillator (frequency 5 Mc) with an output power of 250 watts. The length of the tubular electrodes is chosen in such a way that during the time-of-flight of the ions through each electrode the phase of the oscillating voltage changes by 180°. Owing to this situation all three gaps act in the same way and the effective accelerating voltage is twice as large as that provided by the oscillator. The latter voltage is approximately 5 kv.

In the present case the ion bunching takes place at a distance of 193 cm from the output of the system. With an ion current of $I_0 = 67$ μamp in the accelerator and a pulse repetition frequency of five megacycles, the average current at the target is 12 μamp, i.e., 18% of I_0.

In order to make an experimental investigation of the duration of the ion pulses, Flerov and Tamanov used the converted oscilloscope which is shown in Fig. 7. The secondary electrons which are produced by the ions at the quartz plate (13) are focused on the screen. The accelerating voltage in the tube is 9 kv and the beam is swept at a frequency of 5 Mc . Careful investigation showed that the duration of the ion pulses at the target was less than $5 \cdot 10^{-10}$ sec under certain conditions. In this case, the pulse current was increased by a factor of 70 as compared with the current when ion bunching was (absolute magnitude was 5 ma).

A similar method of ion bunching has been used by Nakada et al. [14-16] with a Cockcroft-Walton accelerator which provided deuterons with an energy of 500 kev.

A disadvantage of the method is the beam divergence which arises as a result of the preliminary chopping; this divergence is undesirable because it is necessary to have a large distance between the output of the modulator and the target. A reduction in this distance can be achieved only by increasing the bunching voltage; this is inconvenient since it leads to an increase in the energy spread. Inasmuch as the divergence angles of the beam are not very large, this shortcoming can be avoided through the use of some kind of focusing system which is applied to the beam after it passes through the modulator.

The unavoidable small nonmonochromaticity of the beam (10-20 kev) which arises in bunching is not an important shortcoming in reactions which yield neutrons with energies of several million electron volts.

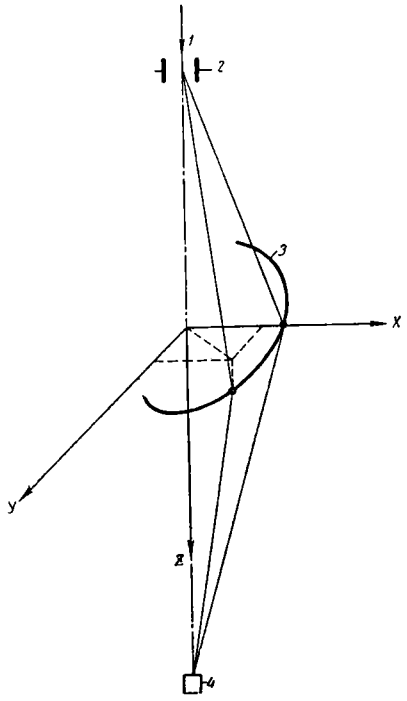

Fig. 48. Diagram showing ion-bunching scheme proposed by Shapiro [17]. 1) Ion beam; 2) deflection plates; 3) target in the form of a spiral; 4) scatterer.

Flerov and Tamanov indicate the possibility of using this method to obtain short, intense ion pulses at energies of several million electron volts by locating the modulator between the ion source and the accelerator of a van de Graaff generator. It is possible, however, that this arrangement may lead to certain difficulties due to the focusing conditions in the generator.

A unique method of increasing the pulse intensity of a neutron beam has been suggested by Shapiro [17]. By displacing the beam over a target which is bent into a spiral (Fig. 48) it is possible to achieve conditions in which neutrons produced later traverse an appropriately shorter path to the detector. It is apparent that the bunching conditions are satisfied only for a narrow range of neutron energies. The author believes that this method can be used to increase the intensity of the neutron flux by two orders of magnitude.

It is possible that this method of bunching will be useful for studying secondary neutron spectra when the primary neutrons are monochromatic and it is possible to satisfy the bunching conditions at the scatterer. Furthermore, in this case the requirements on certain complexities of target construction are relieved.

§ 2. Use of the Inherent Modulation of a Cyclotron Beam

The acceleration mechanism in a cyclotron is such (see, for example, [18, 19]) that at the terminal radius there are only particles which pass through the gap between the dees at some definite phase of the radio-frequency accelerating voltage (RF). The ejection of particles from the chamber by means of an electrostatic deflector compresses the phase interval still further. As a result, particles which are accelerated in a cyclotron are ejected from the cyclotron in short pulses, once per RF period. As a rule, the duration of the particle pulse from a fixed-frequency cyclotron is less than several percent of the RF period.

Bloom [20, 21] has measured the width of the particle pulse for particles accelerated at the 46-cm cyclotron at the Brookhaven laboratory (USA) by studying the coincidences of γ-rays from the target with pulses synchronized with the RF; it was found that the pulse width was 1-2 mμsec (the RF period was 54 mμsec).

According to measurements made by Grismore and Parkinson [22] the duration of the deuteron pulse at the target of the one-meter cyclotron at the University of Michigan (USA) is 4 mμsec (the RF period is about 100 mμsec).

The one and one-half meter cyclotron of the Institute for Atomic Energy Academy of Sciences, USSR, with proper adjustment, gives particle pulses at the target which are less than 3 mμsec long (the RF period is about 100 mμsec) [23].

This same pulse duration is obtained at the 80-cm cyclotron of the Nobel Institute of Physics (Sweden) (RF period 82 mμsec [24]) and the two-meter variable energy cyclotron at Livermore (USA [25]).

The width of the particle pulse depends on the adjustment of the cyclotron. It has been shown experimentally, as is to be expected, that the width of the pulse increases with increasing RF amplitude. It also depends on the voltage at the deflection plate and is reduced with resonance detuning (for example, by changing the magnetic field). For a value of the deflection voltage close to threshold particle pulses shorter than $5 \cdot 10^{-10}$ sec can be obtained [20, 26].

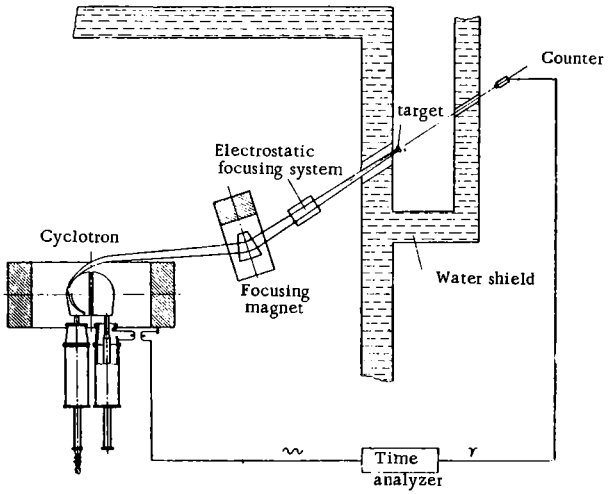

Fig. 49. Arrangement of the neutron spectrometer at the $1^1/_2$ meter cyclotron at the Institute for Atomic Energy, Academy of Sciences, USSR.

In cyclotrons which are designed for neutron work, in order to reduce the background the beam which is extracted from the chamber is focused on a target which is located at a great distance from the cyclotron and is behind a concrete or water shield (for example, at the cyclotron of the Institute for Atomic Energy this distance is 12 meters) (Fig. 49) while at the cyclotron of the Nobel Institute this distance is 8 meters). Thus, the width of the particle pulse at the target (Δt_{pulse}) may be greater than the width of the pulse upon leaving the cyclotron (Δt_1) as a consequence of the energy spread of the accelerated particles; for an extracted beam in which no special monochromatization measures have been taken this quantity is approximately 1% [27-29].

We now consider the effect of nonmonochromaticity on the duration of the proton pulse. If the proton energy is $E \pm \Delta E$, after passing over a distance L the width of the pulse due to the energy spread is

$$\Delta t_2 (\text{m}\mu\text{sec}) = \frac{72{,}3L\,(\text{m})}{\sqrt{E\,(\text{Mev})}} \cdot \frac{\Delta E}{E}.$$

With $\Delta E/E = 0.01$, $L = 12$ m and $E = 9$ Mev (the cyclotron at the Institute for Atomic Energy) we find $\Delta t_2 = 3$ mμsec. If Δt_1 and Δt_2 are independent, $\Delta t_{pulse} = \sqrt{\Delta t_1^2 + \Delta t_2^2}$. Measurements at a remote target give $t_{pulse} < 3$ mμsec. This may be a result of the fact that Δt_1 and Δt_2 compensate each other; apparently the faster particles leave the cyclotron later.

In certain cases a noticeable additional broadening of the pulse is produced by the focusing system because of differences in behavior of different parts of the beam (for example, when a magnetic prism with a large deflection angle is used). This effect is easily avoided by collimating the beam, although this procedure leads to a reduction by a factor of 2 or 3 in the current.

In most cyclotrons the current at a remote target is of the order of 10 μamp.

From what has been indicated it is apparent that a cyclotron is a very convenient "natural" pulsed neutron source.

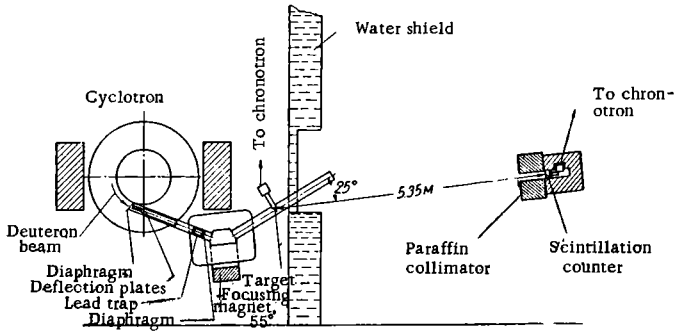

Fig. 50. General arrangement of the neutron spectrometer at the University of Michigan (USA) [22].

In the first spectrometers used with cyclotrons the natural modulation of the beam was used directly [30, 31]. In this case the allowable length of the flight path is limited by the very high repetition rates of the accelerated particle bunches (approximately 10 Mc). Since the beam current of a cyclotron is rather large, the frequency at which the particle bunches appear at the target can be reduced. For a spectrometer resolving time of 3-5 mμsec, in order to obtain a resolving power of the order of 1% for fast neutrons the optimum frequencies turn out to be 1-2 Mc (see § 3, Chapter VIII).

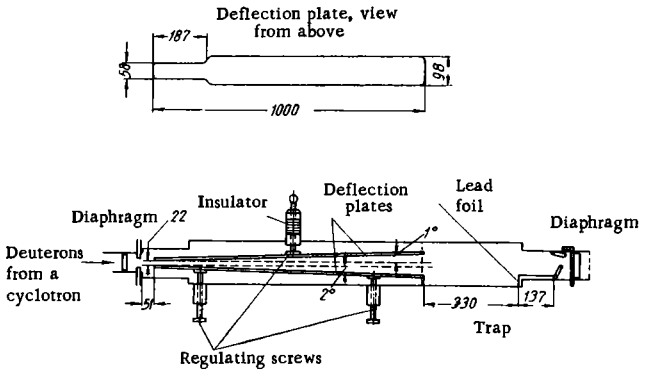

Fig. 51. Deflection system for reducing the pulse repetition rate of the cyclotron beam [22]. The lower plate is grounded and the deflection voltage is applied to the upper plate.

One of the possible methods of reducing the pulse-repetition frequency of a cyclotron has been used by Grismore and Parkinson [22] at the University of Michigan cyclotron (USA). A pair of deflection plates is located directly at the output from the chamber (Figs. 50 and 51); a fixed high voltage is applied to these plates and causes deflection of the beam in a direction perpendicular to the plane of rotation of the particles in the cyclotron. Under these conditions the beam strikes a "trap" covered with lead and cooled by water. By the application of a short high-voltage pulse of the opposite polarity at the required instant of time the beam is deflected into

the normal position and one particle bunch strikes the target. The main element of the apparatus is a pulse generator which consists of two stages. The first stage is a trigger unit which provides pulses 0.6-μsec long at an amplitude of 800 volts. This is synchronized with the cyclotron RF generator through a decade scaler system with with a scaling factor of 10^4. The high-voltage pulse generator is triggered by the trigger circuit and provides at the deflection plates a triangular pulse with rounded top which has a half-width of 0.1 μsec (the RF period is approximately 0.1 μsec) at amplitudes of up to 40 kv. The system is phased with the RF system in such a way that each generator pulse causes the extraction of only one particle bunch. The frequency at which bunches appear at the target is approximately 1 kc (10^4 times smaller than the original RF frequency) and is limited by the time for bringing the pulse generator back to operating condition.

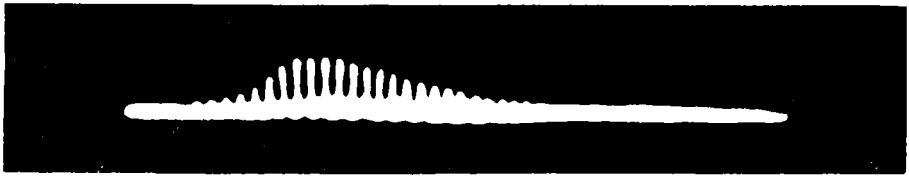

Fig. 52. Oscillogram showing the particle pulses in a cyclotron obtained by modulation of the ion source. The individual ion bunches are clearly visible; one bunch is obtained from the chamber per cycle by the deflection voltage pulse.

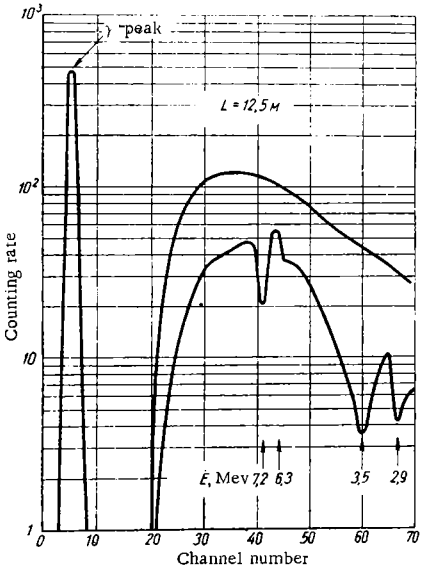

Fig. 53. Time-of-flight distribution of neutrons and γ-rays emitted from a beryllium target bombarded by a deuteron beam from the 1½ meter cyclotron obtained by Draper [32]. The lower curve is the spectrum for neutrons which pass through a carbon absorber.

A similar method of reducing the repetition frequency of cyclotron pulses has been used by Draper at the one and one-half meter cyclotron at Brookhaven laboratory (USA) [32, 33]. The difference in this method from the one considered above is the fact that the deflection plate is used directly as the modulator; to this plate is applied a deflection voltage in the form of short pulses, approximately 50 mμsec long, (the RF period is 90 mμsec), synchronized with the RF in such a way that each pulse causes the extraction of one ion bunch. As in the system used by Grismore and Parkinson, the pulse generator operates at a very low frequency (400-1400 cps).

In order to avoid contamination of the cyclotron by the accelerated particles in the intervals between pulses and to reduce the background Draper used modulation of the ion source, as is conventional for "chopped" cyclotrons and synchronized the operation with the deflection pulse generator. He noted that under these conditions it was possible to increase the instantaneous current (as compared with continuous operation) by almost a factor of 10. In Fig. 52, is shown an oscillogram of the pulses of accelerated particles obtained by modulation of the ion source. The individual ion bunches are clearly seen; one bunch is emitted from the chamber per pulse of deflection voltage.

In Fig. 53 is shown the time-of-flight distribution obtained by Draper for γ-rays and neutrons from a beryllium target bombarded by deuterons with an energy

of 22 Mev. The flight distance is 12.5 m. The counting rate for neutrons in the scintillation counter (a plastic scintillator 5 cm in diameter and 3 cm high) is approximately 100 pulses/sec. The time-of-flight range between 0 and 560 mμsec was investigated. The absence of pulses between the γ-peak and the upper limit of the neutron spectrum is evidence that there is no superposition of spectra of different order.

In spite of the fact that the frequency of the neutron pulses is 1000 times smaller than the optimum frequency, the intensity of the neutron fluxes produced by a large cyclotron is found to be more than sufficient for most experiments in fast-neutron spectroscopy. Sources of this kind are usually convenient for time-of-flight spectroscopy of kilovolt neutrons.

The optimum frequency for fast-neutron spectroscopy (1-2 Mc) can be obtained only through the use of sinusoidal deflection fields as is done in electrostatic generators. In a cyclotron this problem is technologically more complicated because of the high energy and because of the deterioration of the geometric parameters of the beam (the large angular divergence and cross section).

It is natural that the deflection plates of the chopper should comprise part of the resonant oscillatory circuit. The chopper can be located after the deflection system of the cyclotron along the trajectory of the beam. However, it is possible to use the deflection system of the cyclotron itself as a chopper [34]. A modulation scheme of this kind is the simplest possible and will be considered below.

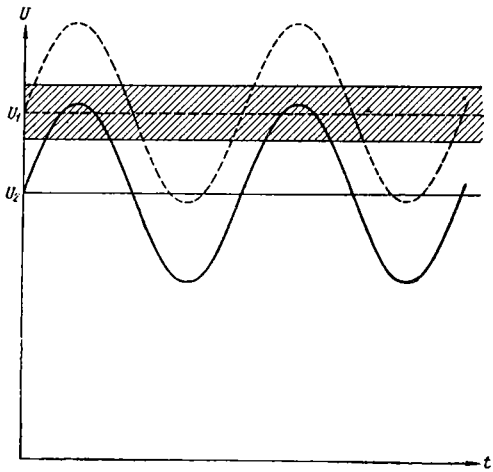

Fig. 54. Possible modes of operation of a system for reducing the repetition frequency of cyclotron pulses by applying a sinusoidal voltage to the deflection system.

The dependence of the current of the extracted beam of the cyclotron on the voltage applied to the deflection plate indicates that there is a region in which the plates are "transparent." Thus, for example, in deuteron acceleration at 14 Mev at the cyclotron of the Institute of Atomic Energy this region extends from 50 to 70 kv. For power economy it is desirable to apply to the deflection plate both high-frequency and dc voltages since the transparency region, as a rule, is several times smaller than the mean deflection potential.

In Fig. 54 are shown two possible modes of operation:

1) The fixed potential U_1 can be chosen in such a way that in the absence of the high-frequency voltage the beam passes through the deflection system without interference (dashed line on the figure);

2) The fixed potential U_2 is chosen so that with no high-frequency voltage the deflection system is "closed," it is "opened" at the peaks of the sinusoidal high-frequency voltage (the solid lines on the figure).

In the latter case, during the time in which the ion bunches pass through the deflection system the voltage applied to the system remains essentially constant and close to the optimum value. This situation helps to maintain a constant intensity of the bunches which pass through the system. Moreover, this mode of operation does not require precise phasing of the high-frequency voltage at the deflection plates with respect to the accelerating voltage of the cyclotron.

§ 3. Obtaining "Time Markers"

In order to analyze the neutron distribution by time-of-flight it is necessary to have "time markers," i.e., control or reference signals which are synchronized with the neutron pulses.

The most direct method for obtaining time markers is to use the electric pulses which are produced in the target when it is struck by the charged particles. This method would seem to be convenient in work with the cyclotron since any problem of phase instability is avoided. However, in practical cases, it turns out to be very inconvenient and is used only rarely.

In Fig. 55 is shown a scheme used by Grismore and Parkinson [22] for obtaining pulses from the target of a cyclotron at the University of Michigan (the general set-up is shown in Fig. 50).

The accelerated particles are completely absorbed in a lead plate. They strike it through a lead foil window in an electrostatic shield. The other side of the shield has the same sort of covering. The target material is deposited on the foil of one of the windows. When the holder is rotated through 180° the other window is placed in front of the beam and the background is measured.

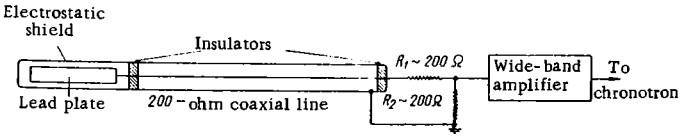

Fig. 55. Scheme for obtaining electric pulses from the cyclotron target [22].

Pulses from the target are 20 mμsec long (the pulse duration is determined by the choice of resistances R_1 and R_2 for the best operation of the chronotron) for accelerated-particle pulse lengths of approximately 4 mμsec at the target. At average beam intensity the pulse amplitudes are approximately 10 millivolts. Before being applied to the chronotron the pulses are amplified in a wide-band amplifier.

A disadvantage of this system is the dependence of pulse amplitude on beam current. In addition, this system imposes certain limitations on the construction of the target which are not always compatible with the requirements of the experiment. These shortcomings are less important when the accelerator target is used as a source of monochromatic neutrons for studying secondary processes.

Another method of obtaining controlled pulses is the detection of some of the accelerated particles by a fast scintillation counter located in front of the target. Malmfors et al. [24] has used a liquid scintillator in a thin-walled aluminum tube with an RCA-5819 photomultiplier for this purpose. The liquid scintillator is used since it is more impervious to the bombarding particles. Apparently the best scintillator for this purpose would be a gaseous scintillator.

Sometimes it is possible to obtain a scintillation pulse directly from a gas target. For example, Smith [3], by bombarding a deuteron gas target with deuterons of about 1.5 Mev energy, was able to obtain pulses with amplitude sufficient for observation on a fast oscilloscope, through the use of an RCA-6328 photomultiplier placed inside the target.

Obtaining controlled pulses by means of a scintillation counter which records the primary particles involves difficulties in carrying out good time analysis: the amplitude of the pulses is strongly affected by the beam intensity.

In practice the most convenient method of obtaining time markers turns out to be "locking" to the sinusoidal voltage used for modulating the beam (the voltage at the electrodes of the chopper placed in the van de Graaff generator [35], or the cyclotron accelerating voltage [23, 30, 36, 37]). In this case the problem of obtaining controlled pulses is simplified since the dependence of pulse position and amplitude on beam intensity is completely eliminated.

In the cyclotron a difficulty arises which is connected with the fact that the phase of particle ejection from the cyclotron depends on its adjustment. Uncontrollable changes in the cyclotron parameters during the time of a measurement of a neutron spectrum can lead to distortion in the results. An experiment on the cyclotron at the Institute for Atomic Energy has shown that with changes in the cyclotron parameters which lead to a reduction in the average current of the target of less than a factor of 10 the position of the γ-peak can change by ± 10 mμsec.

By stabilizing the main parameters of the cyclotron (RF amplitude [38], deflection voltage [39] etc.) it is possible to eliminate uncontrollable phase changes which appear over a long period of time (the period between shutdowns for replacing the source filament) to a magnitude which is negligible compared with the width of the γ-peak. In this case there is a considerable improvement in the stability of the beam current.

The method of "processing" the sinusoidal voltages required for obtaining time markers depends on the time analyzer which is used. Certain analyzers can work directly from the sinusoidal voltages. The majority of multichannel analyzers require standard pulses of fairly high duration (10 mμsec) as time markers. Various generators are used for forming these pulses from the sinusoidal voltages. Certain of these generators are discussed in Chapter VII.

LITERATURE CITED

[1] B. Jennings and G. Griffits, Phys. Rev. 91, 440 (1953).

[2] L. Cranberg and J. S. Levin, Phys. Rev. 103, 343 (1956).

[3] R. V. Smith, Conference on Neutron Physics by Time-of-Flight, Gatlinburg, (Tennessee, USA, 1956), p. 103.

[4] R. E. Holland, F. J. Lynch, and K. Tsukada, Bull. Am. Phys. Soc. Ser. 2, 3, 103 (1958).

[5] L. G. Kuo, Centre d'Etudes Nucleaires de Saclay, France, private communication.

[6] V. E. Parker and R. F. King, Bull. Am. Phys. Soc. Ser. 2, 1, 70 (1956).

[7] H. E. Banta, R. F. King, and J. P. Judish, Bull. Am. Phys. Soc. Ser. 2, 1, 70 (1956).

[8] W. M. Good, J. H. Neiler, and J. H. Gibbons, Bull. Am. Phys. Soc. Ser. 2, 1, 71 (1956).

[9] C. M. Turner and S. D. Bloom, Rev. Sci. Instr. 29, 480 (1958).

[10] W. Bertozzi, F. R. Paolini, and C. P. Sargent, Phys. Rev. 110, 790 (1958).

[11] R. C. Mobley, Phys. Rev. 88, 360 (1952).

[12] R. C. Mobley and B. R. Albritton, Phys. Rev. 98, 232 (1955).

[13] N. N. Flerov and E. A. Tamanov, J. Atomic Energy 3, 44 (1957).

[14] M. P. Nakada, V. J. Ashby, M. Harris, and W. Klein, Bull. Am. Phys. Soc. Ser. 2, 1, 69 (1956).

[15] J. Benveniste, C. C. Gardner, M. P. Nakada, and C. Wong, Bull. Am. Phys. Soc. Ser. 2, 1, 175 (1956).

[16] J. D. Anderson, C. C. Gardner, M. P. Nakada, and C. Wong, Phys. Rev. 110, 160 (1958).

[17] F. L. Shapiro, Inst. and Exp. Tech. (USSR) 1, 33 (1957).

[18] D. Bohm and L. Foldy, Phys. Rev. 72, 649 (1947).

[19] B. L. Cohen, Rev. Sci. Instr. 24, 589 (1953).

[20] S. D. Bloom, Phys. Rev. 98, 233 (1955).

[21] S. D. Bloom, C. Muehlhause, and H. Wegner, Phys. Rev. 99, 654 (1955).

[22] R. Grismore and W. C. Parkinson, Rev. Sci. Instr. 28, 245 (1957).

[23] A. A. Kurashov, F. Linev, B. V. Rybakov, and V. A. Sidorov, J. Atomic Energy 5, 135 (1958).

[24] K. G. Malmfors, J. Kjellman, and A. Nilsson, Nuclear Instruments 1, 186 (1957).

[25] M. P. Nakada, J. D. Anderson, C. C. Gardner, J. McClure, and C. Wong, Phys. Rev. 110, 594 (1958).

[26] J. H. Manley and M. J. Jakobson, Rev. Sci. Instr. 25, 368 (1954).

[27] E. C. Creutz and R. R. Wilson, Rev. Sci. Instr. 17, 385 (1946).

[28] B. V. Rybakov, J. Exptl.-Theoret. Phys. (USSR) 28, 651 (1955).

[29] A. Nilsson, Arkiv för Fysik 13, 280 (1958).

[30] G. F. Bogdanov, A. A. Kurashov, B. V. Rybakov, and V. A. Sidorov, J. Atomic Energy 1, 66 (1956).

[31] C. O. Muehlhause, S. D. Bloom, H. E. Wegner, and G. N. Glasoe, Phys. Rev. 103, 720 (1956).

[32] J. E. Draper, Conference on Neutron Physics by Time-of-Flight (Gatlinburg, Tennessee, 1956), p. 146.

[33] J. E. Draper, Rev. Sci. Instr. 29, 137 (1958).

[34] V. S. Panasyuk, J. Atomic Energy 3, 47 (1957).

[35] W. Weber, C. W. Johnston, and L. Cranberg, Rev. Sci. Instr. 27, 166 (1956).

[36] G. F. Bogdanov, N. A. Flasov, S. P. Kalinin, B. V. Rybakov, and V. A. Sidorov, J. Atomic Energy 3, 204 (1957).

[37] G. N. Glasoe, H. H. Landon, A. J. Elwyn, and S. Oleksa, Proceedings of International Conference on the Neutron Interactions with the Nucleus , Columbia University (New York, 1957), p. 230.

[38] A. V. Antonov, Yu. V. Korshunov, E. A. Meleshko, and V. S. Panasyuk, Inst. and Exp. Tech. (USSR) 1, 41 (1958).

[39] B. S. Kozachina, N. Z. Kub'shkin, and A. I. Nastyukha, Inst. and Exp. Tech. (USSR) (1959).

NEUTRON DETECTORS

The neutron detector in a time-of-flight spectrometer for the megavolt region is usually a scintillation counter with an organic scintillator which detects neutrons by means of the recoil protons. In certain cases it is also possible to use gaseous scintillators. General information on scintillation counters can be found in numerous sources [1-7]. Here we shall consider only those characteristics which are most important for our purposes — neutron-detection efficiency and resolution time.

§ 1. Efficiency of a Counter with an Organic Scintillator

In principle, a scintillation counter which records neutrons by means of the recoil protons is no different from an ionization chamber which is filled with a hydrogenous gas. Just as in an ionization chamber, a device of this type can be used to a study simple neutron spectrum on the basis of the integrated recoil-nucleus spectrum and can be used to make absolute measurements of monoenergetic neutron fluxes, in which case its efficiency is considerably greater than the efficiency of an ionization chamber with the same working volume. However, the applicability of a single scintillation counter is limited to a great extent because of the high sensitivity to γ-rays.

The high efficiency of a scintillation counter and the possibility of making absolute measurements of a neutron flux are realized in a time-of-flight spectrometer, where the counter may be considered a detector for monoenergetic neutrons. In the investigation of an arbitrary neutron spectrum, which is usually accompanied by a γ-ray background, a given channel of a multichannel time analyzer (or a single channel analyzer with a fixed delay) chooses from all the counter pulses only those pulses due to neutrons whose energy is associated with a given time of flight.

The efficiency of a counter for neutrons of a given energy can be easily computed if the energy threshold B is known. From Eq. (16) it follows that the number of recoil protons with energies $E < B$, referred to the total number of protons is:

$$W(B,\ E) = \int_B^E \frac{dE_p}{E} = 1 - \frac{B}{E}\,. \tag{39}$$

Multiplying Eq. (39) by the probability for scattering of a neutron on protons in the scintillator we obtain the counter efficiency for neutrons of energy E

$$\varepsilon = nh\sigma\left(1 - \frac{B}{E}\right), \tag{40}$$

where n is the number of hydrogen atoms in 1 cm^3 of the scintillator; h is the thickness of the scintillator (which is assumed small compared with the mean free path) and σ is the total cross section for n, p scattering.

If the counter threshold is known in units of neutron energy, Eq. (40) gives both the energy dependence of the counter efficiency as well as its absolute value. In order to calibrate the scale of the amplitude selector in energy units (given by the counter threshold) it is sufficient to measure the pulse spectrum of the counter when it is irradiated by monoenergetic neutrons of known energy. The calibration can be carried out using neutrons with a complex spectrum if one makes use of the possibility of selecting neutrons of a given energy by time-of-flight. However, in isolating a narrow energy range from a complicated neutron spectrum one finds a considerable reduction in the counting rate, especially if a differential amplitude spectrum is being measured. For this reason, it is more desirable to use a strong line in the neutron spectrum.

For example, in order to calibrate the single-channel spectrometer at the Institute for Atomic Energy [8] use is made of the neutrons from the T (p, n) He^3 reaction; this reaction is produced by bombarding a tritium-zirconium target on a tungsten base with protons. The neutrons from this reaction are distinguished from the γ-rays and the soft neutrons produced in the interaction of the protons with the zirconium and tungsten by means of a single-channel time analyzer. In this case use is made of a so-called "wide" channel (§ 1, Chapter VII) which covers the entire neutron line and provides 100% efficiency for the fast coincidence circuit at neutron energies greater than 0.3 Mev.

In Fig. 56 are shown the integrated and differential pulse spectra for a scintillation counter with a stilbene crystal (diameter 3 cm, height 2 cm) obtained at a neutron energy of 9 Mev. The shape of the spectra is in excellent agreement with the energy distribution for the recoil protons (16). The smearing of the upper edge of the spectrum is due to the finite amplitude resolution of the counter. The rise close to zero is due chiefly to the nonlinearity in the dependence of scintillator light yield on proton energy.

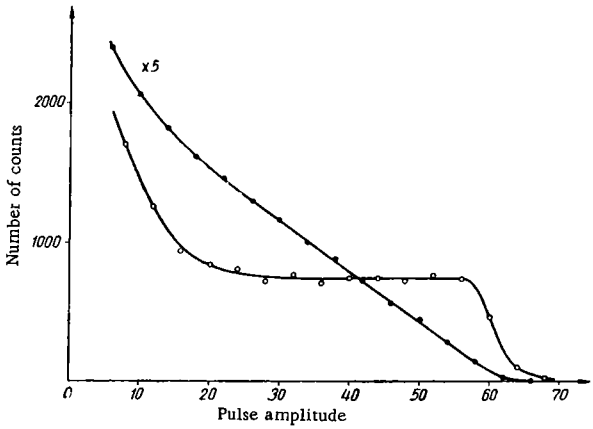

Fig. 56. Integrated and differential pulse spectra for a scintillation counter with a stilbene crystal (diameter 3 cm, height 2 cm) for irradiation by neutrons with an energy of 9 Mev.

The position of the upper edge of the pulse spectrum gives a relation between the pulse amplitude and the proton energy, but only at one value of the energy; this is a result of the nonlinearity in the light yield of the organic scintillator. Investigations of the amplitude spectra for counter pulses at several values of neutron energy show that the size of the pulses corresponding to the spectral limits are in good agreement with the dependence of light yield of stilbene on proton energy obtained in other work [9, 10].

A light yield curve for stilbene is shown in Fig. 57. Along the abscissa axis is plotted the proton energy; the electron energy is plotted along the ordinate axis. A measurement of the light yield in units of electron energy [10] makes it possible to calibrate the counter for γ-rays. When excited by electrons, stilbene exhibits a light yield which is linear even at energies greater than 10 kev.

Using the light-yield curve, by measuring the amplitude spectrum corresponding to one neutron line it is possible to calibrate the scale of the amplitude selector in energy units over a wide region [8, 11].

The accuracy with which the efficiency is determined depends to a large degree on the errors in the determination of the energy threshold of the counter. In Fig. 58 is shown the dependence of the product $\sigma\left(1-\frac{B}{E}\right)$ which determines the energy dependence of the efficiency for several values of B. The rapid increase in efficiency close to threshold is due to the reduction in the ratio $\frac{B}{E}$; the subsequent drop is a result of the dependence of

the n,p cross section on energy. It is apparent that the error in the determination of counter efficiency due to the uncertainty in the determination of the threshold is especially large in the region of the sharp rise close to threshold.

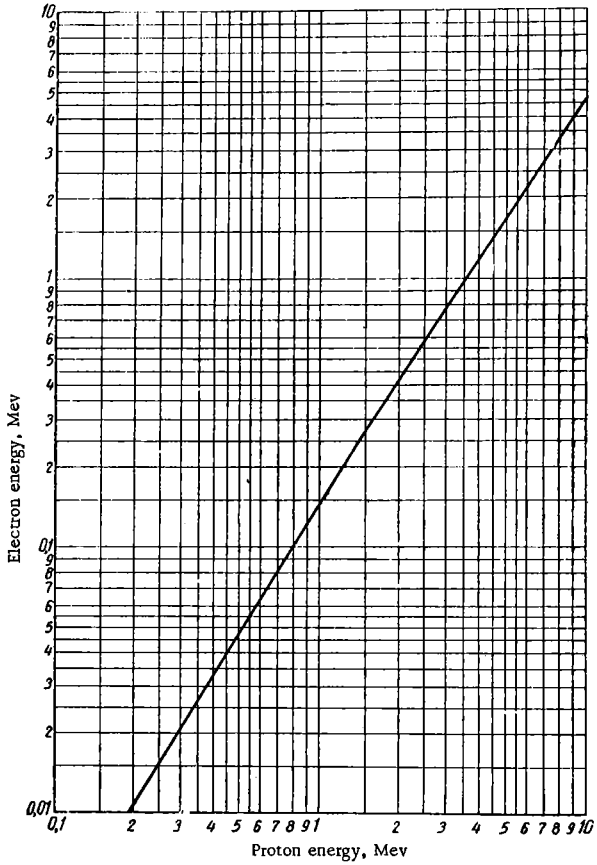

Fig. 57. Light output of stilbene as a function of proton energy. The ordinates and abscissa of points on the curve correspond to the energies of an electron and proton which give the same light pulse.

As is apparent from Eq. (40), the relative error in the determination of the efficiency is equal to the relative error in the determination of the threshold at $E = 2B$; as the energy is reduced, this error increases sharply. Hence, the counter threshold should be made as low as possible. In what follows, we shall assume that the following condition is always satisfied:

$$B < 0.7\,E_{\min}, \tag{41}$$

where E_{min} is the lower limit of the neutron energy being investigated.

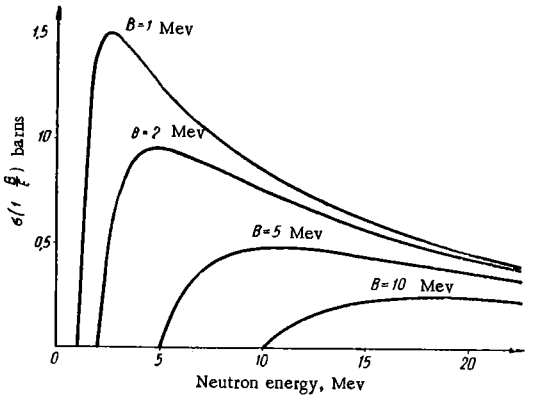

Fig. 58. Energy dependence of the efficiency of a neutron counter with an organic scintillator for several values of the threshold B.

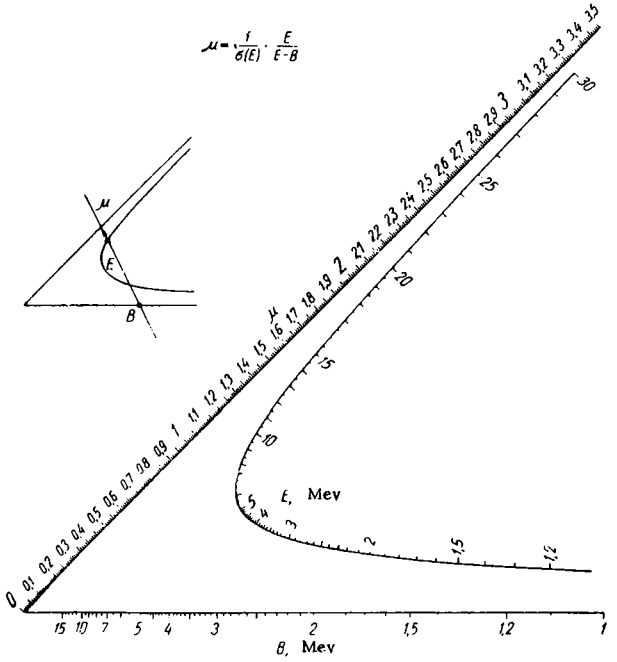

Fig. 59. Nomogram for determining the factor μ (E, B), which takes account of the energy dependence of the efficiency of a neutron counter with an organic scintillator.

In order to take account of the energy dependence of the counter efficiency the experimental data must be multiplied by $\mu(B, E)$:

$$\mu(B,\ E) = \frac{1}{\sigma(E)\left(1-\frac{B}{E}\right)} = \frac{1}{\sigma(E)} \cdot \frac{E}{E-B}.$$

In Fig. 59 is given a nomogram with which it is possible to find the quantity μ rapidly for given values of B and E.

Eq. (40) for the counter efficiency has been obtained taking into account the interaction of neutrons only with the hydrogen in a "thin" scintillator, under the assumption of isotropic n, p scattering. We now analyze the additional effects which can lead to a change in counter efficiency and show that under the conditions which usually obtain, Eq. (40) is valid to within at least 10%.

Interaction of Neutrons with Carbon Nuclei

The usual composition of the majority of organic scintillators is essentially CH. The total cross section of carbon for neutrons in the megavolt region is essentially the same as the cross section for n, p scattering; at E > 10 Mev it becomes greater than the cross section for n, p scattering. Consequently, detection of interaction events between neutrons and carbon nuclei can lead to a considerable difference in efficiency from the expression given in Eq. (40). This increase in counter efficiency has been observed experimentally [12]. The basic role is played by inelastic interactions of neutrons with carbon nuclei, since the pulses due to elastic scattering of neutrons on carbon can be detected only at very low counter thresholds.

The energy transferred to the recoil carbon nucleus by the neutron is less than 0.28 E. Because of the strong reduction in the light yield of an organic scintillator at high ionization density the carbon nucleus produces a flash which is many times smaller than that produced by a proton of the same energy. As a result, the ratio of the maximum counter pulse due to a carbon recoil nucleus to the maximum counter pulse due to a recoil proton is very small. According to measurements made by Draper [13], for neutrons with an energy of 1 Mev, this ratio is less than 0.07. At neutron energies greater than 10 Mev, the probability for inelastic interactions with carbon nuclei becomes significant.

$$C^{12}(n,\ \alpha)Be^{9} \qquad Q = -5{,}75 \text{ Mev}$$
$$C^{12}(n,\ n'\alpha)Be^{8} \rightarrow 3\alpha + n \qquad Q = -7{,}34 \text{ Mev.}$$

The cross section for the C^{12} (n, α) Be^{9} reaction is small. For example, for neutron energies of 14 Mev it amounts to 1% of the cross section for n, p scattering.

TABLE 2

E	$\frac{\sigma}{\sigma} n, 3\alpha$	$E_{3\alpha}$	$E_{p\alpha}$	$E_{p\alpha}/E$
10	—	2,7	0,8	0,080
12	0,20	4,7	1,5	0,125
14	0,32	6,7	2,2	0,157
16	0,53	8,7	2,8	0,175
18	0,56	10,7	3,7	0,205
20	0,50	12,7	4,6	0,230
30	—	22,7	9,5	0,316

The ratio of the cross section for the reaction in which C^{12} divides into 3 α-particles under the effect of neutrons with energies between 10 and 20 Mev to the cross section for n, p scattering is shown in Table 2 for several values of neutron energy. In order to give an idea of the magnitude of the counter pulses which are produced in the disintegration of carbon, in the Table are also shown the total energies for three α-particles obtained in the splitting of C^{12}, $E_{3\alpha}$, and the proton energy $E_{p\alpha}$ for a proton which gives the same pulse as an α-particle with energy $E_{3\alpha}$.

In the "soft" part of the energy region (E < < 10 Mev) where there is only elastic scattering of neutrons on carbon, the counter efficiency is purely "hydrogenous" even when $\frac{B}{E} > 0.07$. In the "hard" part of the region (E > 10 Mev), as is apparent from Table 1,

the "carbon" component of the counter efficiency can be neglected only when $\frac{B}{E} > 0.3$. In actual fact the conditions are somewhat less stringent, because, on the average, the counter pulse due to 3 α-particles with total energy $E_{3\alpha}$ is less than the pulse from a single α-particle with the same energy; this is a result of the non-linearity in the light yield of the scintillator. Whence, it follows that if the counter threshold is fixed, in the hard part, absolute measurements of a neutron flux can be carried out simultaneously only over a narrow range of neutron energy since $\frac{B}{E}$ must be less than 0.7 (41). In this connection it turns out to be very desirable to use the "tracking-threshold" method described in § 2, Chapter VIII.

Attenuation of the Neutron Flux in the Scintillator

If the thickness of the scintillator is comparable with the neutron mean free path, in computing the counter efficiency it is necessary to take account of the attenuation of the neutron flux in the scintillator.

We shall assume that scattering of neutrons on hydrogen removes them from the beam. This assumption is valid in the case in which all recoil protons are recorded since in this case back-scattering of the neutrons on a proton never adds additional counts.

The existence of a finite threshold in the counter means that multiple n, p scattering leads to a somewhat higher efficiency than is indicated by Eq. (40). We consider this effect separately.

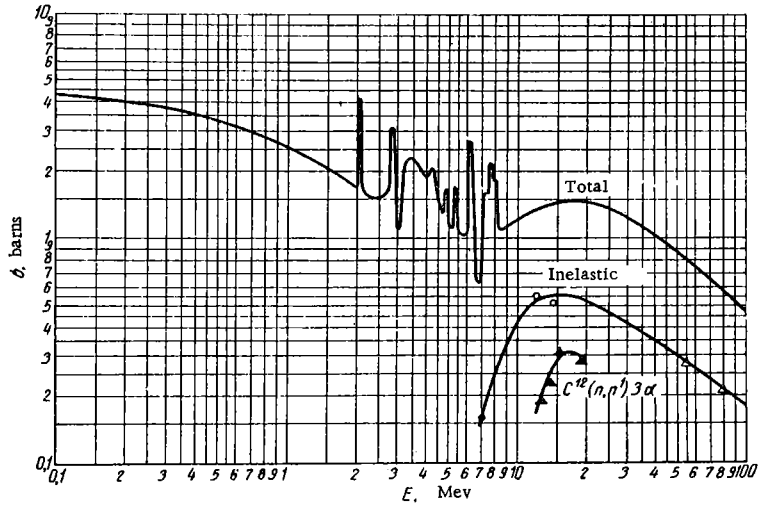

Fig. 60. Cross section for interaction of neutrons with carbon.

For the usual scintillator shape ($r \sim h$), elastic scattering of neutrons on carbon nuclei need not be considered since neutrons are deflected from the original direction with almost no loss of energy (the carbon nucleus is considerably heavier than the neutron). An inelastic interaction of a neutron with a carbon nucleus (which is important in the hard part of the region) leads to the removal of neutrons from the beam if the condition $\frac{B}{E} > 0.3$ is satisfied since the neutron energy is usually small after inelastic scattering.

Thus, taking account of the finite thickness of the scintillator (for an average chemical scintillator composition CH) the counter efficiency is:

$$\varepsilon' = \frac{\sigma}{\sigma + \sigma_c}\left(1 - e^{-nh(\sigma+\sigma_c)}\right), \tag{42}$$

where σ_c is the cross section for inelastic neutron interactions with carbon (Fig. 60).

For the scintillator thickness used in practice the correction for the attenuation of the neutron flux is small and may be conveniently written in the form:

$$\rho = 1 - \frac{nh(\sigma + \sigma_c)}{2}.$$

Thus, the true counter efficiency is

$$\varepsilon' = \varepsilon \cdot \rho,$$

where ϵ is computed from Eq. (40).

Edge Effects

The loss of recoil protons from the scintillator due to recoil protons which are formed near the edges leads to some reduction in the counter efficiency as compared with the expression given in (40). In contrast with an ionization chamber with a hydrogenous gas radiator, in a scintillation counter the edge effect can always be made as small as desired, because the range of a recoil proton in the scintillator is small as compared with the usual scintillator dimensions.

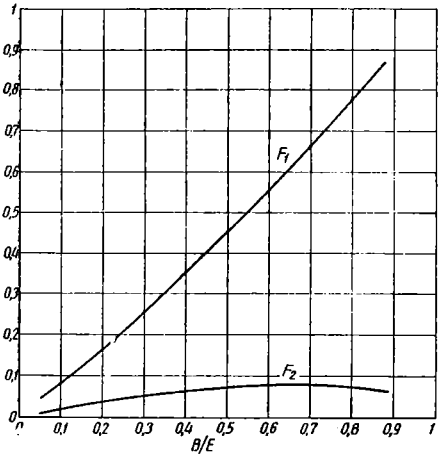

Fig. 61. Curve used for estimating edge effects in a scintillation counter.

Suppose that a neutron flux from a remote source passes through a cylindrical scintillator parallel to the cylinder axis. Some of the recoil protons formed in the scintillator are lost through the side and back surfaces. To estimate the magnitude of the edge effects we make use of the calculations of Rossi and Staub [14], carried out for the usual case of a cylindrical ionization chamber with a gas radiator, using the assumption that the recoil proton range is $R = CE^{3/2}$ and that the proton pulse is proportional to the energy loss in the operating volume of the chamber. Neglecting second-order quantities in R_0/h and R_0/r, where R_0 is the range of a maximum energy recoil proton and $\underline{h}$ and $\underline{r}$ are the height and radius of the scintillator, we obtain the counter efficiency with the edge effect taken into account.

$$\varepsilon'' = nh\sigma\left[1 - \frac{B}{E} + \frac{R_0}{h} D\left(\frac{B}{E}\right) + \frac{R_0}{r} T\left(\frac{B}{E}\right)\right],$$

where D and T are functions of the ratio $\frac{B}{E}$, given in Rossi and Staub.

In actual fact the edge effect in a scintillation counter is smaller because of the nonlinearity in the light yield of the scintillator. For this reason, we can write the symbol $<$ in evaluating the influence of the edge effect on spectrometer efficiency:

$$\frac{\Delta\varepsilon}{\varepsilon} < \frac{R_0}{h} F_1\left(\frac{B}{E}\right) + \frac{R_0}{r} F_2\left(\frac{B}{E}\right).$$
$$F_1 = D\frac{E}{B-E}; \quad F_2 = T\frac{E}{B-E}. \tag{43}$$

The functions F_1 and F_2 are given in Fig. 61. From Fig. 61 and the relation given in (43) it is apparent that with $r \sim h$ the main contribution to the edge effect is due to the loss of protons through the base of the scintillator; this is to be expected since the range of recoil protons is small at large angles.

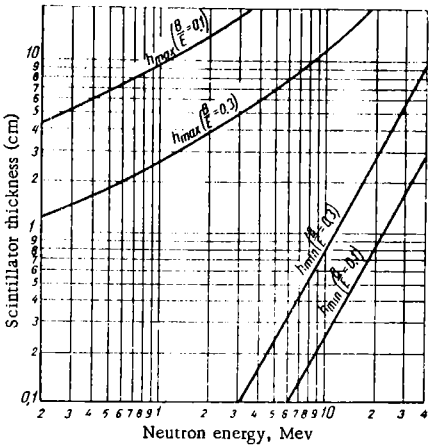

Fig. 62. Limitations imposed on the thickness of a scintillator by edge effects (h_{min}) and multiple scattering (h_{max}).

To illustrate the edge effect the relation in (43) is shown graphically in Fig. 62 (cylindrical scintillator, r = h, composition CH, density 1, $\Delta \epsilon / \epsilon = 10\%$). If the threshold is lower the required scintillator thickness falls off approximately as $\frac{B}{E}$.

Multiple n, p Scattering

If before leaving the scintillator a scattered neutron is scattered a second time, the flashes from the two recoil protons combine and are recorded as a flash due to a recoil proton of high energy formed in a single scattering event. When the probability for this type of event is large the use of Eq. (40) leads to considerable error.

We may estimate the effect due to double scattering. If the counter threshold is B, only protons with energies $E_p > B$, are recorded (the fraction of the total number of recoil protons is $(1 - \frac{B}{E})$. The further fate of a neutron which forms a proton with energy $E_p > B$ in its first scattering event is not of interest since the second scattering event does not change the number of counts. However, a neutron which transfers energy $E_p > B$ to a proton in its first scattering event will be capable of transferring (in a second scattering event) energy to another proton; the counter pulse will be greater than the threshold value and will thus be recorded. After the first scattering event the mean energy of this neutron is $\bar{E} = E - \frac{B}{2}$. The ratio of the number of these neutrons to the number of singly scattered neutrons is:

$$\xi_1 = \frac{B}{E - B}$$

The mean energy of recoil protons with $E_p < B$ is $\frac{B}{2}$. We shall assume that all the neutrons being considered have energies equal to the mean energy and that in the second scattering these give rise to a recoil proton spectrum whose shape corresponds to scattering for monochromatic neutrons. Then, in order that it be recorded, in its second scattering event the neutron must give rise to a recoil proton with energy $E_p > \frac{B}{2}$. The fraction of these neutrons compared with the total number of neutrons which experience double-scattering is:

$$\xi_2 = \frac{\bar{E} - \frac{B}{2}}{\bar{E}} = \frac{1 - \frac{B}{\bar{E}}}{1 - \frac{1}{2}\frac{B}{\bar{E}}}.$$

The probability that a neutron which is not recorded in the first scattering event will be scattered on a proton a second time is

$$\xi_3 = \sigma(E')\, n \cdot \bar{s},$$

where $\bar{s}$ is the distance traversed by the neutron in the scintillator after the first scattering event, averaged over volume, and $E' = E - \frac{B}{2}$.

If a flux of neutrons strikes a cylindrical scintillator of height $\underline{h}$ and radius $r = h$ (perpendicularly to the base) $\overline{s} \approx \frac{h}{2}$. In this case the ratio of the number of neutrons recorded as a result of double-scattering to the number of recorded singly scattered neutrons is:

$$\varkappa = \xi_1 \xi_2 \xi_3 = \frac{B}{E} \cdot \frac{\sigma(E') n \cdot h}{2 - \frac{B}{E}} . \tag{44}$$

Eq. (44) has been obtained without taking account of the nonlinearity of the light yield of the scintillator as a function of recoil-proton energy. Hence, it cannot be used for computing double-scattering corrections and allows us only to find the conditions for which double-scattering can be neglected. It is clear that the nonlinearity in the light yield will reduce the quantity κ considerably (one recoil proton gives a greater flash than two with the same total energy), especially in the low-energy region.

Thus, the relative uncertainty due to the neglect of double-scattering is,

$$\frac{\Delta\varepsilon}{\varepsilon} < \frac{B}{E} \cdot \frac{\sigma(E') nh}{2 - \frac{B}{E}} . \tag{45}$$

To illustrate the limitations imposed by multiple scattering, in Fig. 62, the relation in (45) is shown graphically (cylindrical scintillator, $r = h$, composition CH, density 1, $\Delta\epsilon/\epsilon = 10\%$).

In Fig. 62, which shows the limits due to the edge effect (h_{min}) and effects due to multiple scattering (h_{max}) makes it possible to choose a scintillator thickness for which the errors in efficiency can be made less than 10% in a given region of neutron energy. For optimum scintillator thickness, as determined from the relations in (43) and (45), the errors in efficiency are reduced still more because of the fact that the edge effect and effects due to multiple scattering, which affect the efficiency in opposite ways, partly compensate for each other.

If the ratio $\frac{B}{E}$ is reduced, the limits of allowable scintillator thickness (h_{min} and h_{max}) are extended; conversely, for optimum scintillator thickness, the errors in efficiency are reduced. At neutron energies up to 10 Mev, where $\frac{B}{E}$ can be reduced to 0.1, the edge effect and effects due to multiple scattering impose essentially no limitation on the accuracy of absolute measurements of a neutron flux.

In the hard part of the region, where $\frac{B}{E}$ must be larger than $\frac{E_{p\alpha}}{E}$ (see Table 1) the situation is somewhat worse, but here at least 10% accuracy can also be achieved over a wide range of neutron energy (Fig. 62).

If, the scintillator thickness is the optimum value for each neutron energy at which it is necessary to carry out absolute measurements, the errors due to edge effects and multiple scattering can be reduced to 1%.

Anisotropy in n, p Scattering

Eq. (40), for the efficiency of a scintillation counter, has been obtained under the assumption that the neutron scattering exhibits an isotropic angular distribution in the center-of-mass system; this assumption is valid only for neutron energies less than 10 Mev. At neutron energies above 10 Mev the differential cross section for scattering in the center-of-mass system depends on angle and can be given in the form (25):

$$\sigma_\psi = \sigma_\psi\left(\frac{\pi}{2}\right)(1 + C\cos^2\psi).$$

In order to take anisotropy into account, we substitute (25) in (12) and integrate the resulting expression between the limits ψ' and π, where ψ' is determined by the relation $B = \frac{1}{2} E \cdot (1 - \cos\psi')$ (see 11). Using this procedure we obtain the following expression for the probability of emission of a recoil proton with energy between B and E:

$$W_1(\psi', E) = \frac{2\pi\sigma_\psi\left(\frac{\pi}{2}\right)}{\sigma}\left[(1+\cos\psi') + \frac{C}{3}(1+\cos^3\psi')\right].$$

Going from ψ' to B, we have

$$W_1(B, E) = KW(B, E),$$

where W (B, E) is the probability computed without taking anisotropy into account and

$$K = \frac{1+\frac{C}{3}\left(1-2\frac{B}{E}+4\frac{B^2}{E^2}\right)}{1+\frac{C}{3}} \qquad (46)$$

is a correction factor which takes account of anisotropy in the neutron angular distribution. Values of this function, computed according to Eq. (46) for several values of $\frac{B}{E}$ and C, are shown in Table 3.

TABLE 3

B/E \ C	0,05	0,10	0,25	0,50
0,1	1,00	1,00	0,99	0,98
0,2	1,00	1,00	0,98	0,97
0,3	1,00	0,99	0,98	0,97
0,4	0,995	0,99	0,99	0,98
0,5	1,00	1,00	1,00	1,00
0,6	1,00	1,01	1,02	1,04
0,7	1,005	1,02	1,04	1,08
0,8	1,01	1,03	1,08	1,14

A comparison of the data of Table 3 and Fig. 2 shows that when $\frac{B}{E} \leq 0.5$ the anisotropy in n, p scattering cannot be neglected anywhere in the neutron energy range being considered.

It is of interest to note that when $\frac{B}{E} = 0.5$, the anisotropy in n, p scattering is unimportant in the computation of scintillation counter efficiency, even at neutron energies much greater than 30 Mev.

From what has been indicated, it follows that a scintillation counter with an organic scintillator is an absolute instrument with which it is possible to make measurements of neutron fluxes with great accuracy in the absence of background (for monochromatic neutron fluxes (conditions which are automatically satisfied in a time-of-flight spectrometer).

The possibility of computing the absolute efficiency of a scintillation counter has been verified experimentally. For example, Cross [15] has used 14-Mev neutrons obtained from the T (d, n) He^4 reaction ($E_d \sim$ ~ 100 kev), which is one of the few sources of monochromatic high-energy neutrons and exhibits essentially no accompanying background due to γ-rays and neutrons at other energies. The neutron flux was determined by counting the α-particles formed in this reaction. The calculated efficiency of an anthracene crystal for a counter threshold of 4 Mev coincided within 5% with that found experimentally.

In Fig. 63 are shown experimental values of the efficiency of a counter with a plastic scintillator for several values of neutron energy obtained by Cranberg and Levin [16] with a time-of-flight spectrometer. In order to determine the efficiency, the yield of monochromatic neutrons from the T (p, n) He^3 reaction was measured with a scintillation counter at various proton energies and a comparison was made with the results obtained with a proportional-counter telescope with a thin radiator at E < 1.2 Mev and with an "all-wave" counter at E > 1.2 Mev. The solid curve has been plotted from Eq. (42) for a threshold B = 0.4 Mev. The average chemical composition of the scintillator was CH and the thickness 3.8 cm. Under these conditions the edge effects and effects due to multiple scattering are small for E > 1 Mev (Fig. 62).

As is apparent from Fig. 63, the energy dependence of the counter efficiency computed from Eq. (42), and its absolute value, are in good agreement with the experimental data. The discrepancy at E < 1.2 Mev is apparently explained by errors in the absolute measurement of the neutron flux in the "all-wave" counter.

The necessity for measurements of the entire efficiency curve is due to the fact that the energy threshold of the counter, which is determined by the input trigger of the time analyzer, was not known. If there is an

amplitude selector in the spectrometer, and if the dependence of light yield on proton energy is known for the scintillator, the selector scale can be easily calibrated in energy units; thus, it is possible not only to know the energy threshold of the counter but also to vary this threshold over wide limits.

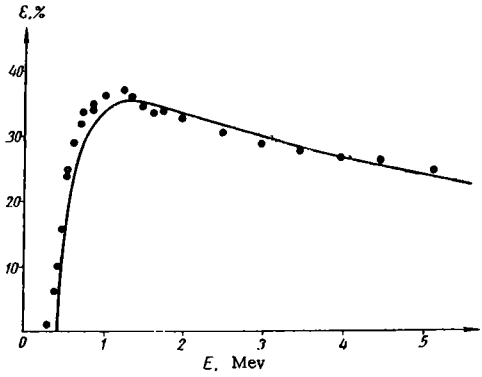

Fig. 63. Energy dependence of the efficiency of a neutron counter with a plastic scintillator. The calculated curve and the experimental points [16] are shown.

§ 2. Resolution Time

In order to fix ideas we will consider a scintillation counter in a time-of-flight spectrometer (Fig. 41). In practice it is extremely difficult to separate the time characteristics of the counter and the time analyzer if no special investigation is made. At the outset, in order to determine the requirements which must be satisfied by a "fast" scintillation counter, we consider a rather idealized picture.

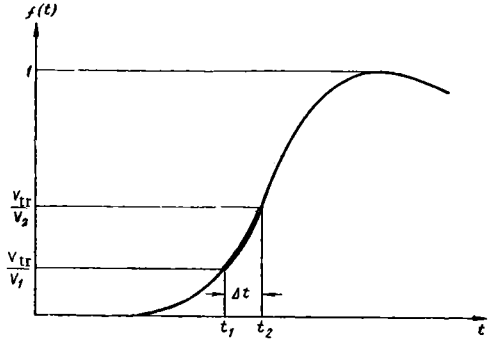

Fig. 64. Curve used for demonstrating the spread in time of operation of the trigger unit caused by the finite range of amplitudes from the scintillation counter.

The number of photoelectrons for a pulse is so large that it is possible to neglect any statistical effects ("large scintillation pulse"). The anode of the multiplier, which operates in a linear mode, is connected to the

input of the trigger circuit. We shall assume that the pulses from the anode of the multiplier differ only in amplitude V_0; their shape is given by the curve $f(t)$ shown in Fig. 64. The time at which the trigger operates is completely determined by the time at which its input potential $V(t) = V_0 f(t)$ reaches some critical value V_{tr} which is the threshold value.

Suppose that at time $t = 0$ a proton is produced in the scintillator with energy higher than E_{tp}, the threshold energy. After a time t_c, the time for the pulse to pass through the counter (usually of the order of 10-100 mμsec), the trigger operates. The resolution time Δt_c will be defined as twice the mean-square spread in this transmission time. Any delay in t_c is in itself not important.

It is apparent (Fig. 64), that if the pulse amplitude lies between V_1 and V_2 the spread in the time of operation of a trigger is $\Delta t = t_2 - t_1$. Consequently, in the idealized case being considered here the resolution time of the counter is completely determined by the amplitude variation of the pulses and the operating portion of the voltage-rise curve at the anode of the photomultiplier. In the case in which an amplitude selector is used (Fig. 41), instead of considering the entire pulse-amplitude range at the anode of the photomultiplier, we need consider only that section which corresponds to pulses which are accepted by the selector.

We consider the small section of the voltage-rise curve at the anode of the photomultiplier corresponding to a dynamic range $1 + \alpha$, where $\alpha \ll 1$.

1. We have

$$V_2 = V_1 (1 + \alpha)$$

$$\frac{V_{tr}}{V_2} = \frac{V_{tr}}{V_1} + \Delta t \left(\frac{d}{dt} \cdot \frac{V}{V_0} \right)_{\substack{V = V_{tr} \\ V_0 = V_1}}$$

where

$$\Delta t = \left| \frac{\alpha}{\left(\frac{d}{dt} \ln \frac{V}{V_0} \right)_{\substack{V = V_{tr} \\ V_0 = V_1}}} \right| .$$

That is to say, for the narrow range of pulse amplitudes in a scintillation counter close to V_1 the resolution time is inversely proportional to the logarithmic derivative of the voltage-rise curve at the point $f(t) = \frac{V_{tr}}{V_1}$. Thus, over a finite dynamic range the resolution time is inversely proportional to the effective value of the logarithmic derivative over the operating proportion of the voltage-rise curve at the anode of the photomultiplier.

The shape of this curve is determined by several factors. We consider these.

1. The excitation time of the scintillator (i.e., the time for a recoil proton to be brought to a stop) in the energy region being considered here is rather small. With an increase in proton energy from 1 to 30 Mev this quantity increases approximately from 0.001 to 0.1 mμsec.

2. To a rough approximation the collection of light from scintillator at the photocathode may be given by $e^{-t/hc}$, where h is a typical linear dimension of a scintillator. The light collection time is unimportant for $h < 10$ cm.

3. The emission from the majority of organic scintillators is described fairly well by an exponential relation [1] so that the rate of rise is a maximum at the starting time. There are indications that in certain scintillators the emission function is a sum of exponents [5] where one reaches a maximum somewhat later than the time of exitation. This "combustion" process has not been investigated to any great extent for organic scintillators. For the scintillators which are used most the combustion time is apparently less than 1 mμsec [17 - 19].

4. The time spread in the flight of photoelectrons to the first dynode (a characteristic of the photomultiplier input) usually makes the basic contribution to the resolution time of a scintillation counter with a photomultiplier with a large photocathode.

5. The pulse spread in the electron multiplication (a characteristic of the multiplication system) is essentially Gaussian for most dynode systems.

The combined effect of these factors determines the shape of the anode pulse of the photomultiplier. The form of the voltage pulse also depends on the time constant of the RC integrating circuit at the anode and on the input of the trigger circuit. In order to increase the rate-of-rise of the voltage pulse it is necessary to reduce the stray capacity at the anode of the photomultiplier, trigger input and other associated circuits.

It can be shown that the logarithmic derivative of the leading edge of the rise pulse is affected by each factor independently so that their combined effect is reduced with increasing t (Fig. 64). Consequently, the closer the working section of the voltage rise curve to the origin, the smaller the time spread due to the finite amplitude range of pulses from the scintillation counter.

In work with a large dynamic pulse-amplitude range the values of the logarithmic derivative at the ends of the working section of the rise curve may differ from each other considerably. Under these conditions, the resolution time depends only weakly on the magnitude of the dynamic range; in practice it is determined by the lower limit V_1. In fast-neutron spectrometers we always deal with this type of operation: the rather large energy spread of the recoil protons leads to a rather large range in the pulses from the photomultiplier because of the nonlinearity in the light yield from organic scintillators.

For a given trigger threshold V_{tr} the operating section of the rise curve can be shifted toward the origin by increasing the amplitudes of the pulses at the trigger input. The use of a wide-band amplifier for this purpose (required band-width approximately 300 Mc) involves a great number of technical difficulties and complications [2]. For this reason, the need for reducing the effective threshold of the time analyzer implies the use of photomultipliers with high gains.

Working with coincidence circuits with germanium diodes in many cases, it is sufficient to use a gain of approximately 10^6. To trigger fast a vacuum-tube circuit, it is necessary to use a multiplier with a gain of $10^8 - 10^9$.

The improvement in resolution time cannot be increased indefinitely by reduction in the effective threshold of the time analyzer. A limitation arises in the statistical nature of the processes which take place in the photomultiplier. It is apparent that the statistical effects will set in earliest at the input of the photomultiplier. A reduction in the effective threshold of the time analyzer below the level corresponding to the detection of a single photoelectron can never reduce the time spread in the arrival of electrons at the first dynode. A reduction in resolving time can, in this case, be achieved only to the extent to which it is determined by the spread in the pulses at the photocathode in the dynode system of the photomultiplier. A high gain in the photomultiplier can, in certain cases, compensate for the shortcomings of its dynode system.

The reduction in resolving time in a time analyzer by the reduction in threshold is limited by purely technical factors in addition to the statistical limitations. If the threshold of the time analyzer is lower than the threshold of the amplitude selector (i.e., a situation in which $B_{tr} \ll B$) there is excessive loading of the input of the analyzer by pulses which are not recorded. When the threshold is lowered below the level corresponding to the detection of one photo-electron, there is a sharp increase in this spurevas effects associated with dark pulses in the photomultiplier.

We now consider the statistical limitations on the resolving time of a scintillation counter. In this analysis we assume that:

1) The excitation time of the scintillator and the time required for collecting light at the photo cathode are negligibly small;

2) The photomultiplier itself does not introduce any time spread;

3) The input trigger of the time analyzer operates when a definite number (Q) of pulses due to individual photoelectrons is received.

We also assume that the emission from the scintillator follows a pure exponential law. Thus, the number of photons emitted by the scintillator at time t is:

$$N(t) = P(1 - e^{-t/\tau_0}),$$

and the emission rate of the scintillator is

$$\frac{dN(t)}{dt} = \frac{P}{\tau_0} \cdot e^{-t/\tau_0},$$

where P is the total number of photons emitted by the scintillator per pulse and τ_0 is the "emission time" of the scintillator.

In this case, the mean-square time spread in the appearance of a Q-th photoelectron is given by an expression with the following asymptotic form [20, 21]:

$$\Delta t \approx \frac{\tau_0}{R} \sqrt{Q}\left(1 + \frac{Q+1}{R} + \dots\right), \quad \text{for} \quad R \gg 1; \tag{47}$$

where R is the total number of photo electrons in a pulse which strike the first dynode of the multiplier. It may be assumed that

$$R = P\varkappa_1\xi\varkappa_2, \tag{48}$$

where $\varkappa_1$ is the photon collection coefficient at the photocathode, ξ is the mean quantum yield of the photocathode in the spectral region corresponding to the scintillator emission; $\varkappa_2$ is the photo electron collection coefficient at the first dynode of the photomultiplier.

From (47) and (48) it is apparent that in order to reduce the statistical component in the resolving time of a scintillation counter, the following are necessary:

1) A high ratio of light yield to scintillator emission time $\frac{P}{\tau_0}$ (i.e., a high initial emission rate for the scintillator).

2) A high photon collection coefficient at the photocathode (consequently, a good reflector, high transparency of the scintillator for its own radiation and a photocathode of large area).

3) High sensitivity of the photocathode in the spectral region corresponding to the emission from the scintillator and complete collection of photoelectrons at the first dynode. (It is also apparent that a high secondary emission coefficient and a high electron collection coefficient in each stage of the photomultiplier, especially the first, are desirable.)

4) A low effective threshold for the time analyzer (reduction of Q to almost unity).

A comparison of various organic scintillators in terms of the parameter $\frac{P}{\tau_0}$ has been carried out by Medvedev et al. [22]. These authors recommend as the scintillators having the best values of $\frac{P}{\tau_0}$ a solution of 8 g/liter PBD* in toluene and a plastic with a polyphenyl toluol base containing 4% terphenyl and 0.1% DPS.** The initial emission rate of these scintillators is approximately twice as high as that of stilbene.

It should be noted that the requirements on a fast photomultiplier which stem from statistical considerations are essentially the same as those for obtaining high amplitude resolution with a scintillation counter.

In many cases the statistical factor does not impose any limitation on the resolving time of a counter in the neutron-energy region being considered here. For example, if B_{tr} corresponds to Q = 10, even at a proton energy of 1 Mev for a counter with a stilbene crystal placed directly at the photocathode and surrounded by a good reflector, $\Delta t \sim 0.1$ mμsec (in making this estimate we assume $\varkappa_1 = \varkappa_2 = 1$, $\xi = 10\%$; the data on the number of photons emitted by stilbene per unit proton energy are taken from [9 and 23]). However, if a large scintillator is used directly with a conventional photomultiplier the poor light collection conditions can cause a considerable increase in Δt. For example, a liquid scintillator (toluene with terphenyl and POPOP, see Table 4)

* PBD is 2 phenyl-5-(4-biphenylyl) 1,3,4 oxdiazole.

** DPS is p,p' diphenyl-stilbene.

with a volume of 1 liter, the emission of which is collected by means of a conical plexiglas light pipe on a photocathode 35 mm in diameter (FEU-33) gives flashes which are approximately 15 times smaller than those obtained with a stilbene crystal (3 cm in diameter and 2 cm high) placed directly at the photocathode for the same proton energy. Under the same conditions considered in the case above, it is found that $\Delta t \sim 1$ mμsec.

TABLE 4

State	Single crystal		Liquid		Plastic	
base material	stilbene	tolane,*	toluene		polystyrol	
Activator (g/liter)			TP** / 4	TP** / 4	TPB*** / 16	TP** / 36
Wavelength shifter (g/liter)	--		--	POPOP**** / 0.1	--	TPB*** / 0.2
Average chemical composition	C_7H_6	C_7H_5	C_7H_8	C_7H_8	CH	CH
Density (g/cm^3)	1.16	1.18	0.867	0.867	1.06	1.06
λ (A) at maximum intensity	4100	3900	3550	4400	4500	4450
Relative pulse amplitude	1	0.75	0.60	0.80	0.60	0.65
Emission time τ_0 (mμsec)	6—8	4—6	2—3	4—6	4—5	3—4

* Tolane-diphenylacetelene.

** TP is p-terphenyl.

*** TPB is 1,1,44-tetraphenyl-1,3,5 butadiene.

**** POPOP is 1,4 di-[2-(5 phenyloxazolyl)]-benzene.

§ 3. Characteristics of Certain Scintillators and Photomultipliers

In Table 4 are shown the basic characteristics of the organic scintillators which find widest application in neutron spectroscopy.

The relative pulse amplitudes were measured with small samples using a photomultiplier with an antimony cesium photocathode with so-called "medium" spectral characteristics which was excited by β-particles. These figures also give the approximate light yields for excitation by protons; the shape of the curve showing the dependence of light yield per unit energy on ionization density is essentially the same for all organic scintillators which are used. The dependence of light yield on proton energy for a stilbene crystal is shown in Fig. 57.

The light yield and emission time of all the scintillators listed in the table are not very different (for small sample dimensions). The choice of one or another of these scintillators is determined mainly by experimental conditions.

The standard stilbene crystal was 3 cm in diameter and 2 cm high or 4 cm in diameter and 4 cm high. The tolane crystal was a cylinder 10 cm in diameter and 5 cm in height [24].

The solution of terphenyl in toluene which gave the best initial emission rate of all the scintillators listed in the table was used only in small containers (several centimeters high). The addition of materials which shift the emission spectrum of the scintillator toward longer wavelengths increases the transparency and light yield and makes it possible to use scintillators of large dimensions.

The light yield of liquid scintillators depends markedly on the purity of the materials which are used; this means that special purification measures are required and that there are limitations on the materials which can

be used in the containers and gaskets. Large containers are frequently made from aluminum and are polished on the inside. The output window is usually sealed by means of teflon or lead. Titanium enamel, which is used frequently for household refrigerators, makes a good reflector. In this case, the container can be fabricated in the form of an iron tank which is enameled on the inside with a thin glass window sealed with BF-2 adhesive. If phenylcyclohexane is used as a solvent it is possible to use a plexiglas container.

The plastics listed in the table have good transparency for their own emission and can be used in large pieces. In a plastic with a wavelength shifter the free path of a photon is approximately 2 m.

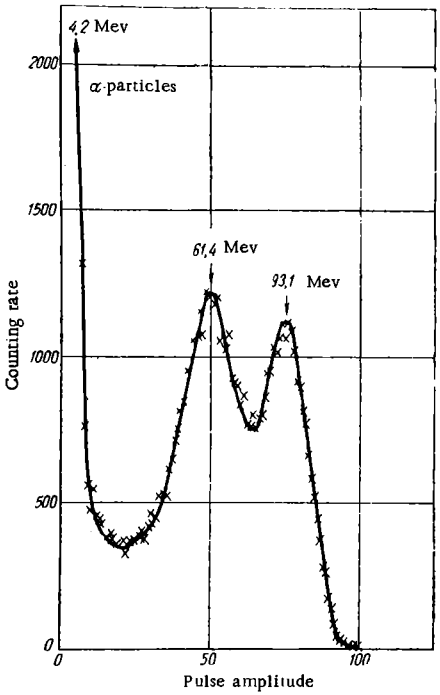

Fig. 65. Pulse spectrum from a gas scintillator counter for detection of α-particles and fission fragments from U^{235}. The counter was filled with xenon. The wavelength shifter is quaterphenyl.

More detailed information on organic scintillators can be found, for example, in [5] (review article), [25, 26] (properties of plastic scintillators), [17-19, 32] (emission time of organic scintillators).

A new technique has been developed rather recently (1955-1957); this technique makes use of gas scintillators in which the emission of noble gases bombarded by ionizing particles is used [33-39]. Along with the relatively slow emission component (tens of millimicroseconds) which depends on the gas pressure (emission due to recombination of ions), there is a fast component (τ_0 of the order of 1 mμsec) due to the emission of excited atoms [35, 37]. The light yields of the better gas scintillators is very high. The difficulty in using these gas scintillators is the fact that the emission spectrum of the noble gases lies in the ultraviolet region. However, in recent years effective spectrum shifters have been developed and these can be used to shift the spectra to the high sensitivity region of the cathode of the photomultiplier. The best of these, quaterphenyl has an emission time less than 8 mμsec so that it can be used in fast counters. In excitation by α-particles from polonium a gas scintillators (a mixture of He and 10% Xe) with quaterphenyl as a wavelength shifter has been used to produce pulses with amplitudes eight times greater than a pulse from a stilbene crystal [39]. Unfortunately, as yet it is still not known what fraction of the light yield of a gas scintillator is to be assigned to the fast component.

The most desirable property of gas scintillators is the fact that the light yield per unit energy is essentially independent of specific ionization and, consequently, the same for different particles.

The properties which have been enumerated for gas scintillators make these devices very desirable for a number of applications in time-of-flight neutron spectroscopy.

Because of its high light yield a gas scintillator can be used as the basis for a fast and effective neutron detector (using recoil protons) which is sensitive to neutrons with energies of several tens of kilo electron volts [4]. For example, in a xenon scintillator it is possible to add a rather large amount of hydrogen without reducing the light yield ($\frac{1}{3}$ H_2 by volume reduces the pulse amplitude by a factor of 2 [34]).

A good scintillator is a mixture of He and Xe [39]. Through the use of this mixture it is possible to build a fast and effective neutron detector for energies of 1 Mev or less which makes use of neutrons from the $He^3(n, p)T$ reaction.

Because the light yield of a gas scintillator shows essentially no reduction with increasing ionization density and the operating time of a gas scintillator is very small, it is possible to distinguish fission fragments against the high background of α-particle which characterize the most active fissionable materials (Fig. 65). Thus, it is possible to use a time-of-flight spectrometer as a selector for studying radiation of fission induced by fast neutrons.

TABLE 5

Photomultiplier designation	FEU					
	1V	2V	1B1V	1B2V	13	33
Diameter of photocathode (mm)	40		75		50	35
Integrated sensitivity of the photocathode (μ amp/lumen)	30—90				30—80	35
Quantum yield of the photocathode λ = = 4047 A (el/photon · 100)	8—16				8—15	10
Operating voltage (kv)	2—2,5				2—2,5	2,5—3
Type of dynode system	circular (channel-shaped dynodes)				venetian blind	linear (channel-shaped dynodes with accelerating grids)
Dynode material	alloy Al—Mg—Si				alloy Cu—Al—Mg	covering Sb—Cs
No. of dynodes	10	12	10	12	12	14
Gain at maximum voltage	10^6	10^7	10^6	10^7	10^7	10^6
Rise time of the scintillation pulse (mμsec)	3	3	5	5	5	2
Maximum pulse output time (ma)	50				>300	>300
Amplitude resolution at Eγ = 0.66 Mev with NaI(Tl)	9—12		9—14		8—10	9—10
Literature reference	[6, 41—45]				[45—48]	[45, 49—51]

In Table 5 are shown the basic characteristics of several domestic photomultipliers used in fast counters.

All the photomultipliers listed in the table have antimony-cesium photocathodes with a maximum sensitivity in the region of 4000 A.

As is apparent from the table, as yet there is only one fast photomultiplier with a gain of the order of 10^8 (FEU-33). Because a high gain is required for the use with fast vacuum-tube circuits, in the first work with the fast-neutron, multichannel, time-of-flight spectrometer at the Institute for Atomic Energy, Academy of Sciences, USSR, a photomultiplier of this type was used [52, 53].

A basic shortcoming of the FEU-33, as concerns its application in a time-of-flight spectrometer, is the small area of the cathode. In principle, the resolving power of a time-of-flight neutron spectrometer can be made as high as desired by the simple expedient of increasing the flight distance. However, when the flight distance is increased, it is necessary tomake a corresponding increase in the scintillator volume in order to maintain spectrometer efficiency. At the present time liquid and plastic scintillators may be made very large; however, their transverse dimensions are limited in practice to about 10 cm because of the necessity for collecting the light from the scintillator on a small photocathode. The use of several photomultipliers which work from a single scintillator involves great technical difficulties if one is to obtain reasonably small resolving time.

Photomultipliers such as the FEU-1B1V and FEU-1B2V which have been developed by Khlebnikov [6, 42], with photocathode areas which are almost five times greater than the area of the photocathode in the FEU-33, have been used successfully in coincidence circuits with germanium diodes but have inadequate gain for operation with fast vacuum tube circuits. Moreover, the resolution time of these tubes is relatively poor.

The most promising photomultiplier in all respects is that designed by Vild'grube [44-48]; this tube uses a venetian-blind construction in the electron multiplier. One version of this design is the FEU-13, the parameters of which are given in Table 5. The possibilities of this design are far from exhausted as far as low resolution time and high gain are concerned [48]. A unique property of the Vild'grube tube is the high stability and reliability in operation at high output currents (an average current of tens of milliamperes can be obtained and the linearity of the light characteristic is as great as 300 ma, pulsed); the tube also has a short transient period, a feature which is very important for operation with accelerators.

LITERATURE CITED

[1] Birks, Scintillation Counters, Izd. IL (1955).

[2] Lewis and Wills, Millimicrosecond Pulse Techniques, Izd. IL (1956).

[3] S. C. Curran, Luminescence and the Scintillation Counter (1956).

[4] N. O. Chechik, S. M. Fainshtein, and T. M. Lifshits, Electron Multipliers GITTL (1957).

[5] R. K. Swank, Annual Review of Nuclear Science 4, 3 (1954); Uspekhi Fiz. Nauk 58, 519 (1956).

[6] N. S. Khlebnikov and A. E. Melamid, Inst. and Exp. Tech. (USSR) 6, 6 (1957).

[7] J. Labeyrie, J. phys. et radium 17, 576 (1956).

[8] G. F. Bogdanov, N. A. Vlasov, S. P. Kalinin, B. V. Rybakov, and V. A. Sidorov, J. Atomic Energy 3, 204 (1957) [USSR].

[9] C. J. Taylor, W. K. Jentschke, M. E. Remley, F. S. Eby, and P. G. Kruger, Phys. Rev. 84, 1034 (1951).

[10] J. Fowler and C. Roos, Phys. Rev. 98, 996 (1955).

[11] J. D. Anderson, C. C. Gardner, M. P. Nakada, and C. Wong, Phys. Rev. 110, 160 (1958).

[12] C. Wong, J. Benbeniste, C. C. Gardner, and M. P. Nakada, Bull. Am. Phys. Soc. Series 2, 175 (1956).

[13] J. E. Draper, Rev. Sci. Instr. 25, 558 (1954).

[14] B. Rossi and G. Staub, Ionization Chambers and Counters, Izd. IL (1951).

[15] W. G. Cross, Phys. Rev. 83, 873 (1951).

[16] L. Cranberg and J. S. Levin, Phys. Rev. 103, 343 (1956).

[17] S. Singer, L. K. Neher, and R. A. Ruehle, Rev. Sci. Instr. 27, 40 (1956).

[18] H. B. Philips and R. K. Swank, Rev. Sci. Instr. 24, 611 (1953).

[19] R. K. Swank and W. L. Buck, Rev. Sci. Instr. 26, 15 (1955).

[20] R. F. Post and L. I. Schiff, Phys. Rev. 80, 1113 (1950).

[21] R. F. Post, Nucleonics 10, 6, 56 (1952).

[22] M. N. Medvedev, E. N. Matveeva, and L. Ya. Zhil'tsova, Izv. Akad. Nauk SSSR Ser. fiz. 22, 44 (1953).

[23] G. T. Wright, Phys. Rev. 91, 1282 (1953).

[24] L. M. Belyaev, B. V. Vitovskii, and G. F. Dobrzhanskii, Growth of Crystals (Academy of Sciences Press, 1957) (Reports to the First Conference on the Growth of Crystals), p. 249.

[25] F. N. Hayes, D. G. Ott, V. N. Kerr, and B. S. Rogers, Nucleonics 13, 12, 38 (1955).

[26] F. N. Hayes, D. G. Ott, and V. N. Kerr, Nucleonics 14, 1, 42 (1956).

[27] W. L. Buck and R. K. Swank, Nucleonics 14, 11, 48 (1953).

[28] G. W. Clark, F. Scherb, and W. B. Smith, Rev. Sci. Instr. 28, 433 (1957).

[29] V. K. Kosmachevskii and M. S. Ainutdinov, Inst. and Exp. Tech. (USSR) 3, 49 (1956).

[30] E. A. Andreeshchev, E. E. Baroni, K. A. Kovyrzina, I. E. Pani, I. M. Rozman, and V. M. Shoniya, Inst. and Exp. Tech. (USSR) 1, 32 (1956).

[31] M. N. Medvedev, E. N. Matveeva, and L. Ya. Zhil'tsova, Inst. and Exp. Tech. (USSR) 3, 45 (1958).

[32] S. F. Kilin, A. A. Pavlov and I. M. Rozman, Inst. and Exp. Tech. (USSR) 2, 50 (1956).

[33] C. Eggler and C. M. Huddleston, Nucleonics 14, 4, 36 (1956).

[34] J. A. Northrop and R. Nobles, Nucleonics 14, 4, 36 (1956).

[35] R. A. Nobles, Rev. Sci. Instr. 27, 280 (1956).

[36] M. Forte, Nuovo Cimento 3, 1443 (1956).

[37] H. Palevsky, R. L. Zimmerman, and R. L. Larsson, Rev. Sci. Instr. 27, 323 (1956).

[38] S. A. Baldin, V. V. Gavrilovskii, and F. E. Chukreev, J. Atomic Energy 3, 331 (1957) [USSR].

[39] A. Sayres and C. S. Wu, Rev. Sci. Instr. 28, 758 (1957).

[40] C. O. Muehlhause, Nucleonics 14, 4, 37 (1956).

[41] G. A. Vasil'ev, Inst. and Exp. Tech. (USSR) 4, 66 (1957).

[42] N. S. Khlebnikov, Izv. Akad. Nauk SSSR, Ser. fiz. 22, 70 (1958).

[43] A. E. Melamid, Izv. Akad. Nauk SSSR, Ser. fiz. 22, 78 (1958); A. E. Lamid, Izv. Akad. Nauk SSSR, Ser. fiz. 22, 78 (1958).

[44] M. N. Medvedev, E. S. Sokolova, I. I. Filippov, and O. N. Tsislyak, Inst. and Exp. Tech. (USSR) 4, 37 (1958).

[45] V. V. Paramonov, B. V. Rybakov, and V. A. Sidorov, Inst. and Exp. Tech. (USSR) (1959) (In press).

[46] Yu. A. Nemilov, V. M. Ovchinnikov, A. N. Pisarevskii, and E. D. Teterin, J. Atomic Energy 4, 51 (1956) [USSR].

[47] G. S. Vil'dgrube, A. P. Zharkov, and E. D. Teterin, Izv. Akad. Nauk SSSR, ser. fiz. 21, 7, 1034 (1957).

[48] G. S. Vil'dgrube, Dissertation (1958).

[49] L. G. Leiteizen, A. G. Berkovskii, I. Ya. Breido, B. M. Glukhovskoi, O. S. Korol'kova, and E. I. Tarasova, Izv. Akad. Nauk SSSR, ser. fiz. 21, 1653 (1957).

[50] L. G. Leiteizen, B. M. Glukhovskoi, and I. Ya. Breido, Crystallography 2, 290 (1957) [USSR].

[51] A. G. Berkovskii, L. G. Leiteizen, and V. G. Pol'skii, Izv. Akad. Nauk SSSR, ser. fiz. 22, 1002 (1958).

[52] A. A. Kurashov, A. F. Linev, B. V. Rybakov, and V. A. Sidorov, J. Atomic Energy 5, 135 (1958).

[53] N. A. Vlasov, S. P. Kalinin, B. V. Rybakov, and V. A. Sidorov, Proceedings of the International Conference on Nuclear Physics (Paris, 1958).

TIME ANALYZERS

During recent years a great number of time analyzers for the millimicrosecond region have been developed and described. We shall consider only the basic time analyzers which are used in neutron spectroscopy.

§ 1. Single-Channel Time Analyzer

The simplest kind of single-channel time analyzer suitable for fast neutron spectroscopy by time-of-flight methods is a coincidence circuit with a resolving time of the order of millimicroseconds. To one branch of the coincidence circuit are applied the pulses from a scintillation counter; the control pulses are applied to the other branch. The dependence of coincidence counting rate on the delay of the control pulse then yields the neutron distribution over time-of-flight.

In one of the first fast-neutron time-of-flight spectrometers [1, 2], used at the one and one-half meter cyclotron, a parallel coincidence circuit employing germanium diodes was employed; the resolving time of this unit was determined by the shape of the pulses applied to it. A fundamental shortcoming of a spectrometer of this type is the dependence of effective channel width (see p. 99) on neutron energy due to the fact that the resolving time of the circuit depends strongly on the amplitude of the counter pulses. Later, on the basis of this circuit a single-channel spectrometer with a "differential" channel was built [2, 3]; this improved unit was free from the disadvantage indicated above and had a higher resolving power.

In spite of the availability of multichannel time analyzers a spectrometer of this type is still of great interest and, being simple in use and construction, has been used to make absolute measurements of neutron flux intensities [4].

The circuit of the time analyzer [3] is shown in Fig. 66. It has two identical channels; each consists of a fast coincidence circuit, a cathode follower and an amplifier with an output discriminator. One input of the coincidence circuit is common. The control pulses are applied to it. The pulses from the scintillation counter, taken from the anode of the photomultiplier, are applied to the second input of the coincidence circuit. A delay Δt is introduced between these two inputs. Both fast coincidence channels and the anticoincidence arrangement between them comprise a differential channel (output D). The anticoincidence circuit, which has a resolution time of 1 μsec, chooses only those events in which there is a pulse in the first channel and no pulse in the second.

If the fast coincidence circuits are identical, and this situation can be realized fairly well by choice of diodes and mode of operation, it will be apparent that the width of the differential channel is essentially equal to the delay time Δt and is independent of the length of the pulses applied to the circuit. The width of each of the fast coincidence channels (outputs 1 and 2) is determined by pulse lengths and can be made considerably larger than Δt.

It should be noted that although the effective width of the differential channel is independent of the amplitude of the pulses from the photomultiplier, if the amplitude of these pulses changes, the position of the channel can be shifted by an amount of the order of the rise time of the photomultiplier pulse. If it is necessary to make an exact determination of the energy of a neutron line, this effect can be eliminated by using a pulse-height discriminator to select a narrow range of pulse amplitudes from the counter. In the present case, the effect is small because when the FEU-2V photomultiplier is used the pulse rise time is 3 mμsec.

The control pulses, which are synchronized with the RF in the cyclotron, are formed in a generator, the basic element of which is an electron-beam tube with a plane deflected beam. The RF voltage is taken from the resonant line of one of the dees in the cyclotron by means of a coupling loop and is then fed to the generator through a phase shifter. After the required amplification the RF is applied to the deflection plates of the electron-beam tube. By proper choice of RF amplitude, it is possible to obtain a pulse of the required duration (from 1 mμsec up to several tens of mμsec) at the collector. Only one control pulse must be produced per RF period; for this reason when the beam of the tube reverses direction, an RF voltage, shifted with respect to the first by 90°, is applied to a blanking electrode (near the cathode of the tube).

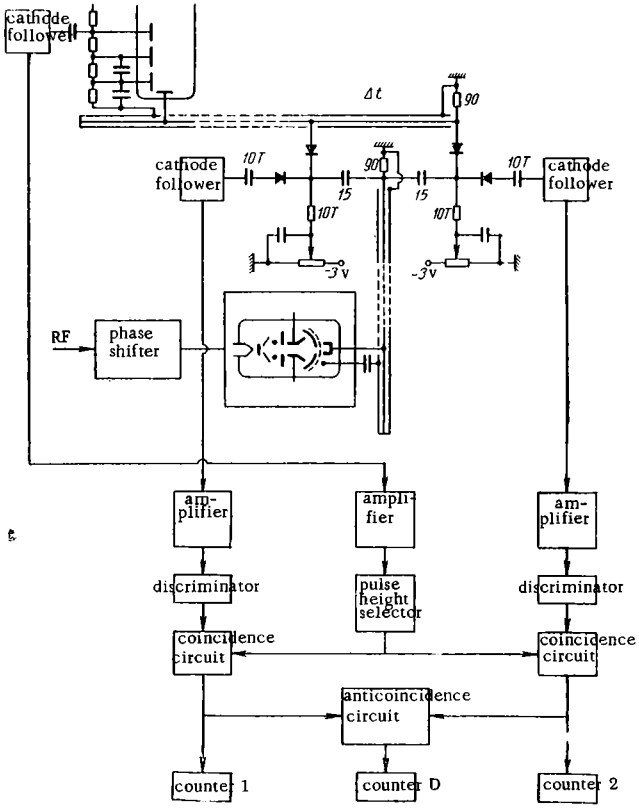

Fig. 66. Differential time analyzer.

The required variation of control-pulse delay needed to obtain the time-of-flight distribution of the neutrons is obtained by means of a phase shifter (Fig. 67) which shifts the RF sine wave before it is applied to the control pulse generator. By means of two 11-position switches, which are used to vary the length of the input cable (RK-2), the sine wave can be shifted between 0 and 120 mμsec in steps of 1 mμsec.

In Fig. 68 are shown characteristic time-analyzer curves for delayed coincidences in all three channels when used to detect γ-rays from the cyclotron target. The delay time is approximately 5 mμsec. The curve for the differential channel has approximately the same width at half-height.

(see § 2, Chapter VIII).

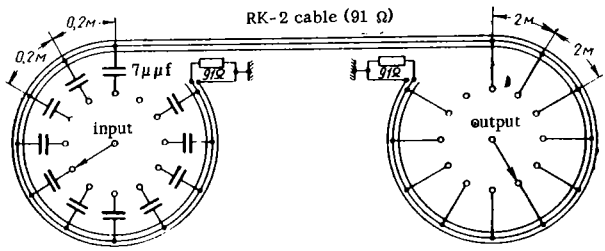

Fig. 67. Diagram of the phase shifter.

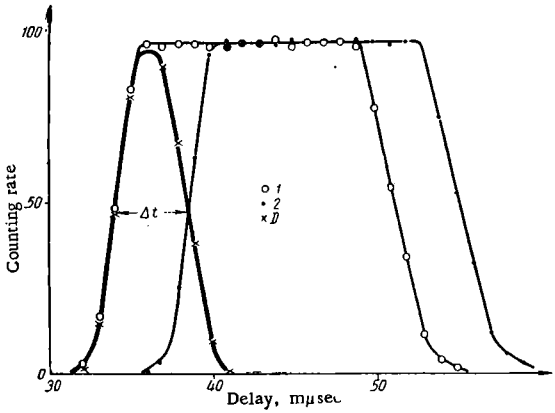

Fig. 68. Curves showing delayed coincidences in three channels of the differential time analyzer.

§ 2. Chronotron

The application of multichannel systems represents an important step forward in the development of time analyzers. It is possible to achieve a marked reduction in the time required for measurements through the use of a multichannel system. In addition, the possibility of making a measurement of the entire spectrum relaxes the requirements on the stability of the neutron source; this last factor is very important in fast neutron work since the stability of many of the neutron sources used in this work (accelerator targets) is frequently not all that might be desired.

One of the simplest multichannel time analyzer systems is the "chronotron" [5], which has found wide application in circuits with two particle counters. The chronotron is essentially a combination of several delayed coincidence circuits which are connected to the counters through sections of cable of different length.

A schematic diagram of the chronotron is shown in Fig. 69. Two cables are used to carry the pulses from the two counters, A and B. (In neutron spectroscopy with a pulsed source one of the counters is replaced by the control pulse generator). The particular coincidence circuit channel which is activated is determined by the time differential between the two pulses. The number of coincidences in each channel is recorded separately.

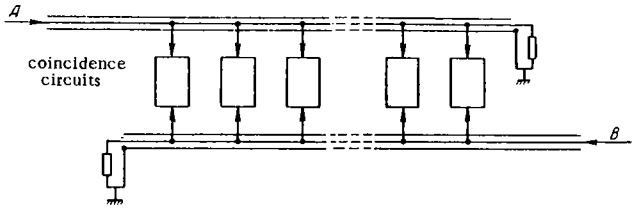

Fig. 69. Schematic diagram of the chronotron.

A shortcoming of this method is the fact that the time width of a channel is not affected by the separation between channels. In this respect the chronotron is no different from a single-channel analyzer. The separation between channels is determined by the length of a section of cable while the width of a channel is determined by the pulse lengths and the sensitivity of the coincidence circuits. The dependence of channel width on the sensitivity of coincidence circuits makes it difficult to obtain good channel uniformity. Just as in the simple coincidence circuit, the width of the channels in a chronotron depends on the amplitude of the counter pulses.

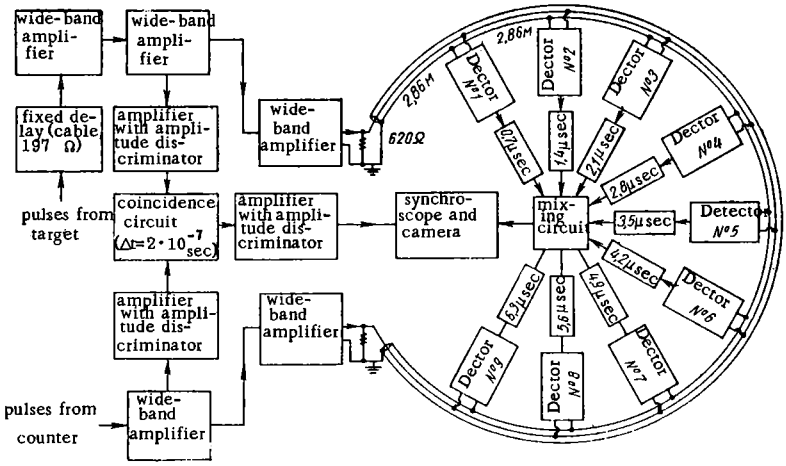

Fig. 70. The chronotron used by Grismore and Parkinson [6].

One method of avoiding the dependence of channel width on pulse amplitude and providing good uniformity is the application of the same principle as that used as a basis for the differential time analyzer described in the preceding section.

The number of channels in a chronotron is usually less than ten. A chronotron with 100 or more channels represents a project of great difficulty and is usually unreliable. A large number of channels leads to difficulties associated with damping of the pulses in the distribution cable because of reflection from discontinuities at the points at which the coincidence circuits are connected.

A chronotron has been used by Grismore and Parkinson [6] as a fast neutron time-of-flight spectrometer with a pulsed neutron source. A block diagram of the time analyzer used by these authors is shown in Fig. 70. The control pulses and the pulses from the neutron detector are applied to opposite ends of a coaxial cable. At various intervals, corresponding to pulse delays of 20 mμsec, are connected 9 diodes which act as peak detectors. A coincidence between a pulse from the scintillation counter and a control pulse results in an increase in the amplitude of the pulse at the output diode. The output pulses of the peak detectors are presented on the screen of an oscilloscope. The distribution of these pulses on the oscilloscope sweep is realized by introducing delays of equal lengths (Fig. 70) between the output of each diode and the mixer at the input of the oscilloscope. The sweep generator of the oscilloscope is triggered by means of an auxiliary coincidence circuit which has a resolution time of $2 \cdot 10^{-7}$ sec, somewhat larger than the total time range measured by the chronotron ($1.6 \cdot 10^{-7}$ sec).

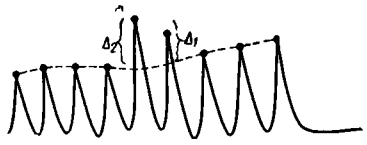

Fig. 71. Oscillogram showing pulses from the chronotron.

The use of peak detectors results in a smooth dependence of pulse amplitude at the output diode on the degree of superposition between the pulse from the scintillation counter and the control pulse. The duration of each of these pulses is about 20 mμsec so that their superposition is observed simultaneously in two neighboring channels (Fig. 71). Using the amplitude ratio of the pulses in these channels Δ_1/Δ_2 it is found possible to determine the point of maximum superposition accurately. The width (at half-height) of the curve which characterizes the inherent resolving time of the chronotron is 0.6 mμsec, which is 30 times smaller than the time corresponding to the section of cable between diodes.

A shortcoming of this system is the low counting rate which results from the need for photographing each detection event. The requirement for careful measurement by photography is additional difficulty in the processing of the results; the work is almost equivalent to that involved in using photographic emulsions.

§ 3. Fast Oscilloscope

In many laboratories which were concerned with fast-neutron spectroscopy by time-of-flight methods in early experiments, the basic element of the millimicrosecond time analyzer was the sweep of a "fast" oscilloscope [7-10]. Let us consider the analyzer used by Malmfors et al. [10], in which this principle was used. The basic element in this system was a fast commercial oscilloscope, the Tektronix 517, which has a short rise time in the vertical amplifier (7 mμsec), a high sweep speed (up to 10 mμsec/cm) and a high accelerating voltage (24 kv), so that it is possible to get good intensity at the screen.

One of the first versions of the time analyzer operated as follows. The pulse from the scintillation counter is used to trigger the horizontal sweep of the oscilloscope while pulses synchronized with the neutron pulses are applied to the vertical plates. The pulse from the scintillation counter is applied to the vertical plates of the oscilloscope through a delay line. The screen of the oscilloscope is photographed by continuously moving film. The measurement of the position of the pulse from the scintillation counter with respect to the control pulses, taken on the same sweep of the oscilloscope beam, makes it possible to avoid errors due to the delays in operation of the trigger for the horizontal sweep of the oscilloscope; these errors can be considerable when the amplitude of the pulse from the scintillation counter is only slightly greater than the threshold value.

In the latest design of the time analyzer [10] the screen of the oscilloscope is photographed on a film which remains fixed throughout the whole series of measurements. In this case only the control pulses are applied to the vertical plates of the oscilloscope; the sweep is triggered by pulses from the neutron counter. In the trigger system for the oscilloscope sweep there is an amplitude selection channel which is used to avoid errors due to delay in triggering of the sweep because of small-amplitude pulses. After differentiation, the control pulses are applied to the modulator of the oscilloscope tube. Thus, the time at which the pulse from the neutron counter is produced is recorded on the photograph by lines which correspond to the front of the control pulse. With this system it is possible to eliminate the tedious process of developing a large number of photographs; instead it is only necessary to make a photometric measurement of a single picture.

In spite of the considerable nonlinearity in the oscilloscope sweep (approximately 10%) the authors were successful in achieving high accuracy in the measurement of the time intervals corresponding to the distance between peaks on the photometry curves. The error (± 0.2 mμsec) was much smaller than the resolution time of the spectrometer.

In Fig. 72 is shown a typical neutron spectra obtained by recording 10,000 pulses and the resulting curve obtained by photometry. The sweep velocity was such that the oscilloscope screen recorded three consecutive periods of the pulses from the neutron source.

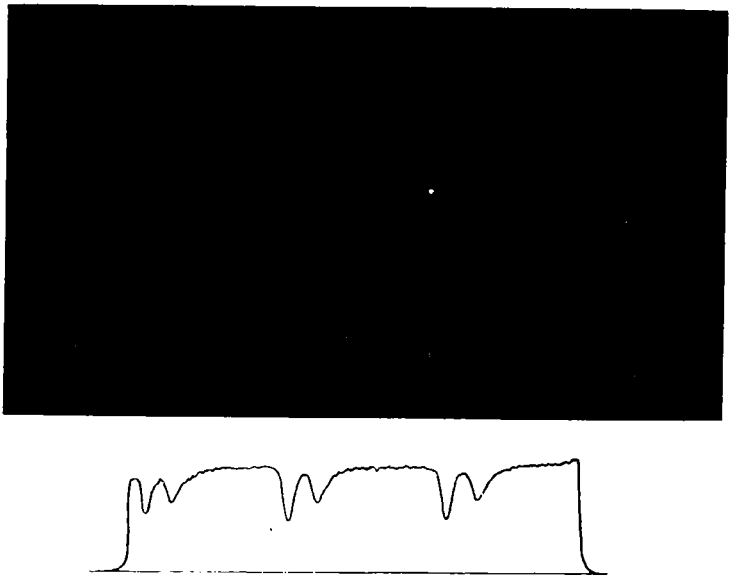

Fig. 72. Photograph of a neutron spectrum and the curve obtained by photometry [10].

The presence in the spectrum of similar peaks, produced in different periods (for example, two neighboring γ-peaks), makes it possible to monitor the time scale. Moreover, the quality of operation of the system at the extremes of the working range is no longer important.

The last remark refers to any time analyzer in a spectrometer with a pulsed neutron source. For this reason it is desirable to make the working range of these analyzers greater than the period of the neutron source.

A basic shortcoming in photometric detection systems is the difficulty making either an absolute measurement or an accurate relative measurement of the intensities of different peaks in the neutron spectrum.

§ 4. "Time-to-Amplitude" Conversion

Among the multichannel millimicrosecond time analyzers which have received widest application are analyzers which work on the so-called "time-to-amplitude" conversion principle [5, 9, 11-18]. The basic element of a system which works on this principle is a condenser which is charged by direct current for a period of time equal to the interval being measured. The voltage pulses formed at the condenser may be analyzed by any multichannel amplitude analyzer. The possibility of applying an available multichannel amplitude analyzer with its recording system (which is always complex for a large number of channels) is the main advantage of this type of time analyzer and has been the reason for its popularity.

Technically, it is more convenient to carry out the time-to-amplitude conversion by means of a double-gated beam tube (type 6AZP or American 6BN6). The sharp cutoff at both ends of the characteristic makes it possible to obtain pure direct current for charging the condenser connected to the anode of this tube.

The measurement of the interval of time between two pulses applied to the converter can be carried out as follows. In the quiescent state one grid is closed and the second is open. The first pulse actuates a trigger which generates a pulse of length greater than the maximum time interval being measured. The positive pulse from the trigger is applied to the blanked grid of the tube and opens it. A second pulse, corresponding to the end of the interval being measured, actuates the second trigger unit, cutting off the beam tube at the second grid. It is apparent that the length of the pulse from the second trigger circuit must be greater than the length of the pulse from the first trigger circuit. The condenser which is then charged is discharged with a time constant considerably greater than the time being measured.

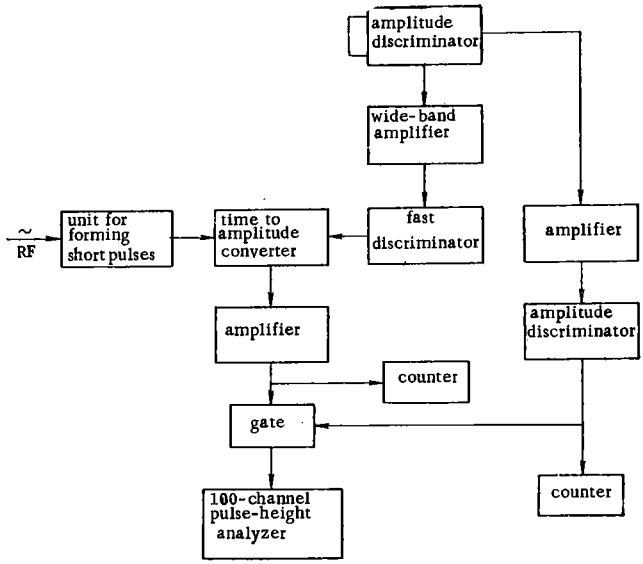

Fig. 73. Block diagram of a time analyzer which uses time-to-amplitude conversion.

The application of this principle for time analysis in a spectrometer with a pulsed neutron source requires taking account of certain special conditions which obtain; in arrangements of this kind, periodic pulses, at a high repetition frequency (control pulses), are applied to one of the inputs of the analyzer. These pulses can only be used for cutting off the beam tube. Under these conditions the charging time of the condenser will not be proportional to the time interval being measured (the time-of-flight of a neutron over a given distance) but a quantity which is the complement of this interval in the control-pulse repetition period.

In Fig. 73 is shown a block diagram of a time analyzer [11], used by Cranberg et al. [19-23]. The pulses from the scintillation counter are amplified by a wide-band amplifier and applied to a fast discriminator. The pulses from the fast discriminator are applied to the input of the "time-to-amplitude" converter, to the other input of which are applied the control pulses.

In the spectrometer used by Cranberg the neutron source is a van de Graaf generator in which the beam is modulated by means of a simple chopper (see Fig. 42). The control pulses are formed from a sinusoidal voltage which is applied to the deflection plates of the chopper; each period of the sign wave corresponds to a single control pulse.

Because of the fact that there are two neutron pulses for each control pulse (the forward and reverse motion of the beam in the chopper) the time analyzer measures a time interval equal to two periods of the neutron source. This is very important in the present case because a time analyzer of the type being considered here has a good characteristic only in the central portion of the working range. The distortions which arise are due to the finite length of the pulse fronts of the pulses produced by the trigger and occupy a region of about 20 mμsec at both extremes of the time range being investigated.

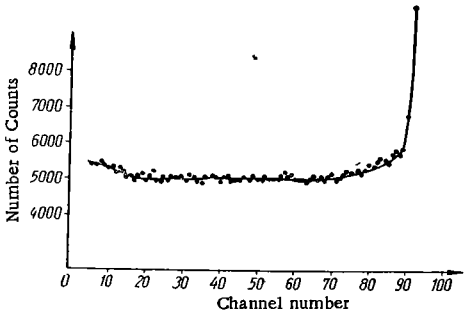

Fig. 74. The observed time distribution of pulses from a scintillation counter used to detect radiation from a radioactive source [11].

The quality of operation of the time analyzer is shown in Fig. 74 in which the observed distribution of counter pulses is given in the detection of γ-rays from a radioactive source. Along the ordinate axis are plotted the amplitudes of the output pulse from the converter, which are proportional to the time interval between the pulse from the counter and the control pulse. Since the counter pulses exhibit a statistical time distribution, in proper operation of the time analyzer there should be a uniform distribution of pulses over channels. As is apparent from Fig. 74, in the central portion of the range, this requirement is satisfied.

In Fig. 75 is shown the neutron spectrum obtained by scattering neutrons with an energy of 2.45 Mev [20] on titanium. The time scale goes from right to left. One of the two periods of the neutron source scanned by the analyzer lies completely within the linear portion of the range. The channel width of the time analyzer is 2.5 mμsec. The widths (at half-height) of the γ-peak and the peak corresponding to elastic neutron scattering are approximately equal, both being approximately 5 mμsec.

In the present case the resolution time of the spectrometer is determined by the resolving time of the scintillation counter. Generally speaking, the resolution time depends on the amplitude of the pulses from the scintillation counter which are applied to the fast discriminator (Fig. 73). In Fig. 76 is shown the dependence of the delay in the operation of the discriminator on its threshold setting for a given trigger-pulse amplitude. In order to obtain this characteristic, standard pulses from a special generator, having a rise time of approximately 1.5 mμsec, were applied to the discriminator. It is apparent from Fig. 76 that when the discriminator threshold is close to the pulse amplitude the discriminator operates with a delay greater than 10 mμsec. In recording pulses from a scintillation counter this situation can lead to a considerable smearing of the lines since the counter produces a continuous amplitude spectrum.

It is apparent from Fig. 76 that this smearing can be eliminated by limiting the pulse amplitudes which are used to values which are several times greater than the fast-discriminator threshold. This limiting operation can be carried out by means of an auxiliary part of the amplitude selector (Fig. 73). The input of a 100-channel amplitude analyzer which records the pulses from the "time-to-amplitude" converter is opened by a pulse from a conventional "slow" discriminator to which are applied pulses from one of the last dynodes of the photomultiplier in the scintillation counter.

It is apparent that the energy threshold of the neutron detector also is given by the "slow" discriminator in this case.

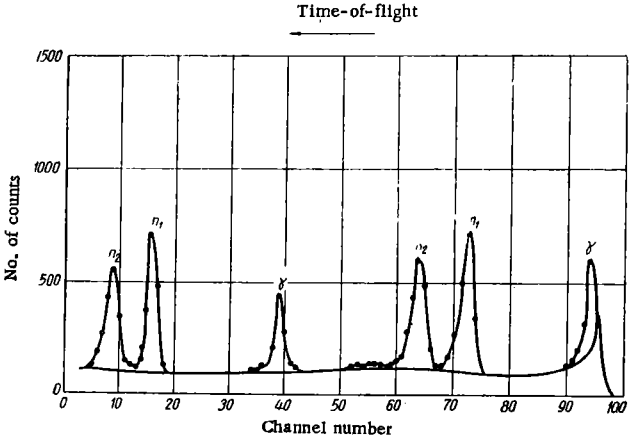

Fig. 75. Neutron spectrum observed at 90° in scattering of 2.45 Mev neutrons on titanium: n_1 is the number of scattered neutrons, n_2 is the neutron group corresponding to excitation of the level at 1.02 Mev in Ti^{48}, γ are peaks corresponding to γ-rays from the scatterer.

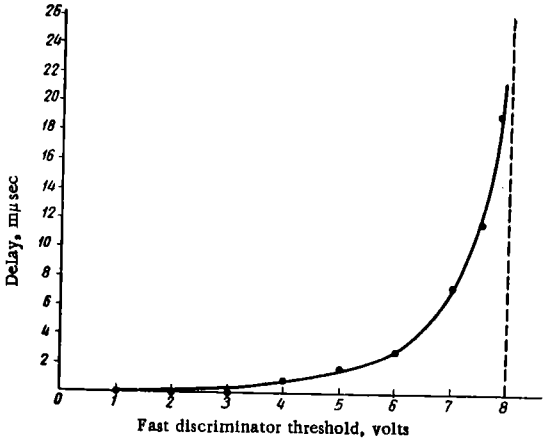

Fig. 76. Delay in the operation of the fast discriminator as a function of threshold setting for a given trigger pulse amplitude. The threshold equal to the amplitude of the pulse is denoted by the dotted line.

§ 5. "Vernier Principle"

A new principle for use in time analysis in the millimicrosecond region has recently become known; this system is called the "vernier" system [25, 26]. A time analyzer which works on this principle has been built at the Institute for Atomic Energy of the Academy of Sciences, USSR [27].

The basis of this analyzer is two generators which produce pulses with repetition periods which are almost the same; the number of operating cycles of one of the generators, counted from some starting time up to the first coincidence of pulses from the two generators serves to measure the time interval between the pulses from the generators at the starting time. The vernier principle is illustrated in Fig. 77 (in the simplest case the generator periods can be taken as T and $T - \Delta t$).

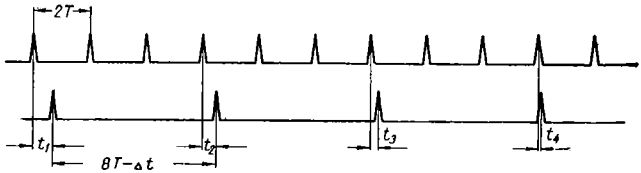

Fig. 77. Principle of the "vernier": 2T is the period of the control pulse oscillator; $(8T - \Delta t)$ is the period of the phased oscillator; t_1 is the position of the first pulse from the phased oscillator with respect to the control pulse; on the fourth cycle of operation of the phased oscillator a coincidence occurs.

If the channel width is of the order of 1 mμsec the time interval being studied (two periods of the neutron source) occupies approximately 200 channels. In the spectrometer use is made of an ELA-2 (an improved version of the ELA-1 [28]) multichannel amplitude analyzer with a "potentialscope" memory having 256 channels with a capacity of 2^{16} pulses in each channel; with this arrangement it is possible to obtain data in the form of a photograph of the screen of the oscilloscope tube.

In order to direct a pulse into a definite channel of the ELA-2 recording system, it is necessary to apply a series of pulses, the number of which is one less than the channel number. The speed of operation of the recording system is such that the repetition frequency of the pulses in the series cannot be much higher than 1 Mc. Thus, for the given channel width (1 mμsec) the problem of time analysis leads essentially to changing the scale by approximately a factor of a thousand. The vernier time analyzer is very convenient in this connection since the source of the pulse series can be the pulse generator itself; the number of cycles of the generator from the starting time to the first coincidence is proportional to the time interval being measured. In this case, the repetition frequency of the pulses from the generator, because of the characteristics of the recording system, must be approximately 10 times smaller than the repetition frequency of the pulses from the neutron source; in the present case the latter frequency is 10 Mc (the frequency of the RF accelerating voltage in the cyclotron).

A block diagram of the spectrometer is shown in Fig. 78. Control pulses, synchronized with the RF, are formed by means of a trigger unit which uses a secondary emission pentode. These pulses are several mμsec in length. The repetition frequency of the neutron pulses T is equal to the RF period. In order to make it possible to study a time interval equal to 2T, the generator which provides the control pulses must provide one pulse for each two RF periods. This relation is obtained by means of a frequency divider which is part of the system; the input of the divider receives a sinusoidal voltage taken by means of a coupling loop from a resonant line of one of the dees in the cyclotron. The control pulses with period 2T are applied directly to the fast coincidence circuit.

A basic part of the time analyzer is the "phased" generator, which is triggered by the pulse from the scintillation counter. It is a trigger unit with delayed inverse feedback which uses a secondary emission pentode. The delay line in the negative feedback system is approximately 150 meters of RK-2 cable. The length of the cable is chosen to make the period of the phased generator $8T - \Delta t$ ($\Delta t \sim 1$ mμsec). As is apparent from Fig. 77, the fact that the period of the phased generator is four times greater than the period of the control pulse generator

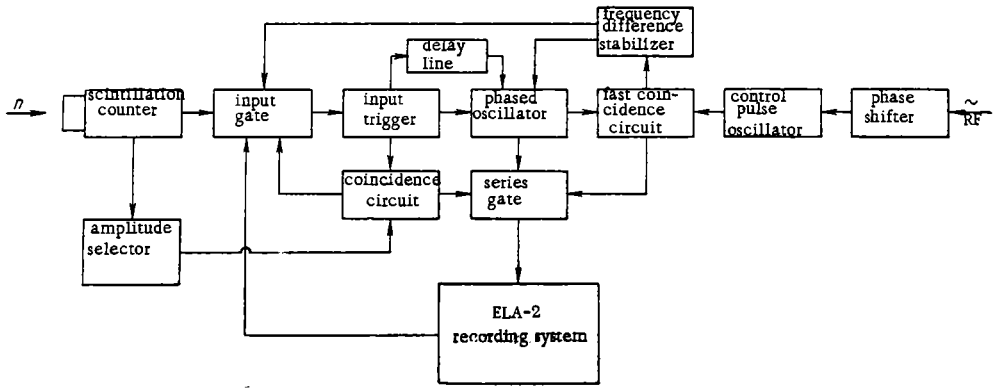

Fig. 78. Block diagram of the neutron spectrometer which uses a vernier arrangement.

has very little effect on the operation of the time analyzer. The position of each subsequent pulse of the phase generator with respect to the control pulse varies by an amount Δt with each cycle of operation ($t_2 = t_1 - \Delta t$; $t_3 = t_2 - \Delta t$, etc.). The total length of the control pulse and the pulse from the phased generator is greater than Δt. Hence, at some cycle (the fourth cycle in Fig. 77) these two pulses become superimposed. This superposition is recorded by the fast coincidence circuit which makes use of a double-gated beam tube (6AZP). The number of cycles of operation of the phase generator from the time at which it is triggered by a pulse from the counter to the time at which the fast coincidence circuit operates is linearly related to the quantity t_1 and, consequently to the neutron time-of-flight being measured. The repetition frequency of the pulses from the phased generator is 1.25 Mc (for an RF frequency of 10 Mc). It produces a series of pulses which are applied to the input of the recording system. The time of the end of the series is fixed by the operation of the fast coincidence circuit. Thus, the width of a channel of the time analyzer is Δt.

The triggering of the phased generator in the quiescent state is accompanied by transient processes which are apparently due to dynode fatigue. These processes cause a change in the generator period which amounts to several mμsec during the course of the first hundred cycles of operation. In order to avoid this effect the pulse from the scintillation counter is not used to trigger but to phase the generator, which is in continuous operation (whence the name "phased" generator). The pulse from the anode of the photomultiplier (FEU-33) passes through the input gate and actuates the input trigger.

Fig. 79. Photograph of the screen of the oscilloscope in the ELA-2 system which records the neutron spectrum in a binary presentation. This same spectrum is given in conventional form in Fig. 80.

The input trigger provides two pulses; one of these shuts off the oscillator while the other triggers it again at a phase corresponding to the time of detection of the neutron. The oscillator is turned off in a time of approximately 2.5 μsec; this time is determined by the charge of the trigger pulse by means of a line consisting of 500 meters of RK-3 cable.

The spectrometer contains a pulse-height selector, to the input of which are applied pulses from one of the last dynodes of the photomultiplier. The pulse-height selector is connected in coincidence with the input trigger so that it is possible to vary the effective threshold of the counter over wide limits. The counter threshold, which is fixed by the amplitude selector, must be at least ten times higher than the threshold for the input trigger unit. If this is not the case, there is a delay in the operation of the input trigger which can be greater than 10 mμsec close to the threshold value.

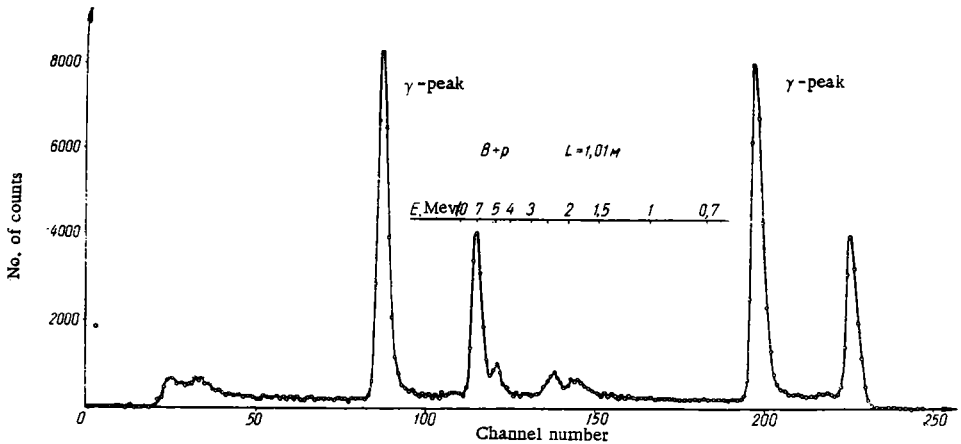

Fig. 80. Neutron spectrum observed in the bombardment of boron by 9.8 Mev protons. The channel width is 0.874 mμsec. The counter with a stilbene crystal (diameter 3 cm, height 2 cm) was located at a distance of 1.01 m from the target at an angle of 0° with respect to the direction of the proton beam. The counter threshold, as determined by the amplitude selector was 1.0 Mev.

The coincidence circuit closes the input gate and opens the gate for the series of pulses of the phased generator in the ELA-2 recording system. The gate is closed by a pulse from the fast coincidence circuit. The recording system records a pulse in the appropriate channel of its memory and generates a signal which opens the input gate. During the operation of the regenerative recording system in its memory [28] the system closes the input gate.

The operation of a vernier time analyzer requires a constant difference in the frequencies of the oscillators which are used. If the frequencies of these oscillators are independent very high stability is required. Thus, in the case being considered here, to provide a 1% stability in the channel width it is necessary that the frequency stabilities of the RF oscillator in the cyclotron and the phased oscillator be better than 0.001%. Neither one of these oscillators has a stability of this kind. Hence, a circuit for stabilizing the frequency difference (channel width) is used in the analyzer. The sensing unit for the stabilizer measures the time interval between two pulses at the output of the fast coincidence circuit. The measurement is made with the closing of the input gate. In this case, the interval being measured is equal to the maximum length of the series applied to the input of the recording system. This time period is $16\,\frac{T^2}{\Delta t}$ and is inversely proportional to the channel width. The stabilizer works by shifting the time of operation of the phased oscillator. A change in the time of operation changes the period of the phased oscillator.

The operation frequency of the stabilizer is 50 cps and is derived from the line frequency. Hence, the stabilizer cannot correct for frequency modulation of the phase oscillator and RF oscillator in the cyclotron due to the power supply. In order to reduce these effects to a reasonably low level, it is necessary to supply the filaments of the tubes in the phased oscillator with direct current and to use an RF oscillator which is independently excited. Stable operation of the cyclotron with an independently excited oscillator was found possible only after the development of a system for automatic adjustment of the resonant frequency of the cyclotron chamber.

An important characteristic of a multichannel analyzer is the uniformity of the channel width. The uniformity of the channel width of the time analyzer can easily be checked by measuring a time distribution of pulses from a counter which is exposed to a radioactive source. Measurements carried out in this way show that the deviation of the channel width from the mean value is less than 1%.

To illustrate the operation of the spectrometer, in Fig. 79, is shown a photograph of the screen of an oscilloscope of the ELA-2 recording system using a binary system to record the neutron spectrum obtained by bombarding boron with 9.8 Mev protons.

The scintillation counter was located at a distance of 1.01 meters from the target at an angle of 0° with respect to the proton beam. The same spectrum is shown in Fig. 80.

LITERATURE CITED

[1] G. F. Bogdanov, A. A. Kurashov, B. V. Rybakov, and V. A. Sidorov, J. Atomic Energy 1, 66 (1956).

[2] G. F. Bogdanov, Dissertation (1957).

[3] G. F. Bogdanov, N. A. Vlasov, S. P. Kalinin, B. V. Rybakov, and V. A. Sidorov, J. Atomic Energy 3, 204 (1957). [USSR].

[4] G. F. Bogdanov, N. A. Vlasov, S. P. Kalinin, B. V. Rybakov, L. N. Samoilov, and V. A. Sidorov, J. Exptl.-Theoret. Phys. (USSR) 36, 643 (1959).

[5] Lewis and Wills, Millimicrosecond Pulse Techniques, IIL (1956).

[6] R. Grismore and W. C. Parkinson, Rev. Sci. Instr. 28, 245 (1957).

[7] R. V. Smith, Conference on Neutron Physics by Time-of-Flight, (Gatlinburg, Tennessee, 1956), p. 103.

[8] L. Cranberg, G. Frye, N. Nereson, and L. Rosen, Phys. Rev. 103, 662 (1956).

[9] A. B. Smith, P. R. Fields, and J. H. Roberts, Phys. Rev. 108, 411 (1957).

[10] K. G. Malmfors, J. Kjellman, and A. Nilsson, Nuclear Instruments 1, 186 (1957).

[11] W. Weber, C. W. Johnston, and L. Cranberg, Rev. Sci. Instr. 27, 166 (1956).

[12] H. L. Schultz, G. F. Pierer, and L. Rosler, Rev. Sci. Instr. 27, 437 (1956).

[13] G. N. Glasoe, H. H. Landon, A. J. Elwyn, and S. Oleksa, Proceedings of International Conference on the Neutron Interactions with the Nucleus (Columbia University, New York, 1957), p. 230.

[14] W. M. Good, J. H. Gibbons, and J. H. Neiler, Proceedings of International Conference on the Neutron Interactions with the Nucleus, Columbia University (New York, 1957), p. 162.

[15] J. P. Scanlon, G. N. Stafford, J. J. Threshner, and P. H. Bowen, Rev. Sci. Instr. 28, 749 (1957).

[16] W. Bertozzi, F. R. Paolini, and C. P. Sargent, Phys. Rev. 110, 790 (1958).

[17] J. D. Anderson, C. C. Gardner, M. P. Nakada, and C. Wong, Phys. Rev. 110, 160 (1958).

[18] L. G. Kuo, Centre d'Etudes Nucleaires de Saclay, Paris, private communication.

[19] L. Cranberg and J. S. Levin, Phys. Rev. 100, 434 (1955).

[20] L. Cranberg and J. S. Levin, Phys. Rev. 103, 343 (1956).

[21] L. Cranberg, A. H. Armstrong, and R. L. Henkel, Phys. Rev. 104, 1639 (1956).

[22] J. D. Seagrave and L. Cranberg, Phys. Rev. 105, 1816 (1957).

[23] L. Cranberg, R. K. Beauchamp, and J. S. Levin, Rev. Sci. Instr. 28, 89 (1957).

[24] L. Cranberg and J. S. Levin, Phys. Rev. 109, 2063 (1958).

[25] C. Cottini and E. Gatti, Nuovo Cimento 4, 1950 (1956).

[26] R. L. Chase and W. A. Higinbotham, Rev. Sci. Instr. 24, 448 (1957).

[27] A. A. Kurashov, A. F. Linev, B. V. Rybakov, and V. A. Sidorov, J. Atomic Energy 5, 135 (1958)[USSR].

[28] G. P. Mel'nikov, L. I. Artemenkov, and Yu. M. Golubev, Inst. and Expt. Tech. (USSR) 6, 57 (1957).

BASIC CHARACTERISTICS OF A TIME-OF-FLIGHT SPECTROMETER

§ 1. Resolving Power

The linewidth of a spectrometer (and consequently its resolving power) can be broken down into several "partial" widths which due to different factors which introduce uncertainties into the determination of the neutron energy. These factors include the finite length of the neutron pulse, the resolution time of the detector, etc. If there is no correlation between the uncertainties in the determination of neutron energy and they have a Gaussian distribution in amplitude, in determining the resultant of the partial widths for computing total resolving power of the spectrometer one uses the quadratic form:

$$\delta = \sqrt{\Sigma \sigma_i^2}.$$

In practice the use of this simple method of combining the partial widths does not introduce any significant error even when the distribution of uncertainties, as is frequently the case, is not Gaussian.

The resolving power of a spectrometer for the study of primary neutron spectra is determined by its resolution time Δt and the uncertainty in the flight path ΔL. In addition, the accuracy of the final results of a study of neutron spectra depend on the energy spread of the primary charged particles, the energy thickness of the target which is used as the neutron source, and on the uncertainty in the angle of emission of the neutrons with respect to the beam of charged particles or primary neutrons.

The neutron energy is quadratically related to the time-of-flight and the flight distance. Hence, the relative uncertainty in the determination of the energy will be twice as large as the relative uncertainty in the measurement of the time-of-flight which causes it:

$$\delta_t = 2\frac{\Delta t}{t}\,;\ \delta_L = 2\frac{\Delta L}{L}\,.$$

The time spread is due to the following factors.

The length of the neutron pulse Δt_1 is determined by the duration of the charged particle pulse at the target; at the present time this quantity is 1-5 mμsec in most spectrometers. In certain spectrometers it can be made smaller than a millimicrosecond without any great trouble; however, this is not done because the resolution time of the spectrometer is limited by other factors.

The resolution time of the neutron counter Δt_2 is determined by the properties of the organic scintillators known at the present time and, chiefly, by the time characteristics of presently available photomultipliers; this quantity is of the order of 2-5 mμsec. It cannot be reduced substantially without a radical change in the design of photomultipliers and the application of new scintillators.

The use of spark counters for time-of-flight spectrometers would seem to be desirable at first glance because these have a very small resolution time; however they are not convenient because of their small neutron efficiency (thin hydrogenous radiator).

The resolution time of the time analyzer Δt_3 can easily be made less than a millimicrosecond.

The uncertainty in the synchronization of the electric "control" pulses with the neutron emission time Δt_4 is of importance when the inherent modulation of the cyclotron beam is used and the control pulses are locked to the sinusoidal accelerating voltage of the cyclotron rather than the particle pulses at the target. In this case, the accuracy in the measurement of the time-of-flight depends on the phase stability of the cyclotron.

The total resolution time of the spectrometer Δt is the quadratic sum of the components which have been enumerated. The better fast-neutron time-of-flight spectrometers are characterized by resolution times $\Delta t \sim$ $\sim$ 3 mμsec.

The quantity Δt can be determined experimentally from the width (at half-height) of the peaks due to γ-rays emitted by the accelerator target together with the neutrons; because of the small time-of-flight of the γ-rays the uncertainty in the flight distance does not enter into the width of the γ-peak.

The resolving power of a spectrometer if the uncertainty in the flight distance is neglected is given by the expression

$$\delta(\%) = \frac{2{,}8\sqrt{E\,(\text{Mev})}\,\Delta t\,(\text{m}\mu\text{sec})}{L\,(\text{m})}. \qquad (49)$$

As is apparent from this formula, the resolving power does not remain constant over the energy range but varies in proportion to $\sqrt{E}$. If a wide range of neutron energy is being studied this change in resolution is very inconvenient since it is necessary to increase the flight path to improve the resolution in the hard region of the spectrum; this means a strong reduction in the counting rate in the soft part.

The geometric factor which limits the resolving power of a spectrometer (the uncertainty in the flight distance) is due to the finite thicknesses of the target and the scintillator in the neutron counter and can sometimes be of importance. For example, with Δt = 3 mμsec, h = 5 cm, and l = 5 cm (gas target) it becomes equal to the factor which depends on the resolution time for neutron energies of approximately 6 Mev; it becomes greater than this factor for neutrons with smaller energies. In Fig. 81 is shown the resolving power of the spectrometer at the University of Michigan [1], computed for two values of crystal thickness and two values of L, as a function of neutron energy (l = 0).

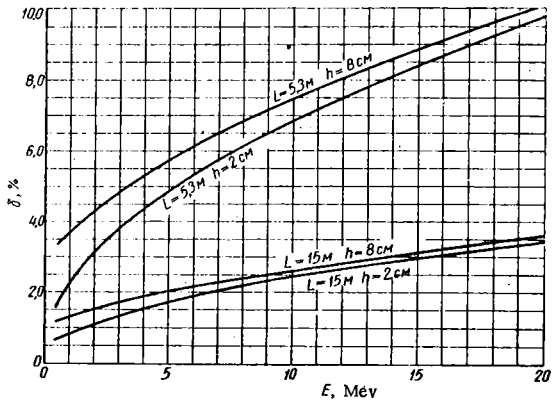

Fig. 81. Resolving power of the spectrometer at the University of Michigan [1] for different values of the flight path and crystal thickness.

The required reduction in scintillator thickness for work with relatively slow neutrons does not necessarily mean a loss in efficiency because the cross section for n, p-scattering increases with a reduction in neutron energy faster than the time-of-flight increases. To illustrate this point, in Fig. 82 are shown the scintillator thicknesses for which the neutron time-of-flight is 3 mμsec and the corresponding probability for scattering of a neutron on hydrogen (for a scintillator of composition CH and density of unity) as a function of neutron energy.

In the study of secondary neutrons it is more difficult to separate out the time and geometric components in the spectrometer resolving power. The errors due to the finite dimensions of the accelerator target, sample,

and scintillator, are simpler to estimate than the time spread. The additional time spread in the investigation of secondary neutrons arises because of the nonmonochromaticity of the primary neutrons which leads to a spread in their time-of-flight from the accelerator target to the sample.

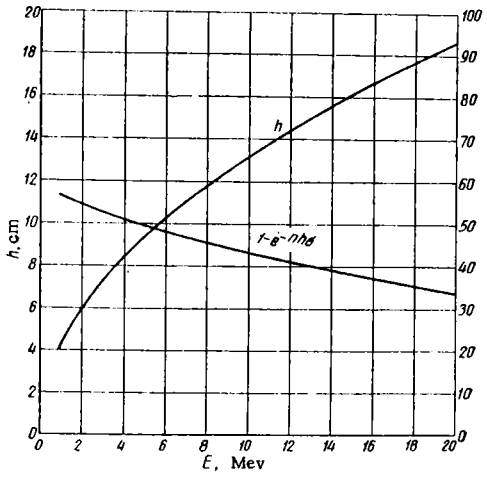

Fig. 82. Thickness of a scintillator for which the time-of-flight of a neutron is 3 mμsec and the corresponding probability for scattering of a neutron on hydrogen (for a scintillator with the composition CH and density of unity).

In Table 6, taken from Smith [2], are enumerated the factors which determine the resolution time of a time-of-flight spectrometer which uses an electrostatic accelerator for the study of neutrons with energies between 2 and 4 Mev.

TABLE 6

Source-time spread	Δt_1, (mμsec)	
	E = 4 Mev	E = 2 Mev
Length of the charged particle pulse	1.0	1.0
Nonmonochromaticity of the primary neutron	0.9	3.2
Target thickness (gas targets)	1.2	1.2
Scatterer dimensions	0.5	1.0
Thickness of the scintillator	0.9	1.3
Photomultiplier (RCA-6342)	2.0	2.0
Time analyzer	0.8	0.8
Δt	3.0	5.5

When used to study secondary processes the resolving power of a spectrometer can be determined by the width of the peak due to γ-rays emitted by the sample or by the width of the peak due to elastic scattering of the primary neutrons.

An important advantage of the time-of-flight method as compared with other methods of neutron spectroscopy is the theoretical possibility of obtaining as high a resolving power as desired by simply increasing the flight

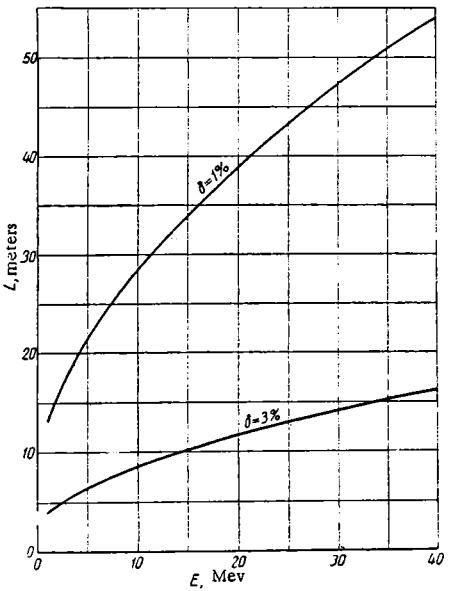

Fig. 83. Length of flight distance required to obtain a resolving power of 3% or 1% for a resolution time of 3 mμsec and a crystal thickness of 5 cm.

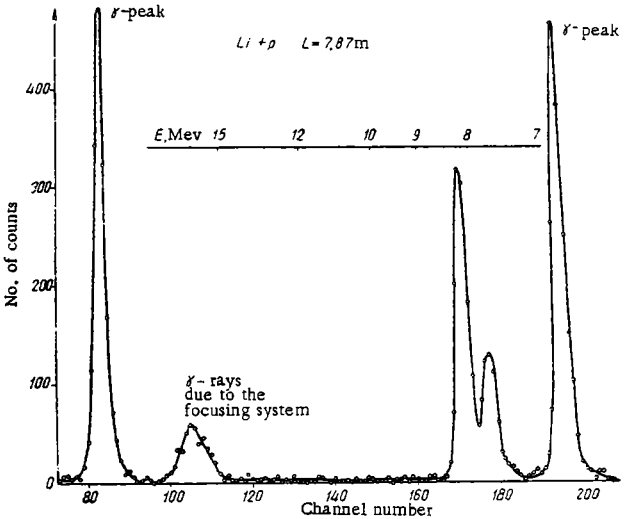

Fig. 84. Neutron spectrum obtained by bombarding lithium with 9.8 Mev protons; this spectrum was obtained with the multichannel spectrometer at the Institute for Atomic Energy [3]. The channel width is 0.865 mμsec. The target thickness is 3 mg/cm^2. A counter with a tolane crystal (diameter 8 cm, height 3 cm) is located at a distance of 7.87 m from the target at an angle of 0° with respect to the proton beam. The counter threshold is 6.1 Mev. The γ-rays due to the electrostatic focussing system can be seen (see Fig. 49).

path (for a fixed resolution time and fixed dimensions of the targets, scatterer, and counter). In Fig. 83 is shown the value of L required, for example, for obtaining δ = 3% and 1% with Δt = mμsec and h = 5 cm as a function of neutron energy.

The actual value of the resolving power achieved in present-day spectrometers is about 3%.

As an example, in Fig. 84 is shown the neutron spectrum obtained by bombarding lithium with 9.8 Mev protons [3]. In this case the length of the flight path is 7.87 m. The two neutron groups from the $Li^7(p, n)Be^7$ reaction (8.2 and 7.8 Mev) corresponding to the ground state and first excited state of Be^7 are clearly visible.

§ 2. Efficiency

The efficiency of a time-of-flight spectrometer with a pulsed neutron source is defined as the efficiency of the scintillation counter ϵ (40) and the solid angle subtended at the source by the counter (2);

$$\eta = \varepsilon \cdot \frac{S}{L^2} = \frac{n_0 \sigma}{L^2}\left(1 - \frac{B}{E}\right), \tag{50}$$

where S is the area of the scintillator cross section; L is the flight distance; n_0 is the total number of hydrogen atoms in the scintillator.

Among other things, Eq. (50) indicates that in computing the efficiency of a spectrometer η (in contrast with the efficiency of a counter ϵ) it is necessary to know the total weight of the scintillator rather than the density which, for organic crystals, depends on the method of fabrication and is a strong function of temperature.

In the determination of both the absolute intensity of a neutron flux as well as its spectrum the channel width of the neutron spectrometer is of great importance. Suppose that a channel of a spectrometer, denoted by the letter $\underline{k}$, records neutrons, with time-of-flight in the interval between $\underline{t}$ and $t + \Delta t_k$. The quantity Δt_k is the channel width. In the general case this quantity depends on $\underline{k}$.

If the time analyzer of the spectrometer is designed in such a way that each pulse of the counter must necessarily be applied to one of the channels and only to one, the channel width is equal to a spacing between neighboring channels. This is a property, for example, of the multichannel time analyzers described in § 4 and 5 of Chapter VII. In this case the counting rate in a spectrometer channel P(k) is related to the neutron spectrum by the expression

$$P(k) = \eta(k)\, V(t)\, \Delta t_k, \tag{51}$$

where $V(t)\Delta t_k$ is the number of neutrons emitted by the source per steradian per second with time-of-flight lying in the range between $\underline{t}$ and $t + \Delta t_k$; $\eta(k)$ is the efficiency of the spectrometer for these neutrons.

Whence we obtain the neutron time-of-flight distribution

$$V(t) = \frac{P(k)}{\eta(k)\,\Delta t_k}.$$

Consequently, in order to find the flux and the spectrum of neutrons from the distribution of counting rates over spectrometer channels, it is necessary to know the absolute value of the channel width and the way in which this channel width varies with the channel number.

If the channel width is constant over the entire working range its absolute magnitude can be defined precisely from the relation

$$\Delta t_k = \frac{T}{N},$$

where T is the repetition period of the neutron pulses; N is the total number of spectrometer channels corresponding to one period (for example the number of channels between neighboring γ-peaks).

In certain simple time analyzer there is no channel width in the sense indicated above. These include, for example, instruments like the chronotron as well as all single-channel analyzers in which the spacing between

"channels" is the magnitude of the step between adjacent measuring points. In these cases one can speak of an effective channel width which is determined by the line shape of the spectrometer.

Suppose that a source emits F_0 monoenergetic neutrons per steradian per second. In the detection of these neutrons by the spectrometer a line is observed; the center of the line coincides with some channel $\underline{k}$, corresponding to a given neutron energy. The counting rates in channels $\underline{k}'$, close to channel $\underline{k}$ are given by some (usually approximately Gaussian) function $f(k - k')$. The effective width of a channel designated by the letter $\underline{k}$ is then given by the relation

$$\Delta t_k = \frac{\Delta_1 t_k}{F_0 \eta(k)} \sum_{k'} f(k - k'),$$

where $\Delta_1 t_k$ is the spacing between neighboring channels, which usually does not change over the entire operating range. In this case the counting rate by channel is given by Eq. (51) for an arbitrary neutron spectrum.

If the time analyzer records all counter pulses which exceed the energy threshold B (50), fixed by the amplitude selector, the counting rate at the maximum of the line observed in recording monoenergetic neutrons is equal to the neutron flux multiplied by the spectrometer efficiency:

$$f(0) = F_0 \eta(k). \tag{52}$$

Thus, if the time analyzer is 100% efficient the effective channel width can be found experimentally on the basis of the relation

$$\Delta t_k = \frac{\Delta_1 t_k \sum_{k'} f(k - k')}{f(0)}. \tag{53}$$

In cases in which the time analyzer records part of the pulses, (for example, because of the time spread in the counter) in measuring $f(0)$ it is possible to set up conditions under which Eq. (52) can be applied by artificially broadening the spectrometer line.

If the effective channel width varies within the working range, in order to determine the dependence on channel number it is necessary to carry out a calibration procedure at several values of the energy, using monoenergetic neutrons.

A very simple calibration of the effective channel width can be made for the single-channel analyzer described in § 1, Chapter VII. The effective width of its "differential" channel, which provides a high resolving power, does not depend on the amplitude spectrum of the counter pulses and is independent of neutron energy. In addition to the differential channel in the spectrometer there is a wide channel which records all counter pulses exceeding the threshold level. It is possible to calibrate the spectrometer using any line, including the γ-peak; in this case, in place of $f(0)$ in Eq. (53) we substitute the counting rate corresponding to the flat top of the wide channel.

We now consider Eq. (50). As has been shown in § 1, Chapter VI, the optimum value of the setting of the counter threshold B in the sense of the best accuracy for the measurements depends on the energy of the neutrons being detected. In cases in which the neutron spectrum being investigated occupies a wide energy region the various parts of the spectrum may be measured most conveniently by using different threshold settings. Usually, a wide spectrum is measured in several sections. It is much more convenient to be able to vary B smoothly over the region being studied. In this case each channel may be assigned an appropriate value of B in accordance with some definite relation, for example, $B = \frac{E}{2}$, where E is the energy of the neutron recorded in a given channel. This method of measurement may be called the "tracking threshold" method.

The method of applying the tracking threshold method is obvious in the case in which a single-channel time analyzer is used, where the distribution of counter pulses in time is found by measuring the counting rate for coincidences with control pulses as a function of the delay of the latter. In this case, the counter threshold can be varied with the delay in accordance with some preassigned relation by an appropriate change in the threshold of the amplitude selector.

When multichannel time analyzers are used the tracking threshold method can still be applied in many cases although a great deal of difficulty is involved; this difficulty stems from the adjustment of the detection system. As an illustration we may consider one of the possible methods of applying the tracking threshold method in the case in which the detection system makes use of a "sequential" principle, i.e., the recording channels are opened one after another after various time intervals (this system is the system which is used in the majority of detection arrangements in present-day multichannel analyzers). If the threshold of the amplitude selector is varied in accordance with some required relation together with the change in the number of the opened recording channel, the counter threshold will be varied as a function of the energy of the neutrons being detected at a given instant of time. An amplitude discriminator with a variable threshold (or a selector with a variable window) can easily be realized for example by means of an oscilloscope. The horizontal sweep of the oscilloscope is moved in synchronism with the operation of the detection system in such a way that the sweep period is equal to the duration of a cycle in the recording system. After the required amplification the pulses from the counter are applied to the vertical plates of the oscilloscope. Part of the screen of the oscilloscope is covered by an opaque shield of the required shape. The appearance of a pulse above the opaque shield is recorded by a photoelectric element. The shape of the opaque shield can be computed in accordance with the required relation to be followed in the variation in the threshold or window of the amplitude selector. In the latter case the opaque shield covers the entire screen of the oscilloscope except for a slit of the required shape and width.

In concluding the present section we consider the dependence of the efficiency of a time-of-flight spectrometer on neutron energy for a given resolving power. From Eqs. (49) and (50), we have:

$$\eta = 1{,}3 \cdot 10^{-5} \left(\frac{\delta}{\Delta t}\right)^2 \frac{n_0 \sigma}{E} \left(1 - \frac{B}{E}\right),$$

where δ is expressed in percent, Δt in mμsec and E in Mev.

For a cylindrical scintillator with r = h, an average chemical composition CH and a density of unity, we have:

$$\eta = 2 \cdot 10^{-6} h^3 \left(\frac{\delta}{\Delta t}\right)^2 \frac{\sigma}{E} \left(1 - \frac{B}{E}\right), \tag{54}$$

where σ is expressed in barns and $\underline{h}$ in centimeters.

Using the relation which has been obtained it is easy to show that over the entire energy range being considered the efficiency of a time-of-flight spectrometer with a pulsed neutron source can be made greater than 10^{-4} for a resolving power of 5%. In this case, it is an easy matter to realize the conditions which provide the possibility of computing the efficiency, so that it is possible to make absolute measurements of the neutron flux with an accuracy no worse than 10%. For purposes of comparison we may note that the efficiency of a telescope with a thin radiator with a resolving power of 5% is 1000 times smaller (34) under optimum conditions.

There is a still greater difference in the counting rates achievable in practice by means of these devices since the background of random coincidences increases sharply as the counter load increases in the telescope and this imposes limitations on the intensity of the neutron flux which can be studied.

The high efficiency of a time-of-flight spectrometer and its ability to withstand high loading makes it possible to study nuclear reactions characterized by a differential cross section for neutron production which is < < 1 millibarn/steradian against a background of reactions which lead to the formation of harder neutrons and γ-rays and which are more probable. For purposes of illustration in Fig. 85 are shown the neutron spectra from the $Li^6 + p$ and $Li^7 + p$ reactions, obtained by means of a single-channel time-of-flight spectrometer [3]. The cross section for the neutron group characterized by an energy of 3.7 Mev for the $Li^6(p, n) Be^6$ reaction (ground state) is approximately 1 millibarn/steradian.

§ 3. Dynamic Range

The resolving power of a time-of-flight neutron spectrometer is usually limited most of all by the intensity of the neutron source since a low source intensity makes it impossible to use a sufficiently large flight distance. Sometimes, however, when the natural modulation of the beam of a large cyclotron is used, the resolving power is not limited by the intensity of the neutron flux but by the pulse-repetition rate.

If the repetition period of the pulses from the source is small, at large values of L it is possible that the fast neutrons from a given pulse can enter the counter before slower neutrons from a preceding pulse. Thus, for a given repetition period the maximum value of L is limited by the requirement for avoiding superposition of neutron spectra of different order and by the size of the required dynamic range $q = \frac{E_{max}}{E_{min}}$, where E_{max} and E_{min} are the maximum and minimum neutron energy which it is desired to measure simultaneously. In order to improve the resolving power and to expand the dynamic range in these cases, it is necessary to artificially reduce the neutron pulse-repetition frequency.

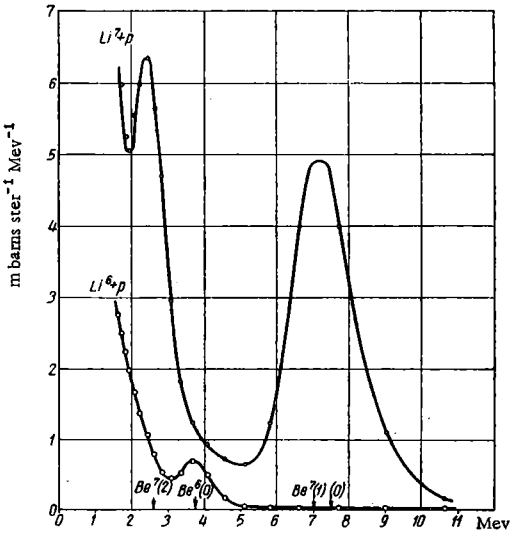

Fig. 85. Neutron spectra for the reactions $Li^6 + p$ and $Li^7 + p$ at an angle of 0° for a proton energy of 9.2 Mev obtained with a single-channel time-of-flight spectrometer [3].

The upper limit of the energy range is determined only by the limiting energy of the neutron spectrum being investigated E_{max}. The lower limit or the minimum neutron energy which can be measured is determined by the energy threshold of the counter B. The dependence of spectrometer efficiency on neutron energy for a given counter threshold has a form such that the accuracy with which the intensity of the neutron flux is measured falls off rapidly as the neutron energy approaches the threshold value. In accordance with Eq. (41), for further estimates we take

$$B = 0{,}7E_{min}.$$

Thus, the actual dynamic range of a time-of-flight spectrometer is

$$q = 0{,}7\,\frac{E_{max}}{B}\,. \tag{55}$$

The superposition of neutrons which are produced in source pulses which follow each other will not occur if the time-of-flight of the slowest neutron of those being recorded (energy B) does not exceed the time-of-flight of the fastest neutrons by an amount greater than the repetition period T:

$$t(B) < t(E_{max}) + T.$$

Under actual conditions, because of the finite resolution this requirement must be somewhat more stringent. Assuming that the two lines do not overlap, if the distance between their maxima is three times greater than the resolving time Δt we have

$$t(B) < t(E_{max}) + T - 3\Delta t. \tag{56}$$

It will be apparent that this condition imposes definite limitations on the dynamic range of the spectrometer. Denoting the quantity $\delta(E_{max})$ by δ_0, from Eqs. (55) and (56), we find that

$$q < 0{,}7\left[1 + \frac{\delta_0}{2}\left(\frac{T}{\Delta t} - 3\right)\right]^2. \tag{57}$$

This condition is shown graphically in Fig. 86 (curve I). The quantity $\left(\frac{T}{\Delta t} - 3\right)$ may be called the effective number of scale points on the spectrometer. The lower scale on the abscissa axis is plotted under the assumption that $\frac{T}{\Delta t} = 35$, corresponding to the effective number of scale points of the spectrometer of the Institute for Atomic Energy, Academy of Sciences, USSR [3]. The curve corresponding to the condition given in (57) separates the region of values of the spectrometer parameters q and δ_0 which can be reached simultaneously for a given effective number of scale points from the region of values of these parameters corresponding to overlapping of neutrons from adjacent periods.

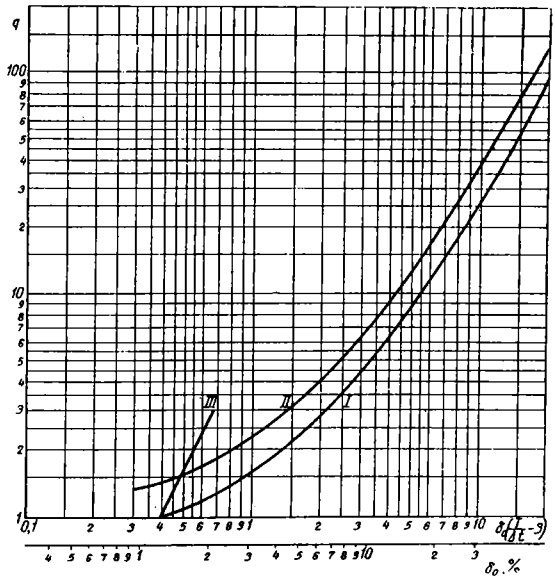

Fig. 86. Maximum dynamic range of a spectrometer when there is no overlap of spectra of different orders. Curve I corresponds to a fixed threshold $B = 0.7\,E_{min}$. Curves II and III correspond to a tracking threshold $B = 0.7\,E$. The lower scale on the abscissa axis refers to the spectrometer at the Institute for Atomic Energy, Academy of Sciences, USSR [3], for which $T/\Delta t = 35$.

In operation with a fixed threshold the part of the spectrometer scale corresponding to neutron energies between E_{min} and B is not used. The application of the tracking threshold method (see preceding section) thus makes it possible to expand the dynamic range of the spectrometer to some extent. In this case, in place of t(B), in Eq. (56), we have $t(E_{min})$:

$$t(E_{min}) < (E_{max}) + T - 3\Delta t,$$

which leads to

$$q < \left[1 + \frac{\delta_0}{2}\left(\frac{T}{\Delta t} - 3\right)\right]^2 \qquad (58)$$

The condition is (58) corresponds to curve II in Fig. 86.

However, the application of the tracking threshold method does not always allow us to use the entire scale of the instrument. If the length of the flight path becomes too large,a situation will occur (earliest of all at the lower limit of the spectrum) in which overlap of neutrons from neighboring periods limits the dynamic range.

Let us assume that the relation chosen between the threshold and the energy is described by the relation B = kE.

Then, in order to avoid overlap we require that

$$t(kE_{min}) < t(E_{min}) + T - 3\Delta t.$$

Assuming that

$$\delta(E_{min}) = \delta(E_{max})\sqrt{\frac{E_{min}}{E_{max}}} = \frac{\delta_0}{q},$$

we have

$$q < \frac{k}{4(1-\sqrt{k})^2}\cdot\delta_0^2\left(\frac{T}{\Delta t} - 3\right)^2.$$

When k = const = 0.7,

$$q < 6{,}6\delta_0^2\left(\frac{T}{\Delta t} - 3\right)^2. \qquad (59)$$

This condition is shown by curve III in Fig. 86.

As is apparent from Fig. 86, in order to increase the dynamic range of a spectrometer for a given resolving power or, to improve the resolving power for a given dynamic range, it is necessary to increase the effective number of scale points. This can be achieved either by reducing the resolving time or by increasing the neutron pulse-repetition period. Usually the first means has been pushed to the limit and only the second remains.

The dynamic range of the spectrometer is not only limited by the effects associated with overlapping of neutrons from neighboring periods. As has already been mentioned, in the targets of large accelerators (and in the study of secondary processes, in the neutron samples) in addition to the neutrons many γ-rays are produced. Because of the high efficiency of a neutron scintillation counter to γ-rays,narrow γ-peaks appear in the pulse-time distribution of the counter. In secondary processes, in addition to the γ-peak there is usually a peak associated with primary neutrons. The appearance of γ-peaks or primary neutron peaks in the working region of the time scale of the spectrometer makes it difficult to carry out exact measurements. Hence, a judicious choice of the conditions of measurement is very important in order to make good use of the capabilities of the spectrometer.

We now consider the limitation which are imposed on the region of allowable values of the parameters q and δ_0 by the condition that there be no γ-peaks in the working part of the spectrometer time scale:

$$t(E_{min} < t(\gamma) + mT - 3\Delta t$$
$$t(\gamma) + (m-1)T < t(E_{max}) - 3\Delta t.$$

Here m is the order number of the RF period during which the measurements are made, counting from the γ-peak corresponding to the neutron being studied.

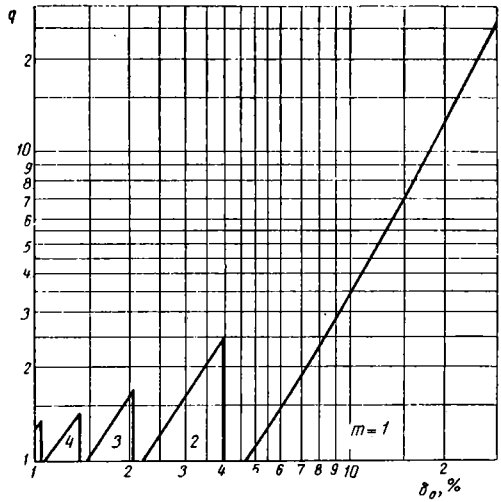

Fig. 87. Limitations imposed on the region of useable values of the dynamic range q and resolving power δ_0 if there are to be no γ-peaks in the operating portion of the spectrometer scale for $T/\Delta t = 35$ and $E_{max} = 30$ Mev.

After some manipulation, assuming that

$$t(\gamma) = 3{,}34L = 0{,}046\frac{\Delta t}{\delta_0}\sqrt{E_{max}},$$

we have

$$\frac{\delta_0}{2}\left(m\frac{T}{\Delta t} - 3\right) > \sqrt{q} - 0{,}046\sqrt{E_{max}}$$
$$\frac{\delta_0}{2}\left[(m-1)\frac{T}{\Delta t} + 3\right] < 1 - 0{,}046\sqrt{E_{max}}. \qquad (60)$$

In Fig. 87 the relation in (60) is shown for $\frac{T}{\Delta t} = 35$ and $E_{max} = 30$ Mev. It is apparent that even in the second period the dynamic range is less than two. The use of higher periods is essentially useless in practice.

If it is necessary to obtain a high resolving power over the entire spectrum in studying a wide spectrum, one must measure the spectrum in parts, using different values of the flight distance and the counter threshold.

As an example, we may consider the measurement of the neutron spectrum obtained by bombarding deuterium by 8.6 Mev protons; this work has been carried out with the multichannel spectrometer of the Institute for Atomic Energy, Academy of Sciences, USSR [4]. In Fig. 88 is shown the time-of-flight distribution for neutrons from the D(p, n) 2p reaction obtained with a flight distance of 1.58 m at an angle of 0° with respect to the proton

beam. The measurements were made with the target filled with deuterium and then with the target empty. The difference of the results obtained in these measurements is shown together with the background associated with the empty target. Close to the upper limit of the spectrum a separate narrow peak is shown, due to the interaction of two protons in the final state. The width and position of this peak is of great interest for comparison with theory [5]. However, with L = 1.58 m the width of the peak is approximately the same as the apparatus width. In order to carry out a more detailed investigation of the hard part of the spectrum measurements were also made with L = 5.15 m, corresponding to observations in the second period of the neutron source (Fig. 89). In this case, the width of the peak is considerably greater than the apparatus width.

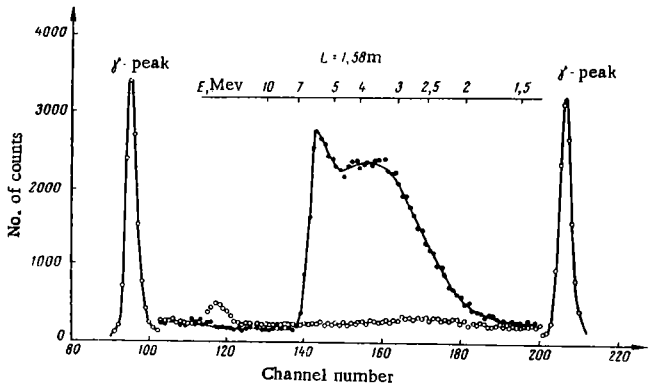

Fig. 88. Time-of-flight distribution for neutrons from the reaction D(p, n) 2p at an angle 0° for a proton energy of 8.6 Mev. The distance from the target to the counter is 1.58 m. The channel width is 0.876 mμsec. The counter threshold is 1.6 Mev. The background due to the empty target is shown.

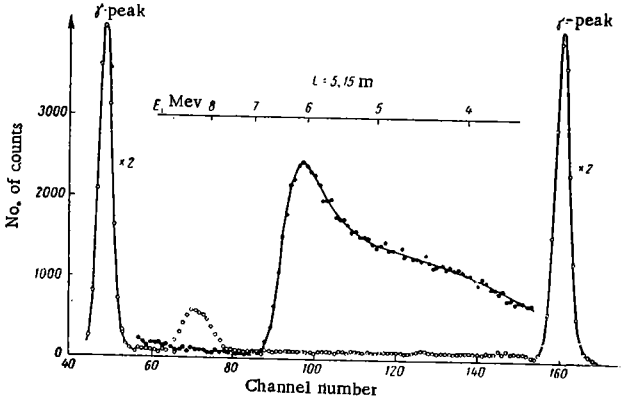

Fig. 89. Time-of-flight distribution for neutrons from the D(p, n) 2p reaction at an angle of 0° for a proton energy of 8.6 Mev. The distance from the target to the counter is 5.15 m. The channel width is 0.866 mμsec. The counter threshold is 2.7 Mev. The background due to the empty target is shown.

In Fig. 90 is shown the neutron spectrum obtained as a result of both measurements. It consists of two parts, with overlap between 4 and 5 Mev. For comparison the points corresponding to L = 1.58 m are given completely. For E > 5 Mev they are not.

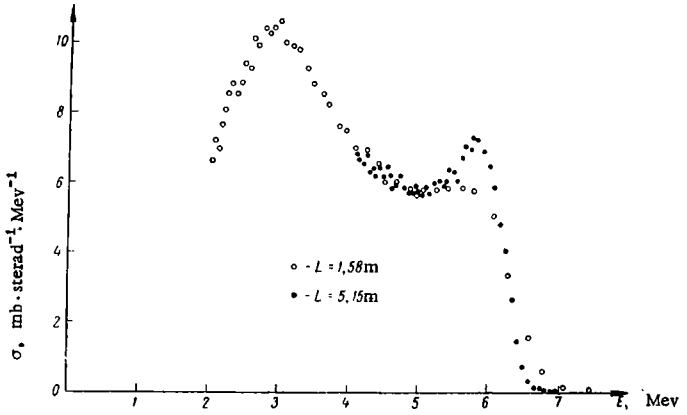

Fig. 90. Neutron spectrum obtained in the D(p, n) 2p reaction at an angle of 0° for proton energy of 8.6 Mev. The solid circles correspond to target-counter distances of 5.15 m, the open circles correspond to a target-counter distance of 1.58 m.

In the case of a line spectrum, the width and position of the individual lines can be measured in the third and higher periods. In Fig. 91 is shown the time-of-flight distribution of the neutron group from the reaction $Li^6(p, n)Be^6$ with the formation of Be^6 in the ground state (observed in the third period) and the doublet neutron group from the $Li^7(p, n)Be^7$ reaction corresponding to the ground state and the first excited state of Be^7 (observed in the second period), obtained with a single channel spectrometer [6]. The repetition period of the pulses from the neutron source is 96 mμsec. The first peak at t = 24 mμsec corresponds to the detection of γ-rays formed in the target (L = 7.3 m). It is possible to distinguish the γ-peak from the neutrons by replacing the target with a flag or by varying L. The zero on the time-of-flight scale is established from the identification of the γ-peak.

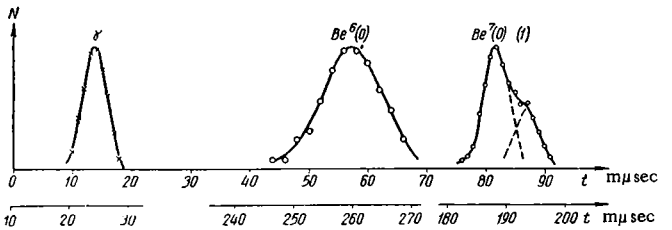

Fig. 91. Time-of-flight distribution for neutron groups from the $Li^6(p, n)Be^6$ reaction with the formation of Be^6 in the ground state and the doublet group from the $Li^7(p, n)Be^7$ reaction corresponding to the ground state and the first excited state of Be^7. Along the abscissa axis is plotted the quantity t' of the control pulse in a scale with an arbitrary zero position. Below are plotted the true values of the time-of-flight t for each group. The group corresponding to $Be^6(0)$ is observed in the third period from the neutron source as computed from the γ-peak, (a period is 96 mμsec) while the group corresponding to Be^7 (0; 1) is observed in the second period.

The resolution time of the spectrometer (width of the γ-peak at half-height) is $\Delta t = 5$ mμsec. The corresponding resolving power for neutrons from the reaction $Li^6(p, n)Be^6(0)$ (neutron energy 3.7 Mev) is 3.7%; for neutrons from the $Li^7(p, n)Be^7$ reaction (0.1) (the energy of the doublet line is 7.8 and 7.4 Mev) this quantity is 5.3%. The actual resolution is poorer (especially in the first period) because of the energy spread in the proton beam and the finite thickness of the target.

LITERATURE CITED

[1] R. Grismore and W. C. Parkinson, Rev. Sci. Instr. 28, 245 (1957).

[2] R. V. Smith, Conference on Neutron Physics by Time-of-Flight (Gatlinburg, Tennessee, USA, 1956), p. 103.

[3] A. A. Kurashov, A. F. Linev, B. V. Rybakov, and V. A. Sidorov, J. Atomic Energy 5, 135 (1958).

[4] N. A. Vlasov, S. P. Kalinin, B. V. Rybakov, and V. A. Sidorov, Proceedings of the International Conference on the Physics of the Nucleus (Paris, 1958).

[5] A. B. Migdal, J. Exptl.-Theoret. Phys. (USSR) 28, 3 (1955).

[6] G. F. Bogdanov, N. A. Vlasov, S. P. Kalinin, B. V. Rybakov, and V. A. Sidorov, J. Atomic Energy 3, 204 (1957).

APPENDIX

TIME-OF-FLIGHT-ENERGY TABLES

The neutron energy E (Mev), which corresponds to time-of-flight per meter, $\tau \left(\frac{\text{m}\mu\,\text{sec}}{\text{m}}\right)$, is computed from the relation

$$E = E_0\left(\frac{1}{\sqrt{1-\beta^2}} - 1\right) \approx 52{,}2680\left(\frac{10}{\tau}\right)^2 + 4{,}3617\left(\frac{10}{\tau}\right)^4 + 0{,}4044\left(\frac{10}{\tau}\right)^6 + 0{,}0394\left(\frac{10}{\tau}\right)^8 + 0{,}0039\left(\frac{10}{\tau}\right)^{10}.$$

In the range of variation of τ between 10 and 50 $\frac{\text{m}\mu\,\text{sec}}{\text{m}}$ the difference in the table entries is 0.02 $\frac{\text{m}\mu\,\text{sec}}{\text{m}}$; in the range between 50 and 150 $\frac{\text{m}\mu\,\text{sec}}{\text{m}}$ the differences in the table entries are 0.1 $\frac{\text{m}\mu\,\text{sec}}{\text{m}}$. The tables cover the energy range from 0.2 up to 57 Mev.

τ	0	2	4	6	8
10,0	57,08	56,83	56,58	56,34	56,09
10,1	55,85	55,61	55,37	55,13	54,90
10,2	54,66	54,43	54,20	53,97	53,74
10,3	53,52	53,29	53,07	52,85	52,62
10,4	52,40	52,19	51,97	51,76	51,54
10,5	51,33	51,12	50,91	50,70	50,49
10,6	50,29	50,08	49,88	49,68	49,47
10,7	49,28	49,08	48,88	48,68	48,49
10,8	48,30	48,10	47,91	47,72	47,53
10,9	47,35	47,16	46,97	46,79	46,61
11,0	46,42	46,24	46,06	45,88	45,71
11,1	45,53	45,35	45,18	45,00	44,83
11,2	44,66	44,49	44,32	44,15	43,98
11,3	43,82	43,65	43,49	43,32	43,16
11,4	43,00	42,84	42,68	42,52	42,36
11,5	42,20	42,05	41,89	41,74	41,58
11,6	41,43	41,28	41,13	40,98	40,83
11,7	40,68	40,53	40,38	40,24	40,09
11,8	39,95	39,80	39,66	39,52	39,38
11,9	39,24	39,10	38,96	38,82	38,68
12,0	38,54	38,41	38,28	38,14	38,01
12,1	37,87	37,74	37,61	37,48	37,35
12,2	37,22	37,09	36,96	36,83	36,70
12,3	36,58	36,45	36,33	36,20	36,08
12,4	35,96	35,83	35,71	35,59	35,47
12,5	35,35	35,23	35,11	35,00	34,88
12,6	34,76	34,64	34,53	34,41	34,30
12,7	34,18	34,07	33,96	33,85	33,74
12,8	33,62	33,51	33,40	33,29	33,18
12,9	33,08	32,97	32,86	32,76	32,65
13,0	32,54	32,44	32,33	32,23	32,13
13,1	32,02	31,92	31,82	31,72	31,62
13,2	31,52	31,42	31,32	31,22	31,12
13,3	31,02	30,92	30,82	30,73	30,63
13,4	30,54	30,44	30,35	30,25	30,16
13,5	30,06	29,97	29,88	29,78	29,69
13,6	29,60	29,51	29,42	29,33	29,24
13,7	29,15	29,06	28,97	28,88	28,80
13,8	28,71	28,62	28,54	28,45	28,37
13,9	28,28	28,20	28,11	28,03	27,94
14,0	27,86	27,78	27,69	27,61	27,53
14,1	27,45	27,37	27,29	27,21	27,13
14,2	27,05	26,97	26,89	26,81	26,73
14,3	26,65	26,57	26,50	26,42	26,34
14,4	26,27	26,19	26,12	26,04	25,97
14,5	25,89	25,82	25,74	25,67	25,60
14,6	25,52	25,45	25,38	25,31	25,24
14,7	25,16	25,09	25,02	24,95	24,88
14,8	24,81	24,74	24,67	24,60	24,54
14,9	24,47	24,40	24,33	24,26	24,20

τ	0	2	4	6	8
15,0	24,13	24,06	24,00	23,93	23,86
15,1	23,80	23,73	23,67	23,60	23,54
15,2	23,47	23,41	23,35	23,28	23,22
15,3	23,16	23,09	23,03	22,97	22,91
15,4	22,85	22,78	22,72	22,66	22,60
15,5	22,54	22,48	22,42	22,36	22,31
15,6	22,24	22,18	22,13	22,07	22,01
15,7	21,95	21,89	21,84	21,78	21,72
15,8	21,66	21,61	21,55	21,50	21,44
15,9	21,38	21,33	21,27	21,22	21,16
16,0	21,11	21,05	21,00	20,95	20,89
16,1	20,84	20,78	20,73	20,68	20,63
16,2	20,57	20,52	20,47	20,42	20,36
16,3	20,31	20,26	20,21	20,16	20,11
16,4	20,06	20,01	19,96	19,91	19,86
16,5	19,81	19,76	19,71	19,66	19,61
16,6	19,56	19,51	19,47	19,42	19,37
16,7	19,32	19,27	19,23	19,18	19,13
16,8	19,09	19,04	18,99	18,95	18,90
16,9	18,85	18,81	18,76	18,72	18,68
17,0	18,63	18,58	18,54	18,49	18,45
17,1	18,40	18,36	18,31	18,26	18,23
17,2	18,18	18,14	18,10	18,05	18,01
17,3	17,97	17,92	17,88	17,84	17,80
17,4	17,75	17,71	17,67	17,63	17,59
17,5	17,55	17,51	17,47	17,42	17,38
17,6	17,34	17,30	17,26	17,22	17,18
17,7	17,14	17,10	17,06	17,02	16,98
17,8	16,94	16,90	16,87	16,83	16,79
17,9	16,75	16,71	16,67	16,64	16,60
18,0	16,56	16,52	16,48	16,45	16,41
18,1	16,37	16,34	16,30	16,26	16,22
18,2	16,19	16,15	16,12	16,08	16,04
18,3	16,01	15,97	15,94	15,90	15,86
18,4	15,83	15,79	15,76	15,72	15,69
18,5	15,65	15,62	15,58	15,55	15,52
18,6	15,48	15,45	15,41	15,38	15,35
18,7	15,31	15,28	15,25	15,21	15,18
18,8	15,15	15,11	15,08	15,05	15,02
18,9	14,98	14,95	14,92	14,89	14,85
19,0	14,82	14,79	14,76	14,73	14,63
19,1	14,66	14,63	14,60	14,57	14,54
19,2	14,51	14,48	14,45	14,42	14,38
19,3	14,35	14,32	14,29	14,26	14,23
19,4	14,20	14,17	14,14	14,11	14,08
19,5	14,05	14,02	14,00	13,97	13,94
19,6	13,91	13,88	13,85	13,82	13,79
19,7	13,76	13,74	13,71	13,68	13,65
19,8	13,62	13,60	13,57	13,54	13,51
19,9	13,48	13,46	13,43	13,40	13,37

τ	0	2	4	6	8
20,0	13,35	13,32	13,29	13,26	13,24
20,1	13,21	13,18	13,16	13,13	13,10
20,2	13,08	13,05	13,02	13,00	12,97
20,3	12,95	12,92	12,90	12,87	12,84
20,4	12,82	12,79	12,77	12,74	12,72
20,5	12,69	12,66	12,64	12,61	12,59
20,6	12,56	12,54	12,51	12,49	12,46
20,7	12,44	12,42	12,39	12,37	12,34
20,8	12,32	12,30	12,27	12,25	12,22
20,9	12,20	12,18	12,15	12,13	12,10
21,0	12,08	12,06	12,04	12,01	11,99
21,1	11,96	11,94	11,92	11,90	11,87
21,2	11,85	11,83	11,80	11,78	11,76
21,3	11,74	11,71	11,69	11,67	11,65
21,4	11,62	11,60	11,58	11,56	11,54
21,5	11,52	11,49	11,47	11,45	11,43
21,6	11,41	11,39	11,36	11,34	11,32
21,7	11,30	11,28	11,26	11,24	11,22
21,8	11,20	11,18	11,15	11,13	11,11
21,9	11,09	11,07	11,05	11,03	11,01
22,0	10,99	10,97	10,95	10,93	10,91
22,1	10,89	10,87	10,85	10,83	10,81
22,2	10,79	10,77	10,75	10,73	10,71
22,3	10,69	10,67	10,65	10,63	10,61
22,4	10,59	10,57	10,56	10,54	10,52
22,5	10,50	10,48	10,46	10,44	10,42
22,6	10,40	10,38	10,37	10,35	10,33
22,7	10,31	10,29	10,27	10,26	10,24
22,8	10,22	10,20	10,18	10,16	10,15
22,9	10,13	10,11	10,09	10,08	10,06
23,0	10,04	10,02	10,00	9,986	9,968
23,1	9,951	9,933	9,916	9,898	9,881
23,2	9,864	9,847	9,829	9,812	9,795
23,3	9,778	9,761	9,744	9,727	9,710
23,4	9,694	9,677	9,660	9,643	9,627
23,5	9,610	9,593	9,577	9,560	9,544
23,6	9,528	9,511	9,495	9,478	9,462
23,7	9,446	9,430	9,414	9,398	9,382
23,8	9,366	9,350	9,334	9,318	9,302
23,9	9,287	9,270	9,255	9,239	9,223
24,0	9,208	9,192	9,177	9,161	9,146
24,1	9,131	9,115	9,100	9,085	9,069
24,2	9,054	9,039	9,024	9,009	8,994
24,3	8,979	8,964	8,949	8,934	8,919
24,4	8,904	8,890	8,875	8,860	8,845
24,5	8,830	8,816	8,802	8,787	8,772
24,6	8,758	8,743	8,729	8,715	8,701
24,7	8,686	8,672	8,658	8,644	8,629
24,8	8,615	8,601	8,587	8,573	8,559
24,9	8,545	8,532	8,518	8,504	8,490

τ	0	2	4	6	8
25,0	8,476	8,462	8,449	8,435	8,421
25,1	8,408	8,394	8,380	8,367	8,354
25,2	8,340	8,327	8,314	8,300	8,287
25,3	8,274	8,260	8,247	8,234	8,221
25,4	8,208	8,195	8,182	8,169	8,156
25,5	8,143	8,130	8,117	8,104	8,092
25,6	8,079	8,066	8,053	8,040	8,028
25,7	8,015	8,002	7,990	7,977	7,965
25,8	7,952	7,940	7,927	7,915	7,902
25,9	7,890	7,878	7,866	7,853	7,841
26,0	7,829	7,816	7,804	7,792	7,781
26,1	7,768	7,756	7,744	7,732	7,720
26,2	7,708	7,696	7,685	7,673	7,661
26,3	7,649	7,637	7,625	7,614	7,602
26,4	7,590	7,579	7,567	7,556	7,544
26,5	7,533	7,521	7,510	7,498	7,487
26,6	7,475	7,464	7,453	7,441	7,430
26,7	7,418	7,407	7,396	7,385	7,374
26,8	7,363	7,352	7,341	7,330	7,318
26,9	7,308	7,297	7,286	7,275	7,264
27,0	7,253	7,242	7,231	7,220	7,210
27,1	7,199	7,188	7,177	7,167	7,156
27,2	7,146	7,135	7,124	7,114	7,103
27,3	7,093	7,082	7,072	7,061	7,051
27,4	7,040	7,030	7,020	7,009	6,999
27,5	6,989	6,978	6,968	6,958	6,948
27,6	6,938	6,928	6,917	6,907	6,897
27,7	6,887	6,877	6,867	6,857	6,847
97,8	6,837	6,827	6,817	6,807	6,797
27,9	6,787	6,778	6,768	6,758	6,748
28,0	6,739	6,729	6,719	6,710	6,700
28,1	6,690	6,681	6,671	6,662	6,652
28,2	6,642	6,633	6,623	6,614	6,605
28,3	6,595	6,586	6,576	6,567	6,558
28,4	6,548	6,539	6,530	6,520	6,511
28,5	6,502	6,492	6,483	6,474	6,465
28,6	6,456	6,447	6,438	6,429	6,420
28,7	6,411	6,402	6,393	6,384	6,375
28,8	6,366	6,357	6,348	6,339	6,330
28,9	6,321	6,312	6,304	6,295	6,286
29,0	6,278	6,269	6,260	6,251	6,242
29,1	6,234	6,225	6,217	6,208	6,199
29,2	6,191	6,182	6,174	6,165	6,156
29,3	6,148	6,139	6,131	6,123	6,114
29,4	6,106	6,098	6,089	6,081	6,072
29,5	6,064	6,056	6,048	6,039	6,031
29,6	6,023	6,015	6,007	5,998	5,990
29,7	5,982	5,974	5,966	5,958	5,950
29,8	5,942	5,934	5,926	5,918	5,910
29,9	5,902	5,894	5,886	5,878	5,870

τ	0	2	4	6	8
30,0	5,862	5,854	5,846	5,838	5,831
30,1	5,823	5,815	5,807	5,799	5,792
30,2	5,784	5,776	5,768	5,761	5,753
30,3	5,745	5,738	5,730	5,723	5,715
30,4	5,707	5,700	5,693	5,685	5,677
30,5	5,670	5,662	5,655	5,647	5,640
30,6	5,632	5,625	5,617	5,610	5,603
30,7	5,595	5,588	5,581	5,573	5,566
30,8	5,559	5,551	5,544	5,537	5,530
30,9	5,522	5,515	5,508	5,501	5,494
31,0	5,487	5,480	5,472	5,465	5,458
31,1	5,451	5,444	5,437	5,430	5,423
31,2	5,416	5,409	5,402	5,395	5,388
31,3	5,381	5,374	5,367	5,360	5,353
31,4	5,346	5,340	5,333	5,326	5,319
31,5	5,312	5,305	5,299	5,292	5,285
31,6	5,278	5,272	5,265	5,259	5,252
31,7	5,245	5,238	5,231	5,225	5,218
31,8	5,212	5,205	5,198	5,192	5,185
31,9	5,178	5,172	5,165	5,159	5,152
32,0	5,146	5,139	5,133	5,127	5,120
32,1	5,114	5,107	5,101	5,094	5,088
32,2	5,082	5,075	5,068	5,063	5,056
32,3	5,050	5,044	5,037	5,031	5,026
32,4	5,019	5,012	5,006	5,000	4,994
32,5	4,988	4,981	4,975	4,969	4,963
32,6	4,957	4,950	4,944	4,938	4,932
32,7	4,926	4,920	4,914	4,908	4,902
32,8	4,896	4,890	4,884	4,878	4,872
32,9	4,866	4,860	4,854	4,848	4,842
33,0	4,836	4,830	4,825	4,819	4,813
33,1	4,807	4,801	4,795	4,790	4,784
33,2	4,778	4,772	4,766	4,760	4,755
33,3	4,749	4,743	4,738	4,732	4,726
33,4	4,720	4,715	4,709	4,703	4,698
33,5	4,692	4,686	4,681	4,675	4,670
33,6	4,644	4,658	4,653	4,647	4,642
33,7	4,636	4,631	4,625	4,620	4,614
33,8	4,609	4,603	4,598	4,592	4,587
33,9	4,581	4,576	4,571	4,565	4,560
34,0	4,554	4,549	4,543	4,538	4,533
34,1	4,527	4,522	4,516	4,511	4,506
34,2	4,501	4,495	4,490	4,485	4,480
34,3	4,474	4,469	4,464	4,459	4,453
34,4	4,448	4,443	4,438	4,432	4,427
34,5	4,422	4,417	4,412	4,407	4,401
34,6	4,396	4,391	4,386	4,381	4,376
34,7	4,371	4,366	4,361	4,356	4,351
34,8	4,346	4,341	4,336	4,331	4,326
34,9	4,321	4,316	4,311	4,306	4,301

τ	0	2	4	6	8
35,0	4,296	4,291	4,286	4,281	4,276
35,1	4,271	4,266	4,261	4,256	4,252
35,2	4,247	4,242	4,237	4,232	4,228
35,3	4,223	4,218	4,213	4,208	4,204
35,4	4,199	4,194	4,189	4,184	4,180
35,5	4,175	4,170	4,165	4,161	4,156
35,6	4,151	4,147	4,142	4,137	4,133
35,7	4,128	4,123	4,119	4,114	4,109
35,8	4,105	4,100	4,096	4,091	4,086
35,9	4,082	4,077	4,073	4,068	4,063
36,0	4,059	4,054	4,050	4,045	4,041
36,1	4,036	4,032	4,027	4,023	4,018
36,2	4,014	4,010	4,005	4,001	3,996
36,3	3,992	3,987	3,983	3,979	3,974
36,4	3,970	3,965	3,961	3,956	3,952
36,5	3,948	3,943	3,939	3,935	3,930
36,6	3,926	3,922	3,918	3,913	3,909
36,7	3,905	3,900	3,896	3,892	3,888
36,8	3,883	3,879	3,875	3,871	3,866
36,9	3,862	3,858	3,854	3,850	3,846
37,0	3,841	3,837	3,833	3,829	3,824
37,1	3,820	3,816	3,812	3,808	3,804
37,2	3,800	3,796	3,792	3,788	3,784
37,3	3,779	3,775	3,771	3,767	3,763
37,4	3,759	3,755	3,751	3,747	3,743
37,5	3,739	3,735	3,731	3,727	3,723
37,6	3,719	3,715	3,711	3,707	3,703
37,7	3,699	3,695	3,691	3,687	3,683
37,8	3,679	3,676	3,672	3,668	3,664
37,9	3,660	3,656	3,652	3,648	3,645
38,0	3,641	3,637	3,633	3,629	3,625
38,1	3,621	3,618	3,614	3,610	3,606
38,2	3,602	3,599	3,595	3,591	3,587
38,3	3,583	3,580	3,576	3,572	3,568
38,4	3,565	3,561	3,557	3,554	3,550
38,5	3,546	3,542	3,539	3,535	3,531
38,6	3,528	3,524	3,520	3,517	3,513
38,7	3,509	3,506	3,502	3,498	3,495
38,8	3,491	3,488	3,484	3,480	3,477
38,9	3,473	3,470	3,466	3,462	3,459
39,0	3,455	3,452	3,448	3,445	3,441
39,1	3,438	3,434	3,430	3,427	3,423
39,2	3,420	3,416	3,413	3,409	3,406
39,3	3,402	3,399	3,395	3,392	3,389
39,4	3,385	3,382	3,378	3,375	3,371
39,5	3,368	3,364	3,361	3,358	3,354
39,6	3,351	3,347	3,344	3,341	3,337
39,7	3,334	3,331	3,327	3,324	3,320
39,8	3,317	3,314	3,310	3,307	3,304
39,9	3,300	3,297	3,294	3,290	3,287

τ	0	2	4	6	8
40,0	3,284	3,280	3,277	3,274	3,271
40,1	3,267	3,264	3,261	3,258	3,254
40,2	3,251	3,248	3,245	3,241	3,238
40,3	3,235	3,232	3,228	3,225	3,222
40,4	3,219	3,216	3,212	3,209	3,206
40,5	3,203	3,200	3,196	3,193	3,190
40,6	3,187	3,184	3,181	3,177	3,174
40,7	3,171	3,168	3,165	3,162	3,159
40,8	3,156	3,153	3,150	3,146	3,143
40,9	3,140	3,137	3,134	3,131	3,128
41,0	3,125	3,122	3,119	3,116	3,113
41,1	3,110	3,106	3,103	3,100	3,097
41,2	3,094	3,091	3,088	3,085	3,082
41,3	3,079	3,076	3,073	3,070	3,067
41,4	3,064	3,061	3,058	3,056	3,052
41,5	3,050	3,047	3,044	3,041	3,038
41,6	3,035	3,032	3,029	3,026	3,023
41,7	3,020	3,017	3,014	3,012	3,009
41,8	3,006	3,003	3,000	2,997	2,994
41,9	2,991	2,988	2,286	2,983	2,980
42,0	2,977	2,974	2,971	2,969	2,966
42,1	2,963	2,960	2,957	2,954	2,952
42,2	2,949	2,946	2,943	2,940	2,938
42,3	2,935	2,932	2,929	2,926	2,924
42,4	2,921	2,918	2,915	2,913	2,910
42,5	2,907	2,904	2,902	2,899	2,896
42,6	2,893	2,891	2,888	2,885	2,882
42,7	2,880	2,877	2,874	2,872	2,869
42,8	2,866	2,864	2,861	2,858	2,856
42,9	2,853	2,850	2,848	2,845	2,842
43,0	2,840	2,837	2,834	2,832	2,829
43,1	2,826	2,824	2,821	2,818	2,816
43,2	2,813	2,811	2,808	2,805	2,803
43,3	2,800	2,798	2,795	2,792	2,790
43,4	2,787	2,785	2,782	2,780	2,777
43,5	2,774	2,772	2,769	2,767	2,764
43,6	2,762	2,759	2,757	2,754	2,752
43,7	2,749	2,746	2,744	2,741	2,739
43,8	2,736	2,734	2,731	2,729	2,726
43,9	2,724	2,721	2,719	2,716	2,714
44,0	2,711	2,709	2,707	2,704	2,702
44,1	2,699	2,697	2,694	2,692	2,689
44,2	2,687	2,684	2,682	2,680	2,677
44,3	2,675	2,672	2,670	2,668	2,665
44,4	2,663	2,660	2,658	2,655	2,653
44,5	2,651	2,648	2,646	2,644	2,641
44,6	2,639	2,636	2,634	2,631	2,629
44,7	2,627	2,624	2,622	2,620	2,617
44,8	2,615	2,613	2,610	2,608	2,606
44,9	2,604	2,601	2,599	2,596	2,594

τ	0	2	4	6	8
45,0	2,592	2,589	2,587	2,585	2,583
45,1	2,580	2,578	2,576	2,573	2,571
45,2	2,569	2,566	2,564	2,562	2,560
45,3	2,558	2,555	2,553	2,551	2,548
45,4	2,546	2,544	2,542	2,539	2,537
45,5	2,535	2,533	2,530	2,528	2,526
45,6	2,524	2,522	2,519	2,517	2,515
45,7	2,513	2,510	2,508	2,506	2,504
45,8	2,502	2,500	2,497	2,495	2,493
45,9	2,491	2,489	2,486	2,484	2,482
46,0	2,480	2,478	2,476	2,473	2,471
46,1	2,469	2,467	2,465	2,463	2,460
46,2	2,458	2,456	2,454	2,452	2,450
46,3	2,448	2,446	2,444	2,441	2,439
46,4	2,437	2,435	2,433	2,431	2,429
46,5	2,427	2,424	2,422	2,420	2,418
46,6	2,416	2,414	2,412	2,410	2,408
46,7	2,406	2,404	2,402	2,400	2,398
46,8	2,396	2,394	2,391	2,389	2,387
46,9	2,385	2,383	2,381	2,379	2,377
47,0	2,375	2,373	2,371	2,369	2,367
47,1	2,365	2,363	2,361	2,359	2,357
47,2	2,355	2,353	2,351	2,349	2,347
47,3	2,345	2,343	2,341	2,339	2,337
47,4	2,335	2,333	2,331	2,329	2,327
47,5	2,325	2,323	2,321	2,319	2,317
47,6	2,315	2,313	2,311	2,310	2,308
47,7	2,306	2,304	2,302	2,300	2,298
47,8	2,296	2,294	2,292	2,290	2,288
47,9	2,286	2,284	2,283	2,281	2,279
48,0	2,277	2,275	2,273	2,271	2,269
48,1	2,267	2,265	2,264	2,262	2,260
48,2	2,258	2,256	2,254	2,252	2,250
48,3	2,248	2,247	2,245	2,243	2,241
48,4	2,239	2,237	2,236	2,234	2,232
48,5	2,230	2,228	2,226	2,224	2,223
48,6	2,221	2,219	2,217	2,215	2,213
48,7	2,212	2,210	2,208	2,206	2,204
48,8	2,202	2,201	2,199	2,197	2,195
48,9	2,193	2,191	2,190	2,188	2,186
49,0	2,184	2,183	2,181	2,179	2,177
49,1	2,176	2,174	2,172	2,170	2,168
49,2	2,167	2,165	2,163	2,161	,160
49,3	2,158	2,156	2,154	2,153	2,151
49,4	2,149	2,148	2,146	2,144	2,142
49,5	2,140	2,139	2,137	2,135	2,134
49,6	2,132	2,130	2,128	2,127	2,125
49,7	2,123	2,122	2,120	2,118	2,116
49,8	2,115	2,113	2,111	2,110	2,108
49,9	2,106	2,104	2,103	2,101	2,099

τ	0	1	2	3	4
50	2,098	2,089	2,082	2,073	2,064
51	2,016	2,008	2,000	1,992	1,985
52	1,939	1,932	1,924	1,917	1,909
53	1,866	1,859	1,852	1,845	1,838
54	1,798	1,791	1,784	1,778	1,771
55	1,733	1,726	1,720	1,714	1,708
56	1,671	1,665	1,659	1,653	1,648
57	1,613	1,607	1,602	1,596	1,590
58	1,558	1,552	1,547	1,542	1,536
59	1,505	1,500	1,495	1,490	1,485
60	1,455	1,450	1,446	1,441	1,436
61	1,408	1,403	1,399	1,394	1,390
62	1,363	1,358	1,354	1,350	1,345
63	1,320	1,316	1,311	1,307	1,303
64	1,279	1,275	1,271	1,267	1,263
65	1,240	1,236	1,232	1,228	1,224
66	1,202	1,199	1,195	1,191	1,188
67	1,167	1,163	1,160	1,156	1,153
68	1,132	1,129	1,126	1,123	1,119
69	1,100	1,097	1,093	1,090	1,087
70	1,069	1,065	1,062	1,059	1,056
71	1,039	1,036	1,033	1,030	1,027
72	1,010	1,007	1,004	1,002	0,9988
73	0,9823	0,9796	0,9770	0,9743	0,9717
74	0,9560	0,9533	0,9508	0,9482	0,9457
75	0,9306	0,9281	0,9256	0,9232	0,9207
76	0,9062	0,9038	0,9015	0,8991	0,8968
77	0,8828	0,8805	0,8782	0,8760	0,8737
78	0,8603	0,8581	0,8559	0,8537	0,8515
79	0,8386	0,8365	0,8344	0,8323	0,8302
80	0,8178	0,8157	0,8137	0,8116	0,8096
81	0,7977	0,7957	0,7937	0,7918	0,7898
82	0,7783	0,7764	0,7745	0,7726	0,7708
83	0,7596	0,7578	0,7560	0,7542	0,7524
84	0,7416	0,7399	0,7381	0,7364	0,7346
85	0,7243	0,7226	0,7209	0,7192	0,7175
86	0,7075	0,7059	0,7042	0,7026	0,7010
87	0,6913	0,6897	0,6882	0,6866	0,6850
88	0,6757	0,6741	0,6726	0,6711	0,6696
89	0,6606	0,6591	0,6576	0,6561	0,6547
90	0,6460	0,6445	0,6431	0,6417	0,6402
91	0,6318	0,6304	0,6290	0,6277	0,6263
92	0,6182	0,6168	0,6155	0,6141	0,6128
93	0,6049	0,6036	0,6023	0,6010	0,5997
94	0,5921	0,5908	0,5896	0,5883	0,5871
95	0,5797	0,5785	0,5772	0,5760	0,5748
96	0,5677	0,5665	0,5653	0,5641	0,5629
97	0,5560	0,5549	0,5537	0,5526	0,5514
98	0,5447	0,5436	0,5425	0,5414	0,5403
99	0,5337	0,5327	0,5316	0,5305	0,5295

5	6	7	8	9	c
2 056	2,048	2,040	2,032	2,024	50
1,977	1,969	1,962	1,954	1,946	51
1,902	1,895	1,888	1,881	1,873	52
1,831	1,825	1,818	1,811	1,804	53
1,765	1,758	1,752	1,745	1,739	54
1,702	1,695	1,689	1,683	1,677	55
1,642	1,636	1,630	1,624	1,618	56
1,585	1,579	1,574	1,568	1,563	57
1,531	1,526	1,521	1,515	1,510	58
1,480	1,475	1,470	1,465	1,460	59
1,431	1,427	1,422	1,417	1,413	60
1,385	1,380	1,376	1,372	1,367	61
1,341	1,357	1,332	1,328	1,324	62
1,299	1,295	1,291	1,287	1,283	63
1,259	1,255	1,251	1,247	1,243	64
1,221	1,217	1,213	1,210	1,206	65
1,184	1,181	1,177	1,174	1,170	66
1,149	1,146	1,143	1,139	1,136	67
1,116	1,113	1,109	1,106	1,103	68
1,084	1,081	1,078	1,075	1,072	69
1,053	1,050	1,047	1,044	1,042	70
1,024	1,021	1,018	1,016	1,013	71
0,9960	0,9933	0,9905	0,9878	0,9850	72
0,9690	0,9664	0,9638	0,9612	0,9586	73
0,9431	0,9406	0,9381	0,9356	0,9331	74
0,9183	0,9158	0,9134	0,9110	0,9086	75
0,8944	0,8921	0,8897	0,8874	0,8851	76
0,8714	0,8692	0,8670	0,8647	0,8625	77
0,8494	0,8472	0,8450	0,8429	0,8408	78
0,8281	0,8260	0,8239	0,8219	0,8198	79
0,8076	0,8056	0,8036	0,8016	0,7996	80
0,7879	0,7860	0,7840	0,7821	0,7802	81
0,7689	0,7670	0,7652	0,7633	0,7615	82
0,7506	0,7488	0,7470	0,7452	0,7434	83
0,7329	0,7311	0,7294	0,7277	0,7260	84
0,7158	0,7141	0,7125	0,7108	0,7092	85
0,6993	0,6977	0,6961	0,6945	0,6929	86
0,6834	0,6819	0,6803	0,6788	0,6772	87
0,6681	0,6666	0,6650	0,6636	0,6621	88
0,6532	0,6517	0,6503	0,6488	0,6474	89
0,6388	0,6374	0,6360	0,6346	0,6332	90
0,6249	0,6236	0,6222	0,6208	0,6195	91
0,6115	0,6101	0,6088	0,6075	0,6062	92
0,5984	0,5972	0,5959	0,5946	0,5934	93
0,5858	0,5846	0,5834	0,5821	0,5809	94
0,5736	0,5724	0,5712	0,5700	0,5688	95
0,5618	0,5606	0,5595	0,5583	0,5572	96
0,5503	0,5492	0,5480	0,5469	0,5458	97
0,5392	0,5381	0,5370	0,5359	0,5348	98
0,5284	0,5273	0,5263	0,5252	0,5242	99

τ	0	1	2	3	4
100	0,5231	0,5221	0,5210	0,5200	0,5190
101	0,5128	0,5118	0,5108	0,5098	0,5088
102	0,5028	0,5018	0,5008	0,4998	0,4989
103	0,4931	0,4921	0,4912	0,4902	0,4893
104	0,4836	0,4827	0,4818	0,4808	0,4799
105	0,4745	0,4735	0,4726	0,4717	0,4709
106	0,4655	0,4647	0,4638	0,4629	0,4620
107	0,4569	0,4560	0,4552	0,4543	0,4535
108	0,4484	0,4476	0,4468	0,4460	0,4451
109	0,4402	0,4394	0,4386	0,4378	0,4370
110	0,4323	0,4315	0,4307	0,4299	0,4291
111	0,4245	0,4237	0,4230	0,4222	0,4215
112	0,4170	0,4162	0,4155	0,4147	0,4140
113	0,4096	0,4089	0,4082	0,4074	0,4067
114	0,4024	0,4017	0,4010	0,4003	0,3996
115	0,3955	0,3948	0,3941	0,3934	0,3927
116	0,3887	0,3880	0,3874	0,3867	0,3860
117	0,3821	0,3814	0,3808	0,3801	0,3795
118	0,3756	0,3750	0,3743	0,3737	0,3731
119	0,3693	0,3687	0,3681	0,3675	0,3668
120	0,3632	0,3626	0,3620	0,3614	0,3608
121	0,3572	0,3566	0,3560	0,3554	0,3548
122	0,3514	0,3508	0,3502	0,3496	0,3491
123	0,3457	0,3451	0,3446	0,3440	0,3434
124	0,3401	0,3396	0,3390	0,3385	0,3379
125	0,3347	0,3342	0,3336	0,3331	0,3326
126	0,3294	0,3289	0,3284	0,3278	0,3273
127	0,3242	0,3237	0,3232	0,3227	0,3222
128	0,3192	0,3187	0,3182	0,3177	0,3172
129	0,3143	0,3138	0,3133	0,3128	0,3123
130	0,3094	0,3090	0,3085	0,3080	0,3075
131	0,3047	0,3043	0,3038	0,3033	0,3029
132	0,3001	0,2997	0,2992	0,2988	0,2983
133	0,2956	0,2952	0,2947	0,2943	0,2939
134	0,2912	0,2908	0,2904	0,2899	0,2895
135	0,2869	0,2865	0,2861	0,2857	0,2852
136	0,2827	0,2823	0,2819	0,2815	0,2811
137	0,2786	0,2782	0,2778	0,2774	0,2770
138	0,2746	0,2742	0,2738	0,2734	0,2730
139	0,2706	0,2703	0,2698	0,2695	0,2691
140	0,2668	0,2664	0,2660	0,2657	0,2653
141	0,2630	0,2626	0,2623	0,2619	0,2615
142	0,2593	0,2590	0,2586	0,2582	0,2579
143	0,2557	0,2554	0,2550	0,2546	0,2543
144	0,2522	0,2518	0,2515	0,2511	0,2508
145	0,2487	0,2484	0,2480	0,2477	0,2473
146	0,2453	0,2450	0,2446	0,2443	0,2440
147	0,2420	0,2416	0,2413	0,2410	0,2407
148	0,2387	0,2384	0,2381	0,2378	0,2374
149	0,2355	0,2352	0,2349	0,2346	0,2343

5	6	7	8	9	:
0,5179	0,5169	0,5159	0,5148	0,5138	100
0,5078	0,5068	0,5058	0,5048	0,5038	101
0,4979	0,4969	0,4960	0,4950	0,4940	102
0,4883	0,4874	0,4864	0,4855	0,4846	103
0,4790	0,4781	0,4772	0,4763	0,4754	104
0,4700	0,4691	0,4682	0,4673	0,4664	105
0,4612	0,4603	0,4594	0,4586	0,4577	106
0,4526	0,4518	0,4509	0,4501	0,4493	107
0,4443	0,4435	0,4427	0,4419	0,4410	108
0,4362	0,4354	0,4346	0,4339	0,4331	109
0,4284	0,4276	0,4268	0,4260	0,4253	110
0,4207	0,4200	0,4192	0,4184	0,4177	111
0,4133	0,4125	0,4118	0,4111	0,4103	112
0,4060	0,4053	0,4046	0,4039	0,4032	113
0,3989	0,3982	0,3975	0,3969	0,3962	114
0,3921	0,3914	0,3907	0,3900	0,3893	115
0,3854	0,3847	0,3840	0,3834	0,3827	116
0,3788	0,3782	0,3775	0,3769	0,3763	117
0,3724	0,3718	0,3712	0,3706	0,3699	118
0,3662	0,3656	0,3650	0,3644	0,3638	119
0,3602	0,3596	0,3590	0,3584	0,3578	120
0,3543	0,3537	0,3531	0,3526	0,3519	121
0,3485	0,3479	0,3474	0,3468	0,3462	122
0,3429	0,3423	0,3418	0,3412	0,3407	123
0,3374	0,3369	0,3363	0,3358	0,3352	124
0,3320	0,3315	0,3310	0,3304	0,3299	125
0,3268	0,3263	0,3258	0,3253	0,3247	126
0,3217	0,3212	0,3207	0,3202	0,3197	127
0,3167	0,3162	0,3157	0,3152	0,3148	128
0,3118	0,3113	0,3109	0,3104	0,3099	129
0,3071	0,3066	0,3061	0,3057	0,3052	130
0,3024	0,3020	0,3015	0,3010	0,3006	131
0,2979	0,2974	0,2970	0,2965	0,2961	132
0,2934	0,2930	0,2925	0,2921	0,2917	133
0,2891	0,2886	0,2882	0,2878	0,2874	134
0,2848	0,2844	0,2840	0,2836	0,2831	135
0,2807	0,2802	0,2798	0,2794	0,2790	136
0,2766	0,2762	0,2758	0,2754	0,2750	137
0,2726	0,2722	0,2718	0,2714	0,2710	138
0,2687	0,2683	0,2679	0,2676	0,2672	139
0,2649	0,2645	0,2641	0,2638	0,2634	140
0,2617	0,2608	0,2604	0,2601	0,2597	141
0,2575	0,2572	0,2568	0,2564	0,2561	142
0,2539	0,2536	0,2532	0,2529	0,2525	143
0,2504	0,2501	0,2497	0,2494	0,2490	144
0,2470	0,2467	0,2463	0,2460	0,2456	145
0,2436	0,2433	0,2430	0,2426	0,2423	146
0,2403	0,2400	0,2397	0,2394	0,2390	147
0,2371	0,2368	0,2365	0,2362	0,2358	148
0,2340	0,2336	0,2333	0,2330	0,2327	149